Dynamic interactions within the host-associated microbiota cause tumorigenesis in the basal metazoan *Hydra*

Dissertation

zur Erlangung des Doktorgrades

der Mathematisch-Naturwissenschaftlichen Fakultät

der Christian-Albrechts-Universität

zu Kiel

vorgelegt von

Kai Erik Rathje

Kiel, im Oktober 2019

Erstgutachter: Prof. Dr. Dr. h.c. Thomas Bosch
Zweitgutachter: Prof. Dr. Thomas Roeder
Tag der mündlichen Prüfung: 12.12.2019

Table of Contents:

Summary

Interactions between microorganisms and their eukaryotic hosts have shaped the evolution of complex life forms - plants and animals. All extant multicellular organisms contain abundant and diverse microbiota, and are considered as metaorganisms or holobionts. It is widely accepted that an intricate balance between cell dynamics within the host, associated microbiota, and their proper adjustment to the environment maintain the integrity of such a metaorganism. However, it remains unclear, to what extent disturbances in the resident microbiota can compromise an animal's health. The fundamental mechanisms coupling the host homeostasis and microbiota and their evolutionary history remain poorly understood. The use of experimentally traceable and evolutionary informative models, such as cnidarians, may provide deep insights into the fundamental rules governing the host-microbiota interdependency.

Here, I investigate the dynamic interactions between the microbiota and its host within the metaorganism *Hydra*. I demonstrate that alterations in the composition of commensal microbiota cause tumorigenesis in *Hydra*. Natural infestation of *Hydra* by environmental spirochaetes *Turneriella* or their experimental introduction greatly disturb normal development, morphogenesis, and tissue homeostasis of *Hydra*, resulting in tumor phenotype. Surprisingly, elimination of spirochaetes obliterates the tumor, indicating that a persistent presence of these bacteria is necessary to sustain tumorigenesis. I also show that, unexpectedly, virulence of the spirochaetes requires the presence of *Pseudomonas* spec., a member of *Hydra´*s beneficial microbiome. Finally, by integrating genomic and transcriptomic data, I uncover putative molecular mechanisms of the dynamic interactions between the resident bacterium *Pseudomonas*, an environmental spirochaete *Turneriella*, and the host that promote the tumor formation.

Taken together, my observations point to the crucial role of commensal bacteria in maintaining tissue homeostasis and add support to the view that microbial community interactions are essential for disease. My findings in an organism that shares deep evolutionary connections with all animals, including the human human, have significant implications for our understanding of normal homeostasis within a holobiont and tumorigenesis.

Zusammenfassung

Interaktionen zwischen Mikroorganismen und ihrem eukaryotischen Wirt formten die Evolution von komplexen Lebensformen – Pflanzen und Tieren. Alle bestehenden multizellulären Organismen enthalten reichhaltig vorhandene und vielfältige Mikrobiota, bekannt als Metaorganismen oder Holobionten. Es ist weitgehend akzeptiert, dass eine komplexes Gleichgewicht zwischen den Zelldynamiken innerhalb des Wirtes, der assoziierten Mikrobiota und deren korrekte Anpassung an die Umwelt die Intaktheit eines solchen Metaorganismus erhalten. Es bleibt hingegen ungewiss in welchen Ausmaße eine Störung der besiedelnden Mikrobiota die Gesundheit des Tieres beeinflussen. Die grundlegenden Mechanismen, die die Wirtshomöostase, die Mikrobiota und ihre evolutionäre Geschichte verbinden, sind kaum verstanden. Der Gebrauch von experimentell nachvollziehbaren und evolutionär informativen Modellorganismen, wie Cnidarien, vermag es tiefreichende Einblicke in die fundamentalen Regeln zu ermöglichen, die die Wirts-Mikrobiota-Wechselwirkungen steuern.

Hier untersuche ich die dynamischen Interaktionen zwischen der Mikrobiota und ihrem Wirt in dem Metaorganismus *Hydra*. Ich demonstriere, dass Veränderungen in der Zusammensetzung der kommensalen Mikrobiota zur Tumorgenese in *Hydra* führen. Natürlicher Befall von *Hydra* durch den Umwelt-Spirochaeten *Turneriella* oder die experimentelle Indizierung, zerstören in hohem Maße die normale Entwicklung, Morphogenese und die Gewebshomöostase in *Hydra,* was im Tumorphenotype resultiert. Überaschenderweise führt die Eliminierung der Spirochaeten zur Auslöschung des Tumors, was darauf hindeutet, dass eine dauerhafte Anwesenheit der Bakterien nötig ist, um Tumorgenese zu erhalten. Ich konnte zudem zeigen, dass die Virulenz der Spriochaeten die Anwesenheit von *Pseudomonas spec*. erfordert, einem Mitglied von *Hydra*'s nützlicher Mikrobiota. Durch das Integrieren der genomischen und transkriptionellen Daten, decke Ich schließlich mögliche molekulare Mechanismen der dynamischen Interaktionen zwischen dem ansässigen Bakterium *Pseudomonas*, dem Umwelt-Spirochaeten *Turneriella* und dem Wirt auf, welche die Tumorbildung verursachen.

Zusammenfassend deuten meine Beobachtungen auf eine entscheidende Rolle der kommensalen Bakterien zum Erhalt der Gewebshomöostase hin und unterstützen die Hinsicht, dass Interaktionen der mikrobiellen Gemeinschaft essentiell für Krankheiten sind. Meine Resultate, in einem Organismus welcher tiefe evolutionäre Verbindungen zu allen Tieren einschließlich zum Menschen teilt, haben signifikante Auswirkungen für das Verständnis von normaler Gebwebshomöostase innerhalb eines Holobionten und von Tumorgenese.

1 Introduction

1.1 Animals evolve in a bacterial world

For 2.1 billion years, microbes were the only form of life on Earth[1]. The first eukaryotes arose likely by the uptake of an archaeon by a bacteria to form the nucleus[1,2], followed by the uptake of other microbes to establish mitochondria[3] and chloroplasts[4]. Further evolution of eukaryotic organisms and emergence of multicellular life was driven not only by changes within the nuclear genome, but by the admission of entire microbes and horizontal gene transfer from bacteria to the host genome as well, forming the metagenome[1,5]. Thus, over millennia, interactions between eukaryotes and microorganisms have shaped the evolution of complex life forms - plants and animals. All extant multicellular organisms contain abundant and diverse microbiota, sometimes outnumbering their hosts in cell number and genomic information volume[1]. Therefore, all organisms can be considered as multispecies associations of a host and billions of microbes – so called metaorganisms[5,6].

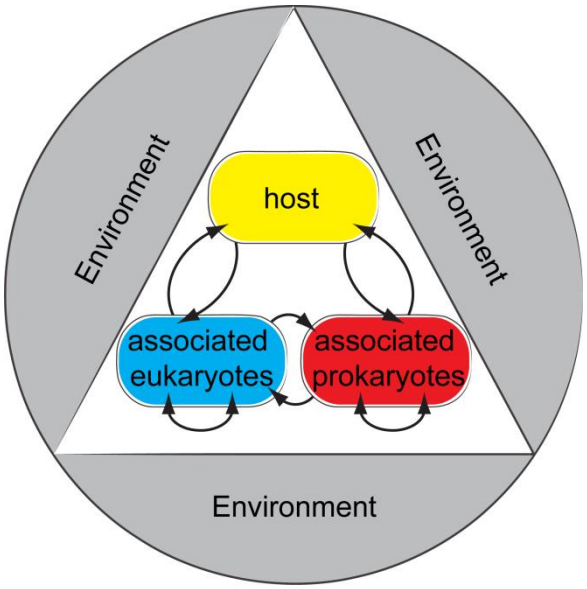

Fig. 1.1: The metaorganism concept. Multicellular organisms are metaorganism encompassing synergistic interdependence with bacteria, archaea, fungi, and numerous microbial and eukaryotic species including algal symbionts on the macroscopic host. (Modified from[5]).

In the recent decade, the interactions between the partners within a metaorganisms were investigated on a broad range of model systems / animal species, from sponges, cnidarians and insects to mouse and the human[5,7]. Collectively, these studies uncovered that a dynamic interplay between the host and its microbiota may affect the host's morphology,

development, behaviour, physiology and resistance to diseases[1,8]. For instance, the microbiome performs some metabolic processes which the hosts cannot carry out themselves, like nitrogen fixation in legumes[9], photosynthesis in corals, molluscs, and sponges[10], or oxidation of inorganic compounds in deep-sea invertebrates[1,11]. Moreover, resident microbes protect animals and plants against pathogens[12,13]. The gut microbiota in humans engage in the production of vitamins and amino acids, breakdown of dietary fiber to short-chain fatty acids, and detoxification of harmful chemicals[14]. Chemical signals from the symbionts trigger organ development[15–17] and patterning[18] in both, invertebrate animals and vertebrates. Studies on vertebrate models highlighted the impact of the microbiome on the nerve system development[19] and the immune system maturation[20]. In spite of these well-documented multifaceted effects that the microbiome exerts onto its host development and physiology, it remains unclear, to what extent do these interactions affect the animal' fitness, life history, and evolution.

1.2 Influence of the microbiome on tissue homeostasis

Emerging studies on mice and human suggest that the microbiome may contribute to maintaining normal tissue homeostasis of the host[21]. On the one hand, the symbiotic bacteria are known to emanate soluble products that support the growth of epithelia in the host. For instance, metabolites produced by the gut microbiota were shown to support the proliferation of the intestinal stem cells[22] and thus contribute to healthy maintenance of the intestinal epithelium homeostasis. On the other hand, multiple observations clearly indicate that a disturbance in the resident microbiota can compromise the tissue homeostasis and the animal's health. Of particular interest is the question, whether changes in the microbiota might disrupt the tissue homeostasis to an extent sufficient to trigger tumor growth and cancer progression[21,23]. Although cancer is recognised as a phenomenon omnipresent in nearly all animal groups[24], little is known about its evolutionary origin and universal principles of tumorigenesis.

Recent studies uncovered that the microbiome is implicated in a remarkably high number of human malignancies[25]: over 20% of tumor cases reported, that equals about 1.2 million cases per year worldwide[26,27], are associated with marked changes in the microbiome. Over 10 members of the human microbiome are currently recognized as triggers of oncogenic transformation in host cells[21]. One of the best-studied bacterium that drives tumorigenesis is *Helicobacter pylori.* It colonizes the human stomach and duodenum and, in some cases, can cause gastric cancer[28,29] and MALT lymphoma[30]. Other known bacteria driving tumorigenesis are *Salmonella typhi*[31,32] linked to gallbladder cancer, *Streptococcus bovis*[33,34] associated with colorectal cancer, and *Chlamydia pneumoniae* involved in lung cancers[35]*.* Collectively,

these bacteria imply multiple molecular mechanisms and target diverse cellular processes – so called hallmarks of cancer[21,36–40] (Fig. 1.2).

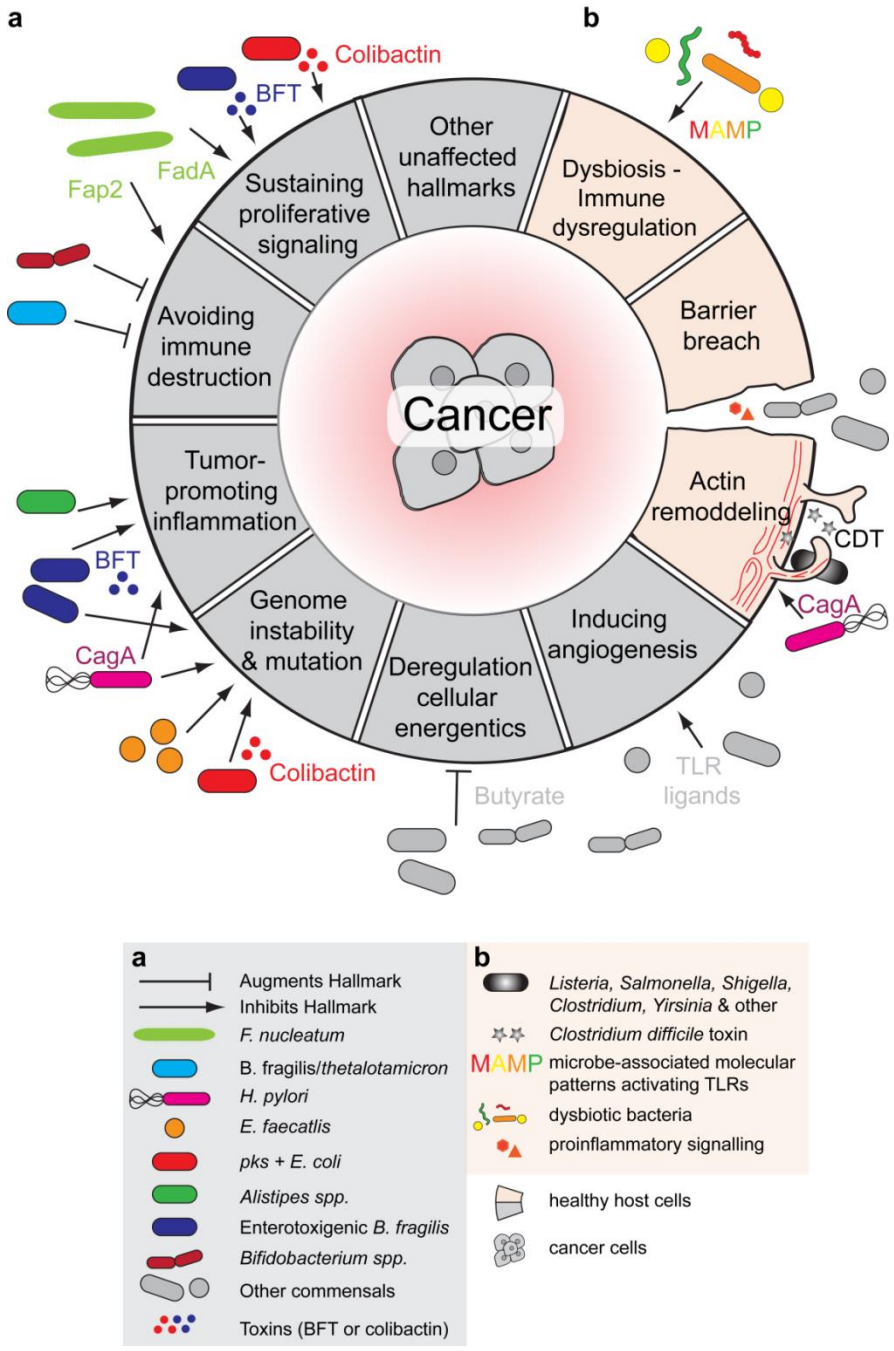

Fig. 1.2: Microbiota-derived signals modulate various cellular processes and interfere with tissue homeostasis through diverse mechanisms to promote carcinogenesis. (a) Microbes deliver a rich toolkit of pathogenicity factors (toxins) into the host cells to interfere with its cellular processes. These effectors modulate *e.g.* the Wnt/β-catenin signaling by activating β-catenin. (b) Dysbiosis and altered microbiota–host interaction can induce carcinogenesis by various mechanisms; increased bacterial translocation and immune dysregulation are shown as examples. (Modified from[41,42]).

Taken together, these findings clearly indicate that microbes are capable of inducing tumorigenesis in mice and humans. However, three important aspects remain virtually unexplored.

First, most of the bacteria with a prominent oncogenic potential are clearly foreign microbes that invade the native host's microbiome. However, accumulating evidence indicates that some members of the normal commensal microbiota may transform within the host and become pathogenic. Such microbes are termed pathobionts[43–45]. Whether and upon what circumstances members of the normal microbiome can become pathogenic and induce tumor formation, remains unclear.

Second, the studies cited above focus on single bacteria as potential inducers of oncogenic transformation and ignore the fact that all microbes form complex communities within their hosts[19,46,47]. Hence, it is conceivable that the microbes interact with their hosts collectively. First observations suggest that it is likely the case. In familial adenomatous polyposis patients (FAP) an interplay between *Bacteroides fragilis* and *Escherichia coli* within the colon mucus promotes cancerogenesis[48]. Whether dynamic interactions within the complex microbiomes can promote tumorigenesis in animals, perhaps - even without a prominent role of single oncogenic bacterium, remains unclear.

Finally, all studies uncovering the role of microbes in tumor formation and progression have been performed on mammalian models – mice and human. However, tumor formation is a universal phenomenon observed throughout the entire animal kingdom. Virtually all animals can develop cancer[24]. What drives tumorigenesis in the groups outside of Mammalia and whether bacteria are also implicated in tumor formation in these species, remains to be uncovered. It is still unclear whether these observations can be generalized to common principles of tumorigenesis. Uncovering these principles and understanding the nature of microbe-driven tumorigenesis may provide essential insights into long-standing questions of cancer biology. Can the exposure to or colonization of specific bacteria prevent or treat certain cancers? What are the critical gene-environmental interactions in cancer susceptibility?[49] Why do specific dietary patterns lead to increased or decreased risk in definite individuals? Why do some medical treatments like chemotherapies, immunotherapies, and preventive drugs fail or succeed for patients, regardless of host germline or cancer genotype? Answering these questions may pave the way to novel approaches to cancer treatment and prevention.

In spite of accumulating evidence for the essential role of bacteria in tumorigenesis, progress in understanding the molecular underpinnings of bacteria-driven tumor growth is hampered

by the complexity of the mammalian systems. The effects of microbes might be indirect and mediated by changes in the host immune system function, nourishment, metabolism of pharmaceuticals[21,50], among others. Additionally, extensive manipulations with the mammalian systems are often limited due to ethical, economical and technical reasons. For instance, the microbial consortia of mammalian intestine are extremely complex[51] and the majority of the gut microbes are actually not culturable[52–54]. These aspects necessitate a use of alternative, less complex animal model systems that are more amenable to experimental manipulations. Additionally, the use of non-mammalian model systems may be informative to trace the role of microbiota in tumorigenesis in the evolutionary perspective. Studying the effects of microbiota onto host tissue homeostasis in phylogenetically distant species that branched of the main vertebrate lineage for hundreds of million years may uncover the most conserved, fundamental principles of host-microbiome interactions.

One possibility to bypass these difficulties is to investigate an organism with lower complexity, including tissue and cell type composition and simple microbial consortia, like the freshwater polyp *Hydra*. This study will reveal insights if the microbiome interferes with the cell homeostasis of a host.

1.3 The *Hydra* holobiont

The freshwater polyp *Hydra* is a multicellular animal of the Cnidarian phylum, which includes solely water-born organisms like the sea anemones, jellyfish and corals. Cnidarians diverged from the Bilateria lineage over 650 Mya[55] and thus allow deep insights into the very early evolutionary history of multicellular animals (Fig. 1.3).

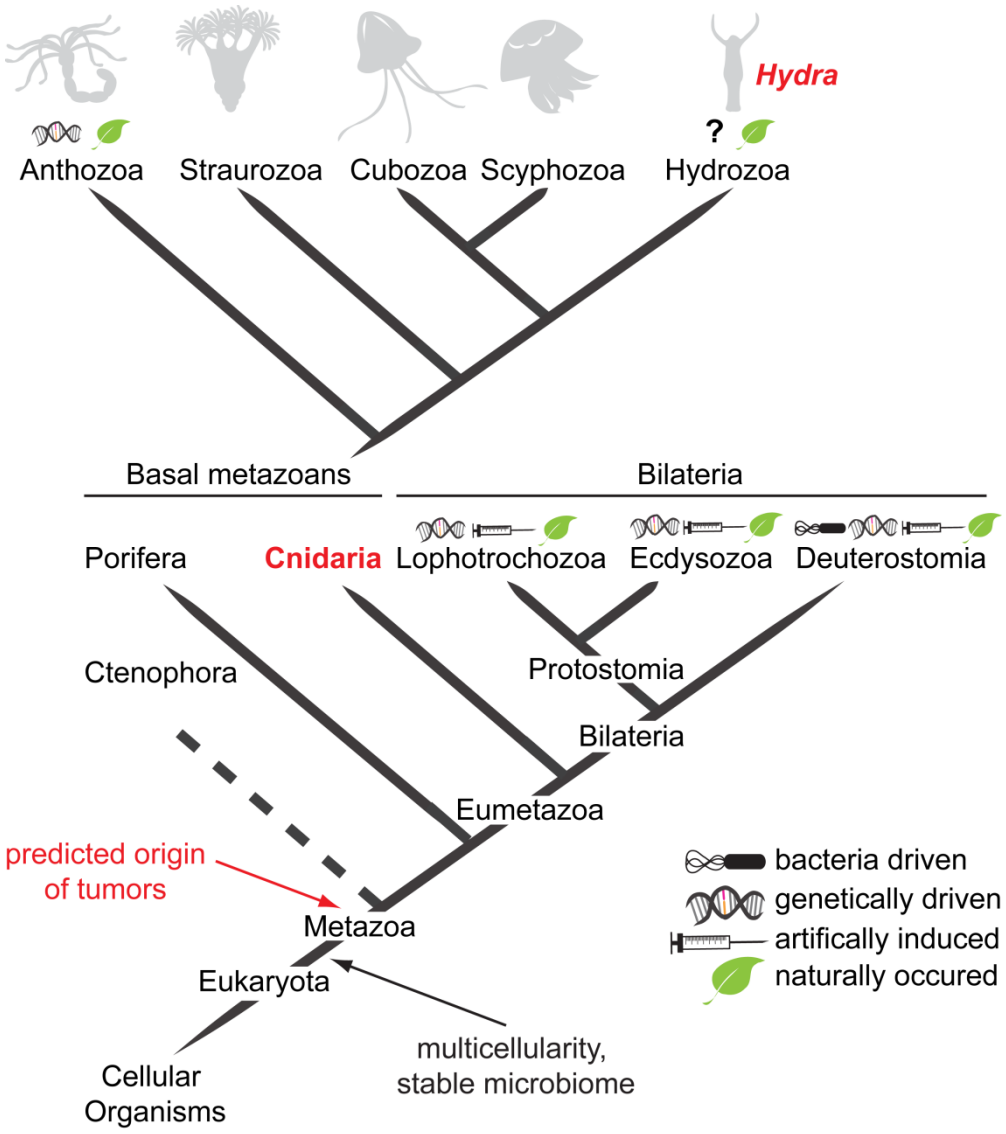

Fig. 1.3: Schematic phylogenetic tree showing main branches of metazoan evolution. The position of Cnidaria is inside the group of pre-bilaterian metazoans. The Cnidaria clade consists of five branches, including Anthozoa, Straurozoa, Cubozoa, Scyphozoa and Hydrozoa. *Hydra* is a multicellular freshwater polyp belonging to the Hydrozoa. (Modified from[56]). For some branches the occurrence and the genesis of cancer cases has been reported. (Modified from[13]). Phylostratic analyses of genes associated with cancer in humans points to their early evolutionary emergence. The evolutionary origin of animal tumors is predicted to the of metazoan tree[57]. The question mark proximate to *Hydra* highlights the unknown etiology of this tumor occurrence which is going to be targeted in this work.

Cnidarians are distinguished from the Porifera and Placozoa by the possession of true tissues joined by cell-cell contacts like tight junctions, and of a nervous system[58–60]. The polyp *Hydra* belongs to the Hydrazoa class and is characterized by absence of a free-swimming medusa stage in the life cycle and by populating exclusively freshwater habitats. Multiple species of *Hydra* are currently used in the labs worldwide. This study focuses on one *Hydra* species, *H. oligactis*, which encompasses the following features:

All *Hydra* species show a remarkably simple body plan and tissue composition. The body of an adult *Hydra* polyp represents a hollow tube of about ~1 cm in length with a head (hypostome with a ring of 6 to 8 tentacles) at the apical end and a foot with a basal disc at the other, with which it attaches to the ground[61,62]. An adult *Hydra* polyp is composed of $\sim 10^5$ cells belonging to less than twenty different cell types[63,64] that are derived from only three stem cell lineages[65,66]. These proliferating stem cells are subsequent induced to undergo specifically regulated differentiation events.

All cell types in a *Hydra* polyp are derived from either of three stem cell lineages: ectodermal and endodermal epithelio-muscular cells and interstitial stem cells[66]. The ectodermal and endodermal epithelio-muscular cells form the body of a polyp and are accountable for all morphogenetic processes[67]. The structure and morphological appearance of the polyps is defined by the epithelial cells[67] and by the actin cytoskeleton organization[68]. Within each of the epithelial layers, the actomyosin cytoskeleton forms cortical networks as well as comprehensive cellular networks of contractile fibers, which span the whole organism. Near the basal side of each layer, these actomyosin fibers are organized along the animal axis in the ectoderm and in a perpendicular (circumferential) direction in the endoderm[69]. Moreover, the actin cytoskeleton interferes with biochemical signaling pathways[70], gene expression[71], cell fate[72], and the reproduction[73] of *Hydra.*

The two epithelial layers are separated by an elastic extracellular matrix (ECM), termed mesoglea (Fig. 1.5). The mesoglea is mainly composed of type IV collagens, laminins, fibronectins, and heparin sulfate proteoglycans[74,75]. Accumulating evidence indicates, that the proper organization of the ECM, it's molecular composition, elasticity, and renewal are essential for correct morphogenetic processes in the polyp. Disruption of the ECM structure results in grave morphological abnormalities of *Hydra*[68,69,76].

Under favorable and stable environmental conditions, *Hydra* reproduces asexually by budding. Here, a new organism develops from an outgrowth of cells. Since budding is the main mode of *Hydra* population expansion, the frequency of bud initiation and rate of bud detachment are directly linked to the population survival and thus are reliable proxy for the

polyp's fitness. Changes of environmental conditions, such as temperature and feeding regime, trigger the gametogenesis, i.e. mitotic proliferation and differentiation of mature gametes from multipotent interstitial stem cells[66,77]. Obviously, rate of gamete production (fecundity) and number of viable embryos (fertility) are also reliable indicator of the polyp's fitness[73,78,79].

Every *Hydra* species is associated with a species-specific and stable multispecies microbial community[80]. The tools to characterize this microbial community by 16S rRNA sequencing and to manipulate it *e.g.* by obtaining pure cultures of germ-free polyps and re-colonization with single isolates or complex consortia, exist[81,82]. The majority of these bacterial colonizers are present on the surface of a polyp. They colonize the glycocalyx - a multilayer mucus covering the outside surface of the ectoderm[83,84]. It is a carbohydrate-rich layer[85] with constantly renewed transmembrane glycoproteins, proteoglycans, and glycolipids[84,86]. The outer surface of *Hydra* is colonized by a specific bacterial community. In some cases, however, bacteria may colonize the mesoglea of diverse *Hydra* species[87] or occur intracellularly[88] (Fig. 1.3). In stark contrast to the mammalian systems, the microbiota in *Hydra* is very simple, composed of only a dozen of species, most of which are culturable[83]. Interestingly, the composition of the microbiota associated with different *Hydra* species mirrors the phylogenetic relatedness between their host species[80]. This strongly suggests highly-specific intricate interactions and a long-term coevolution between the hosts and their associated microbiota[80]. The stability of these interaction suggests that *Hydra* and its associated bacteria achieved a balanced, mutually beneficial state, and thus allows considering this microbiota as commensal microbiota[89–91] (Fig. 1.4).

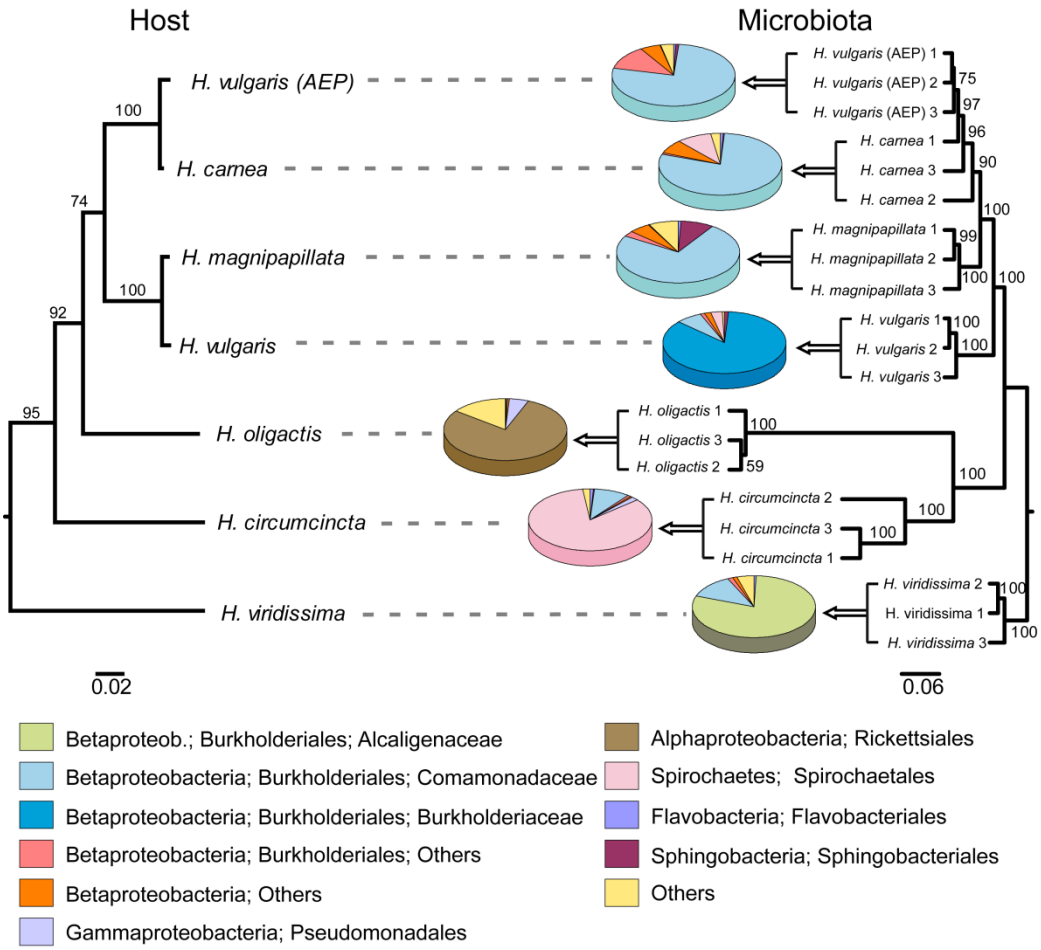

Fig. 1.4: *Hydra* species are colonized by a specific microbiome. (Left) Phylogenetic tree of *Hydra* species. (Right) Phylogenetic tree of 21 environmental bacterial communities from seven *Hydra* species. Pie charts represent mean relative abundance of bacterial orders. The phylogenetic tree of *Hydra* resembles the phylogenetic relations of the associated microbiomes. (Modified from[80]).

The colonization of *Hydra* polyps with bacterial symbionts occurs in the early embryonic development and establishes a robust and reproducible pattern[80]. During asexual reproduction a consortium of bacteria colonizing the budding region of the mother polyp is passed on to the detaching bud, keeping a stable bacterial composition in *Hydra*[92]. Further, throughout the entire lifecycle *Hydra* actively shapes it's microbiome via secretion of a complex mixture of antimicrobial peptides[80,93,94] or by interfering with the quorum sensing signals of the bacteria[95]. Importantly, a *Hydra* polyp demonstrates a remarkable resilience and can effectively re-establish a normal species-specific microbiome after a major disturbance, such as antibiotic treatment[96]. Under steady laboratory conditions, the microbiome of *Hydra* remains remarkably stable, and does not change for decades[92].

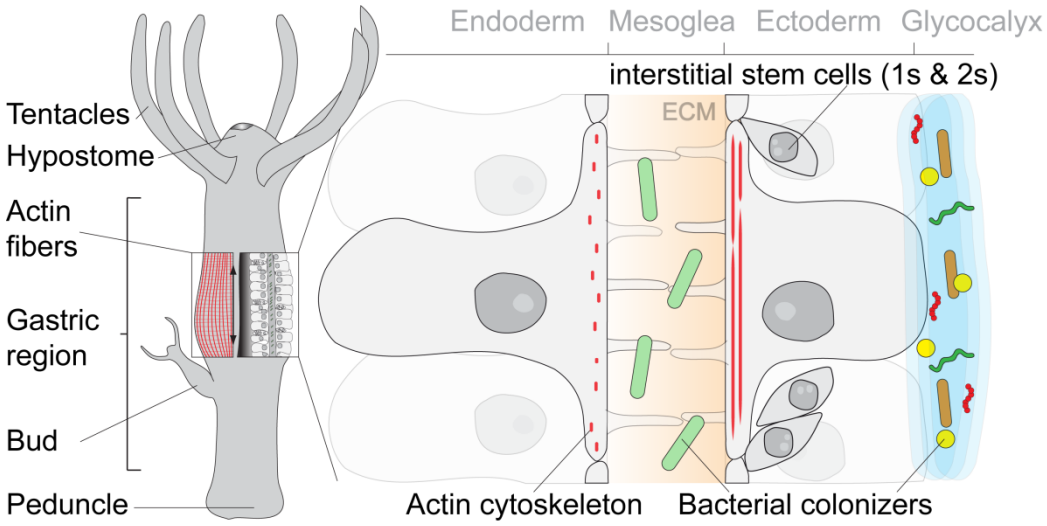

Fig. 1.5: *Hydra* body plan and bacterial colonization. (Left) Schematic representation of a *Hydra* polyp consisting of a head with a hypostome and ~6 tentacles, a gastric region, and a peduncle. *Hydra* polyps normally reproduce asexually by budding. The actin fibers are arranged in a parallel pattern from peduncle to head. (Right) The tissue consists of two epithelial cell layers, the ectoderm and the endoderm, separated by the extracellular matrix (ECM). Interstitial stem cells (1s & 2s) are located in the ectoderm. Bacteria mainly colonize the glycocalyx and the mesoglea/extracellular matrix (ECM).

Once established, a species-specific bacterial consortium exerts diverse beneficial effects onto its host. Recent studies uncovered in the *Hydra* microbiome two bacterial species that provide, likely in a synergistic manner, antifungal protection to their host[83]. Moreover, bacteria interact with the neural activity of the host and promote regular spontaneous body contractions[97], as well as the production of antimicrobial peptides in *Hydra*[94]. Taken together, the observations clearly indicate that the multicellular host *Hydra* and its specific microbiota form a holobiont, which functions, reproduces, and responds to the environmental changes as one entity[98–100].

In sum, the freshwater polyp *Hydra* represents a strategic model to study the host-microbiome interactions. Its simplicity and experimental accessibility allows combining the both, mechanistic insights into complex biological phenomena and a holistic understanding of the entire biological system. This system seems particularly useful for addressing the role of commensal bacteria in the normal tissue homeostasis. The recently described naturally-occurring tumors in *Hydra*[101] may be instrumental in these studies, since the tissue homeostasis is evidently disturbed in these polyps.

1.4 Naturally occurring tumors in *Hydra*

The pathways involved in tumorigenesis are well studied in vertebrates[102], although their evolutionary origin remains unknown. So far, first systematic studies on the occurrence of tumors in invertebrates have been taken[24,103]. Occasional cases of growth abnormalities in phylogenetically basal organisms, like sponges and cnidarians[104,105], have been long reported. Only recently naturally-occurring tumors have been identified in *Hydra* and systematically investigated on cellular and molecular level[101].

Spontaneous tumor formation occurred independently in two species of *Hydra: H. oligactis* and *Pelmatohydra robusta*[101]. Histological, cellular and molecular data revealed that these tumors originated by a differentiation arrest of female germline precursor cells (GCII, Fig. 1.6a-d). In stark contrast to normal temperature-induced oogenesis[79,106], the accumulation of these cells occurs without any environmental trigger, and they are neither able to terminally differentiate into oocytes and nurse cells, nor eliminated by apoptosis[101]. Additionally, tumor formation results in significantly reduced fitness measured by decline in asexual bud production (Fig. 1.6e). The morphological and developmental alterations are reflected in an altered transcriptome of the tumorous polyps, which mimics expression shifts in vertebrate cancers[101]. The presence of aberrant germline cells which proliferate, migrate but do not differentiate[101], the drastic fitness decrease, and the developmental changes, define per definition from the National Cancer Institute (NCI) this type of tumor as a malignant tumor of a precancerous state, termed as dysplasia. Hereinafter, for simplicity further referred as tumor.

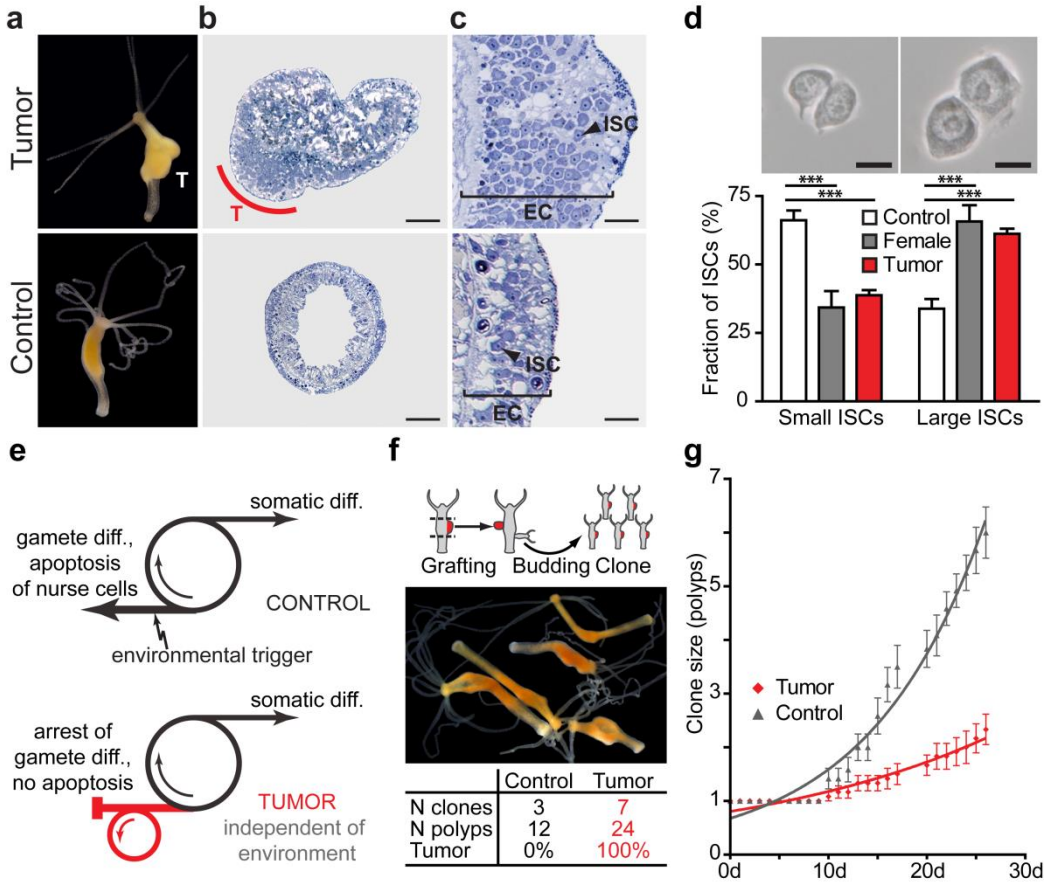

Fig. 1.6: In *Hydra*, uncontrolled proliferation and arrest of differentiation of germline interstitial stem cells causes tumor formation and compromises polyps fitness. (a-d) The morphology of tumorous (Tumor) polyps of *H. oligactis* is disturbed by an accumulation of aberrant germline precursor cells (ISCs) which accumulate in the ectoderm. (scale bar: 50 µm; scale bar: 15 µm). (e-f) In tumor tissue, ISCs become committed to germline differentiation independently of environment, their maturation is arrested, and the cells are not eliminated by apoptosis. These aberrant ISCs are transplantable into a healthy host (experiment outline, top) and induce new tumors in the recipient polyps and in their clonal progeny. (g) Growth curves for tumor and control *P. robusta* cultures demonstrate tumor impact on population growth rate; exponential fit curves. (Modified from[101]).

While the study of Domazet-Lošo and co-authors[101] provided a detailed description of the tumorous phenotype in *Hydra*, the etiology of this tumor formation remained uncertain. It is still unclear, what event has triggered the formation of tumor in the founder polyps. Taking into consideration the essential role of the microbiome in physiology and development of *Hydra* and other animals, and the holobiont paradigm, it is conceivable to consider the driving role of microbiota in the tumor formation in *Hydra*. We hypothesized that the changes in *Hydra*-associated microbiome might have induced the tumorigenesis. In my study, I characterize only one of the previously described lines of tumor-bearing *Hydras* – the *H. oligactis* strain.

For decades, it has been widely accepted that cancer is driven by changes in the genome of an animal cell. In the recent years, however, the leading role of environment and especially the microbiome in tumorigenesis of mammals is being increasingly recognized[21,41,42,107–109]. To which extend do commensal bacteria protect or disturb the cell homeostasis in their hosts? What is the relative contribution of the resident microbiome and the environmental bacteria to tumorigenesis in the animal kingdom? What are the molecular mechanisms utilized by bacteria to interfere with the tissue homeostasis of the multicellular animals? Answering these questions promises a paradigm shift in our understanding of cancer. In this thesis, I attempt to address these questions by investigating the causal relationship between the host, its specific microbiome, and the environmental bacteria in an experimentally accessible system of tumor-bearing *Hydra oligactis*.

1.5 Aims and objectives

All animals, from the ones as simple as *Hydra* to the most complex like man, are prone to tumorigenesis[24,101,110,111]. Studying the cancer instances in the evolutionary distant groups from Bilateria, such as Cnidaria[112], may provide insights into the fundamental mechanisms of tumor growth and the factors eliciting it.

Naturally occurring tumors have been previously described in the basal metazoan *Hydra*[101], however their etiology remained unclear. Here, I investigate the cellular and molecular processes underlying the tumor formation in *Hydra* with a special focus on the role of the microbiome. I hypothesize that the changes in *Hydra*-associated microbiome may trigger tumorigenesis. In order to test this hypothesis, I address the following questions:

1. What is the phenotype of the tumorous polyps? A thorough characterization of the tumorous phenotype is essential for evaluating the putative effects of microbiota on the tumor development.
2. Is the microbiome in tumorous polyps changed in comparison to healthy control polyps?
3. Is an alteration of the microbiome (dysbiosis) sufficient to elicit tumorigenesis in *H. oligactis*?
4. What are the putative molecular mechanisms of the bacterial members which interfere with the tissue homeostasis in *Hydra*? What molecules do bacteria exploit? What molecular pathways are bacteria acting on to cause tumorigenesis in *Hydra*? Do the commensal bacteria protect or disturb the tissue homeostasis?

2 Results

2.1 Detailed phenotype characterization of tumorous *Hydra oligactis*

The overall phenotype and fitness of the tumor-bearing *Hydra* polyps have been previously described[101]. However, in order to evaluate the putative effects of microbiota on the tumorigenesis, a set of strictly defined, ideally – measurable quantitative parameters have to be developed. Therefore, I extended the phenotype description in more detail by adding a few additional parameters. First, I compared the number of tentacles in tumorous and healthy polyps (Fig. 2.1). Surprisingly, the average number of tentacles per polyp was almost doubled in the tumor-bearing polyps compared to controls (Fig. 2.1e). While healthy polyps typically have 6-8 tentacles, a tumorous *Hydra* carry up to 20 tentacles. Remarkably, tumorous polyps demonstrate much higher variance in the number of tentacles. In *Hydra*, the number of tentacles and pattern of their emergence are species-specific traits and are strictly genetically controlled[62,113]. Therefore, our results clearly indicate a loss of a robust tentacle number control in tumorous polyps and therefore suggest, that tumorigenesis gravely affects morphogenesis.

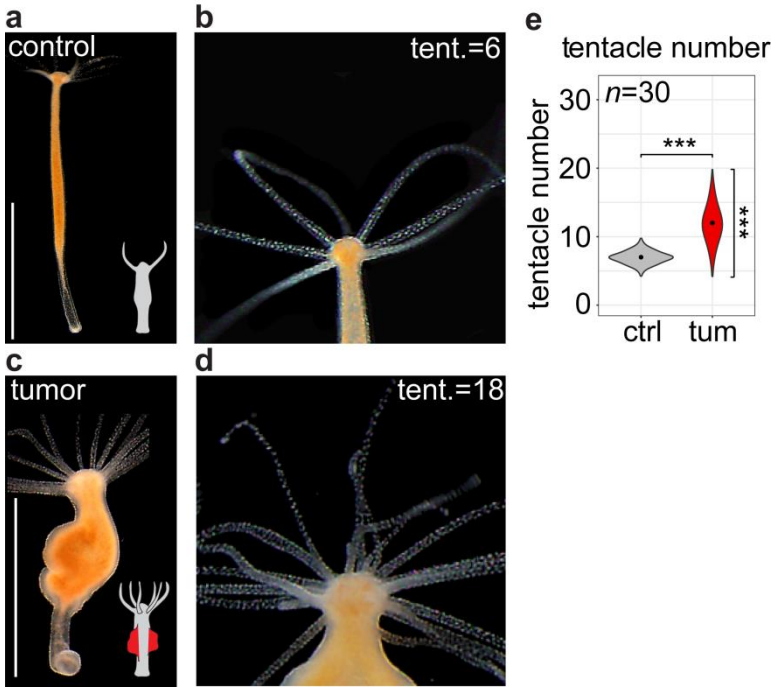

Fig. 2.1: *H. oligactis* tumor polyps demonstrate an altered morphology and increased number of tentacles. (a) Control polyps have a tube shaped body column (right; pictogram of a healthy control polyp used further throughout my thesis) and (b) have typically 6 tentacles (scale bar: 5 mm). (c) Tumor polyps reveal conspicuous tissue bulges in the middle gastric region. (d) The hypostome of a representative tumor-bearing polyp is surrounded by about 18 tentacles. (e) The number of tentacles is significantly increased in tumorous polyps compared to controls (*n*=30; ***:p ≤ 0.001.). The variance between control and tumorous polyps differs significantly (***: p=0,00054).

Furthermore, the number of epithelial cells per polyp was substantially increased in tumorous polyps (Fig. 3.2a). In the tumorous strain a doubled number of epithelial cells per polyp were detected compared to healthy controls. Similarly to the tentacle number, the dispersion of the cell counts was also high in tumorous polyps. Since number of cells per polyp is strictly controlled by highly conserved genetic programs[63,114,115], this observation provides an additional evidence for tumor growth to disrupt normal polyp morphogenesis. Additionally, the thickness of the mesoglea in tumorous polyps more than doubles compared to control polyps (Fig. 2.2b). There is an increase in the variety of epithelial cells in tumor polyps and in the variety of the thickness of the mesoglea in tumorous polyps. This could assume a further indication for the disruption of the tissue homeostasis in tumor polyps.

The bulgy appearance of the tumorous polyps was due to not only the increased number of cells, but to altered extracellular components as well. Morphometric analysis of histologic sections (Fig. 2.2c,d) uncovered that the mesoglea thickness was significantly increased in the tumorous polyps compared to controls (Fig. 2.2b). Since the mesoglea is mainly produced by the epithelial cells of *Hydra*[74], it is plausible that its increased thickness is a direct effect of elevated number of epithelial cells in tumorous polyps. Moreover, since the molecular composition of mesoglea and its structure are essential for proper growth and differentiation in *Hydra*[69,74,75], the severe disturbance of mesoglea structure observed in tumorous polyps points to more general detrimental effects onto the polyp's morphogenesis.

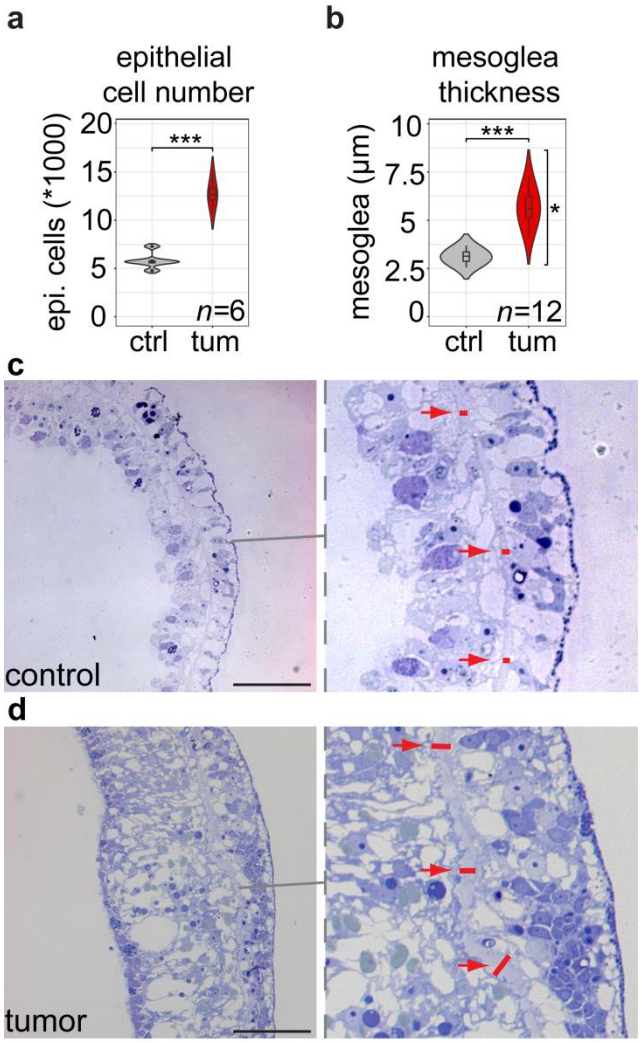

Fig. 2.2: Tumor growth results in increased epithelial cell number and mesoglea thickness. (a) Epithelial cell number doubles in tumorous polyps compared to control polyps (*n*=6) but shows no difference in the variances between control polyps and tumorous polyps (p=0.3022). (b) Thickness of the mesoglea doubles in tumorous polyps compared to control polyps (*n*=12). The variance in mesoglea thickness is significantly higher (p=0.0232) in tumorous polyps than in healthy controls. *:p ≤ 0.1, ***:p ≤ 0.001. **Cross-sections thorough polyp body column demonstrate increased mesoglea thickness in tumorous polyps.** (c) In control polyps, mesoglea forms an evenly thin layer of ~3 µm between the ectodermal (ecto) and endodermal (endo) epithelial layers. Scale bar: 50 µm. (d) In tumorous polyps, mesoglea thickness is substantially increased (~6 µm) and varies visibly. In both cases the mesoglea is highlighted by red arrows and lines were the mesoglea thickness has been counted (scale bar: 50 µm).

As previously reported[101], tumorous polyps are characterized by decelerated asexual growth by budding. To get a quantitative measurement of the growth, I first recorded the cumulative number of buds produced over four weeks by a clone of *Hydra*. Consistently with the earlier observations[101], the tumorous polyps demonstrated a reduced growth rate (Fig. 2.3a). Further, from the population growth curves I derived the time necessary for a polyp to develop and detach a bud (for convenience referred to as the detachment time). In the tumorous polyps the bud detachment time was significantly higher compared to healthy controls (Fig. 2.3b). This indicates that in spite of higher number of cells per polyp the growth

of tumorous polyps is gravely impaired. Since the process of bud initiation, outgrowth and detachment is hard-wired by distinct molecular pathways[116], our observations provide evidence that tumorigenesis interferes with profound genetic programs in *Hydra* cells.

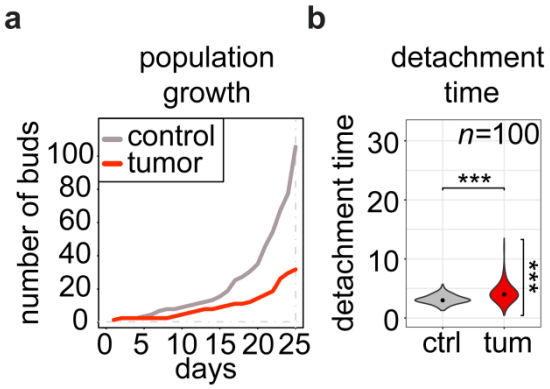

Fig. 2.3: Tumor growth initiates decelerated population growth and prolonged detachment time. (a) Population growth analysis reveals significant decrease in number of buds produced by tumorous polyps compared to control polyps. (b) Bud detachment from tumor polyps is delayed compared to control polyps (*n*=100). The within-group variance differs significantly between control and tumorous polyps ($p=2.2e^{-12}$). ***:$p \leq 0.001$.

The shape of a *Hydra* and some of its morphogenetic processes are defined not only by the epithelial layers and the mesoglea between them[74,117,118], but by the actin cytoskeleton within the epithelial cells as well[68,69,78]. This stimulated us to analyse whether actin cytoskeleton organization is altered in the tumor-bearing polyps. Detection of actin filaments using phalloidin-rhodamine conjugate and confocal microscopy revealed that in control polyps actin fibers are located in a highly organized parallel pattern. Consistently with earlier observations[68], the actin filaments in the ectoderm stretch along the oral-aboral axis of a polyp, while in the endoderm they run circumferentially (Fig. 2.4a). In the tumorous polyps this regular pattern is disorganized, particularly in the regions of the tumor bulges (Fig. 2.4d).

Another essential symptom of tumor formation in *Hydra*, the accumulation of aberrant female germline cells (GCII-cells), was previously described[101]. In my experiments, the presence of aberrant cells in tumor polyps was consistently reproduced. Immunocytochemistry with an antibody against the periculin protein, known to label *Hydra*'s female germline precursor cells[93], revealed numerous periculin-positive aberrant interstitial cells in the tumor tissue (Fig. 2.4e) while control polyps had few if any of GCII-cells in the gastric region (Fig. 2.4b,c). These cells occur in clusters but can also separate, spread, and invade healthy tissue and migrate into a growing bud[101]. Whole mount images of tumor polyps highlight large clusters of this cell type (Fig. 2.4f).

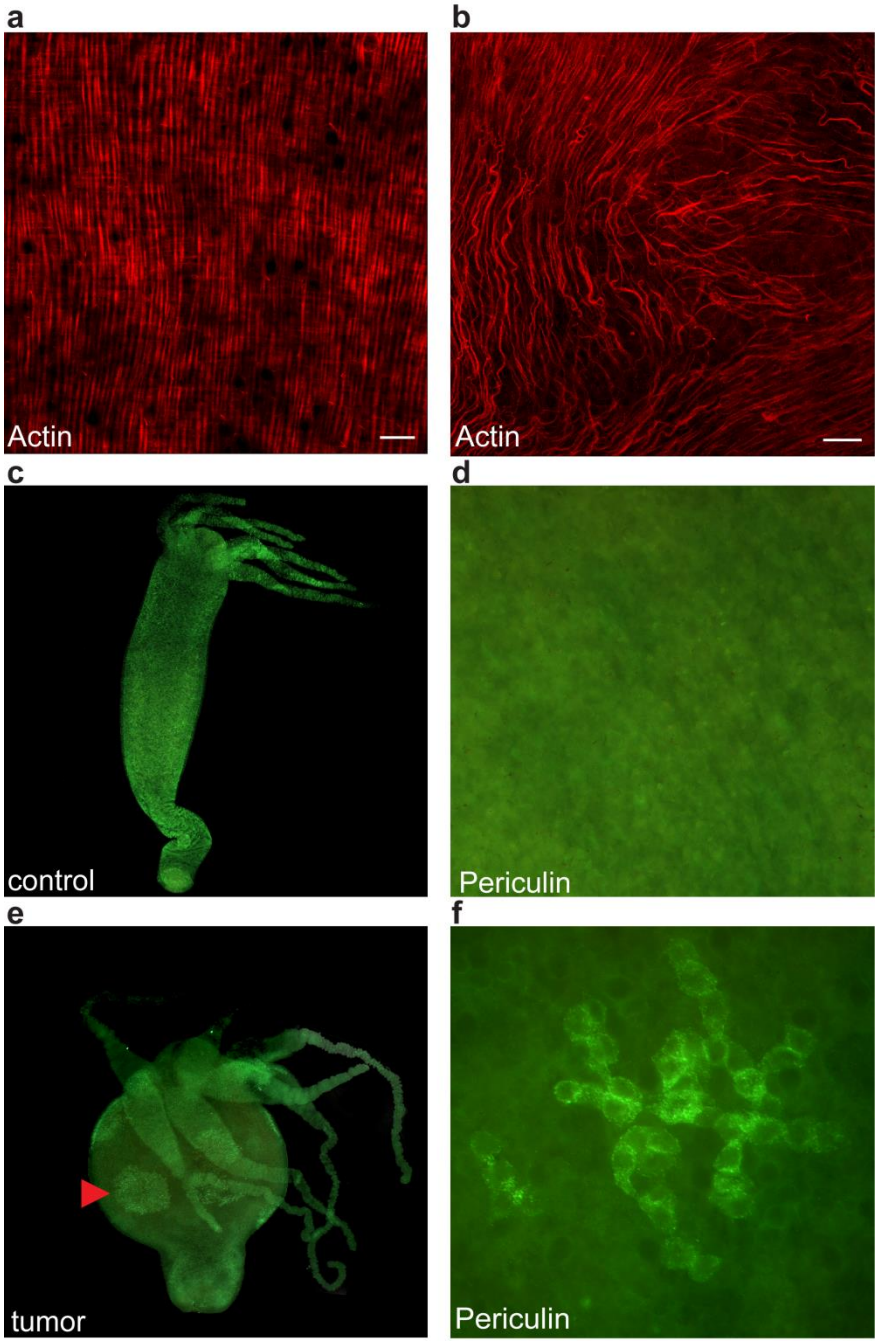

Fig. 2.4: Disturbed tissue homeostasis in tumor polyps. (a) The actin fibers in the epithelial cells are organized in a parallel pattern along the directive (oral-aboral) axis of a polyp (scale bar: 10 µm). (b) Tumor polyps show disorganized actin fibers in the regions of tumor bulges. (c) Under stable environmental conditions, healthy control polyps reproduce asexually and don't show clusters of periculin-positive female germline cells. (d) Close up of a control polyp showing no periculin-positive cells. (e) Whole mount immunocytochemistry staining of a tumorous polyp showing multiple clusters of germline precursor cells (red arrow). (f) Close up of a female germline precursor cell cluster in the gastric region.

Taken together, I identified several new quantitative characteristics of tumor growth: increase in epithelial cell number, mesoglea thickness, and tentacle number. These along with the disturbance of the actin cytoskeleton and the occurrence of aberrant female germline precursor cells can be used further to evaluate the effects of microbiota on tumor growth.

2.2 Microbiome of tumor polyps is dominated by Spirochaetes

Our observations clearly indicate that tissue homeostasis of the both, epithelial and interstitial cell lineages in *Hydra,* is gravely disturbed in tumorous polyps. Since the tissue homeostasis and microbiota composition in *Hydra* are in a mutual interdependence[96,98], I hypothesized that the bacterial community might be altered in the tumorous polyps. To test this hypothesis, I compared the microbiome of tumorous and healthy polyps by 16s rDNA sequencing and computational analysis, and validated the findings using confocal and electron microscopy.

The 16s rDNA sequencing revealed that the microbiota of healthy polyps is dominated by gram-negative bacteria of Pseudomonadales order (Fig. 2.5). In fact, a single bacterium, OTU750018, that can be assigned to the *Pseudomonas* genus (Fig. 2.5c/d), makes up 78% of total bacterial abundance on control polyps. The second dominant group (21% relative abundance) was represented by several species of Sphingobacteriales order, while members of other orders were poorly represented and collectively made up 1% of microbial composition. In the tumorous polyps the abundance of Pseudomonadales OTU750018 was greatly reduced to ~9% (Fig. 2.5b). Instead, bacteria of Leptospirales order dominated (51%) the microbiota of tumor-bearing polyps. Remarkably, this group was actually represented by a single bacterium with characteristic OTU4017244 sequence that can be identified as *Turneriella* bacterium belonging to the Spirochaetes phylum (Fig. 2.5b). The relative abundance of Sphingobacteriales microbes (27%) in the microbiome of tumorous polyps was similar to that of healthy controls. Interestingly, bacteria of other taxonomic groups, poorly represented in control polyps (such as Burkholderiales), greatly expanded in the tumor context.

These findings were statistically supported by LEfSe analysis. The *Pseudomonas* OTU750018 and its higher rank taxonomic categories up to the Proteobacteria phylum were strongly underrepresented in the tumorous polyps compared to controls (Fig. 2.5c). The *Turneriella* OTU4017244 and all the ranks up to Spirochaetes phylum were strongly enriched in the tumorous polyps (Fig. 2.5c). Additionally, two microbes, represented by OTU89333 and OTU59, both belonging to the Comamonadacea phylum, were also enriched in the tumor-bearing polyps compared to control, yet with lower statistical support (Fig. 2.5d).

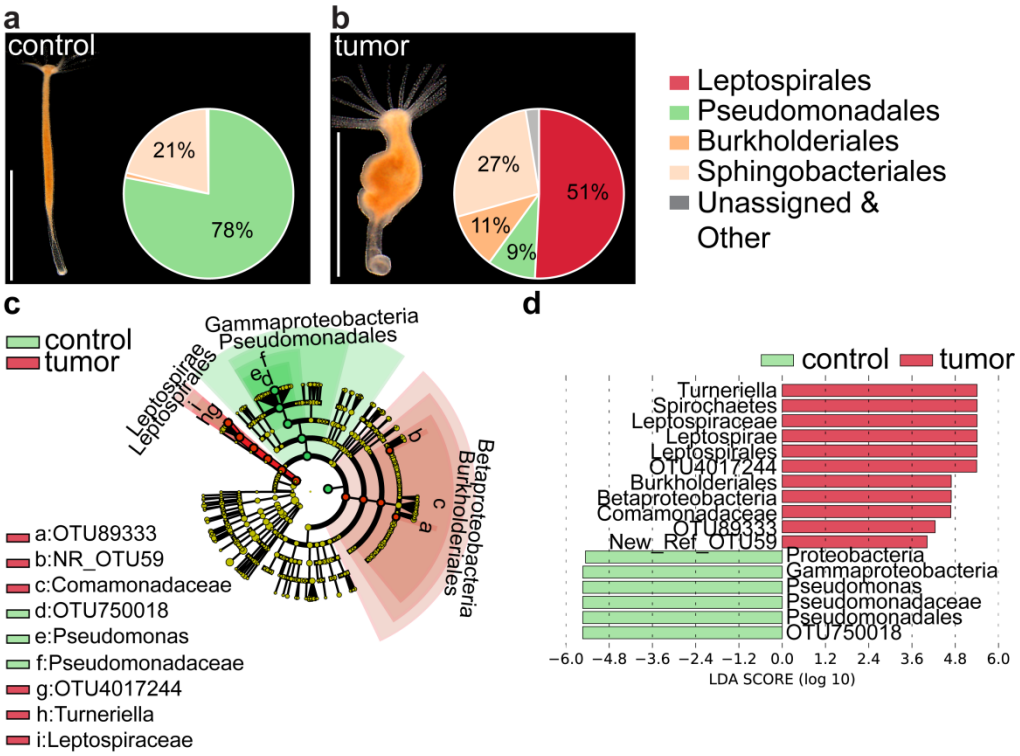

Fig. 2.5: Microbiota of tumor polyps is dominated by the presence of Spirochaetes. (a) Control polyps (scale bar: 0.5 cm) are mainly colonized by two bacteria orders the Sphingobacteriales and the Pseudomonadales. Relative abundance of bacteria estimated using 16s rDNA profiling and resolved at order level (b) The 16s rDNA sequencing of the tumor-bearing polyps. Tumor polyps are colonized by a new bacteria order Leptospirales, while the relative abundance of Pseudomonadales decreases drastically (scale bar: 0.5 cm). (c) Taxonomic cladogram presenting OTUs differentially represented in the microbiota of control and tumor polyps generated using LEfSe analysis; red - taxa enriched in tumor polyps; green – taxa enriched in healthy polyps and under-represented in tumorous polyps. (d) The enrichment of certain taxa in tumor polyps is statistically supported by high positive LDA (linear discriminant analysis) score values (red), and the taxa strongly enriched in control polyps are supported by negative score values (green).

Consistently with these findings, microscopic analysis uncovered dramatic changes in microbial colonization associated with tumor growth. Our preliminary analysis indicated that *Pseudomonas* inhabits the mesoglea of healthy polyps. Therefore, I isolated the mesoglea from the attached epithelial cells like it was performed earlier[119]. In addition, I performed a SYBR-gold staining of bacteria on the isolated mesoglea. In control polyps, a highly abundant rod-shaped bacterium was consistently detected in the extracellular matrix (ECM) (Fig. 2.6a-d) The appearance of these rod-shaped bacteria was very homogeneous and no other morphotypes of bacteria were detected in the ECM of healthy polyps. This bacterium was further isolated from the mesoglea into a pure culture. Sequencing of 16s rDNA from the isolate confirmed this bacterium a *Pseudomonas* OTU750018.

The rod-shaped bacteria were also present on the mesoglea of tumor polyps yet at substantially lower density. In contrary, the ECM of tumor polyps was mainly colonized by numerous helically-coiled bacteria (Fig. 2.6e-h), and the rod-shaped microbes were scarcely

found in the mesoglea (Fig. 2.6g). The presence of the spirochaetes was proven by PCR and sequencing of the 16s rDNA (data not shown).

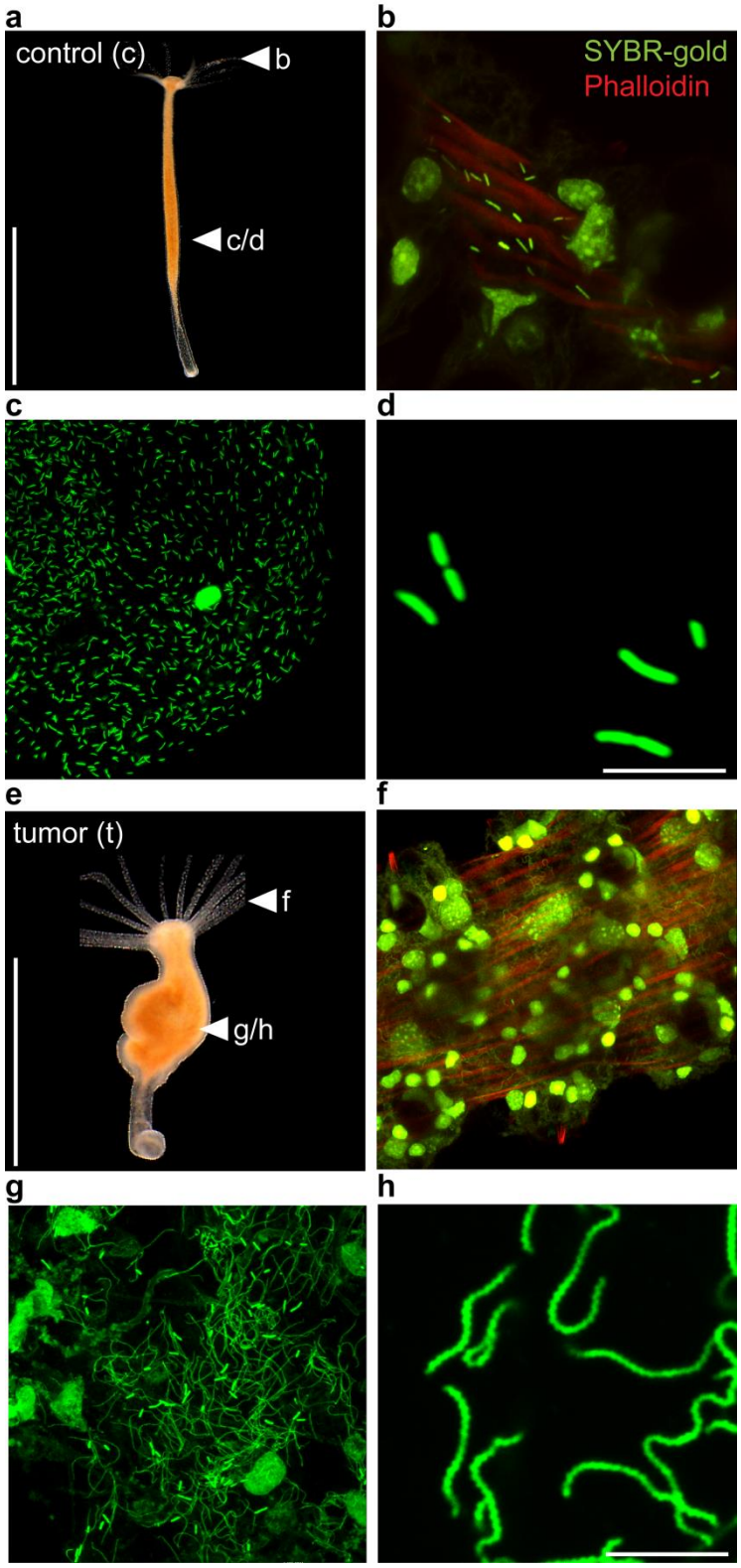

Fig. 2.6: The mesoglea of tumorous polyps is colonized by *Pseudomonas* and spirochaetes. (a) Whole mount image of a *H. oligactis* control polyp (scale bar: 0.5 cm) (white arrows point to investigated regions). *Pseudomonas* colonizes the entire mesoglea of healthy control polyps including (b) the tentacles and (c) the gastric region. (d) Close up of rod-shaped *Pseudomonas* bacteria

colonizing the *Hydra* ECM (scale bar: 5 µm). (e) Whole mount image of a tumor polyp (white arrows point to the investigated regions). In tumor polyps (scale bar: 0,5 cm) the mesoglea including (f) tentacles and (g) the gastric region is densely colonized by helically-coiled spirochaetes while the density of *Pseudomonas* markedly decreases. Importantly, *Pseudomonas* and spirochaetes are found in close proximity. (h) Close up of an area of the mesoglea only colonized by spirochaetes (scale bar: 5 µm).

In order to confirm the presence of the both bacteria on the ECM at higher resolution, I performed transmission electron microscopy (TEM) of ultrathin cross sections of control and tumor polyps. Consistently with the confocal microscopy results, TEM analysis revealed the presence of *Pseudomonas* on the entire ECM of healthy polyps (Fig. 2.7). Rod-shaped bacteria were indeed localized within the fiber-rich mesoglea layer between two epithelia. Interestingly, every cross section of a *Pseudomonas* cell was surrounded by an electron-transparent area free of ECM fibers (red arrows; Fig. 2.7a/b), suggesting that *Pseudomonas* may digest the ECM. In addition, the outer surface of each *Pseudomonas* cell was covered with electron-dense droplet-like structures (red arrows; Fig. 2.7c-f). Such single (Fig.3.8.c) or concatenated (Fig. 3.8d/f) structures were found in direct proximity to the bacterium's outer membrane (Fig.3.8c/d) or detached from the surface (Fig.3.8e). Overall, the localization and appearance of these structures strongly suggests that they represent outer membrane vesicles (OMVs). Formation of similar structures is frequently reported in diverse gram-negative bacteria, including the related species of Pseudomonas – *P.aeruginosa*[120]. The substances released by means of OMVs are known to digest the bacteria environment or even affect the host cell by releasing toxins[121–123].

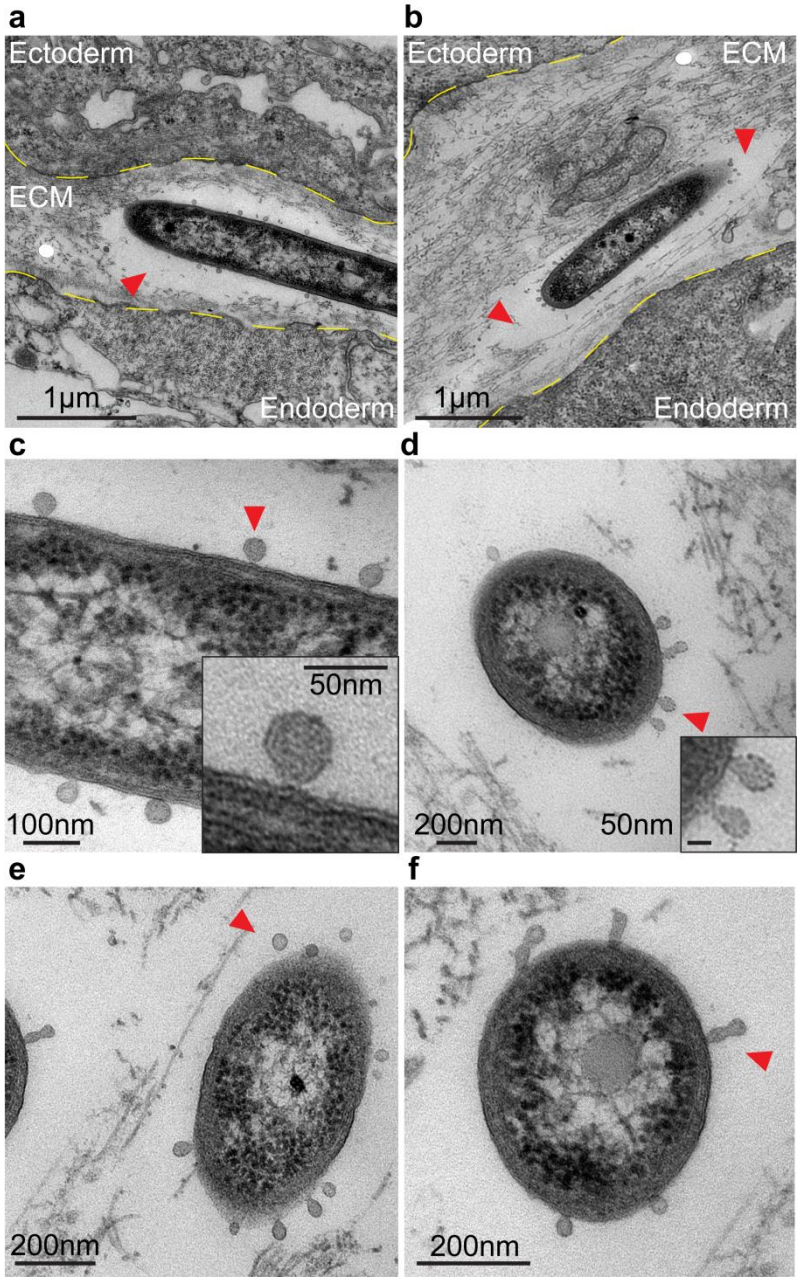

Fig. 2.7: *Pseudomonas* colonizes the extracellular matrix of control polyps and forms outer membrane vesicles. (a-f) Transmission electron microscopy images reveal the presence of *Pseudomonas* in the ECM (epithelial cell layers highlighted with a yellow dashed line). (a/b) Rod-shaped *Pseudomonas* colonizes the mesoglea in high density and may dissolve the ECM as food source (red arrows; scale bar: 1 µm). (c-f) TEM images reveal possible outer membrane vesicles (OMVs) on the surface of every *Pseudomonas* cell (red arrows).

In agreement with the confocal microscopy findings, TEM analysis of cross-sections from tumor revealed a high abundance of helically coiled bacteria similar to detected *Turneriella* spirochaete (Fig. 2.8a/c). *Turneriella* are mostly detected in the ECM between two epithelial layers (Fig. 3.9a-c). In rare cases, however, the helically-coiled electron-dense cells can be observed within the ecto- or endodermal cells of the tumor polyps, surrounded by a membrane. This may suggest a possible elimination of the spirochaetes by the host immune

defence (Fig. 2.8d). Noteworthy, the spirochaetes were detected throughout the entire body of the tumorous polyp, I found them also specifically in close proximity to aberrant germline precursor cells in the ectoderm (Fig. 2.8e/f).

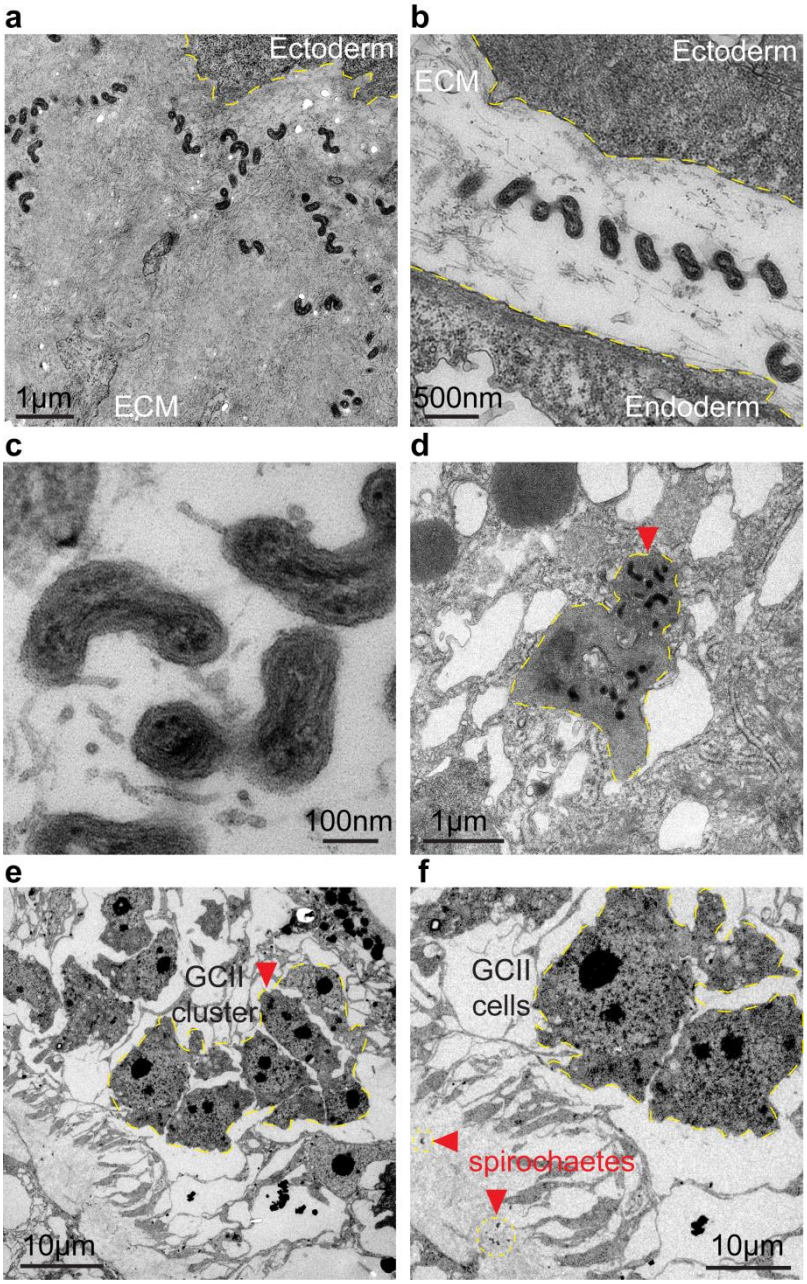

Fig. 2.8: Spirochaetes dominate the ECM in tumorous polyps. (a) Electron microscopy images of the spirochaetes colonizing the ECM (scale bar: 1µm). (b/c) characterized by a helical-coiled cross section (scale bar; 100/500 nm). (d) Spirochaetes only occur in the ectoderm or endoderm in a type of encapsulated form (red arrow, yellow dashed line; scale bar: 1µm). (e) Aberrant germline precursor cells (red arrow, yellow dashed line; scale bar: 10 µm). (f) are in close proximity to the Spirochaetes on the mesoglea (red arrow; yellow dashed lines scale bar: 10 µm).

Phylogenetic analysis of the 16S rDNA provided further insights into the identity of the bacteria colonizing the mesoglea in *Hydra*. Full ITS sequences were used for the

phylogenetic tree construction. The OTU750018 isolated from healthy *H. oligactis* polyps clusters close with the other members of the *Pseudomonas* species earlier isolated from *H. oligactis* and *H. magnipapillata* (unpublished; Fig. 2.9a). The closest well-characterized relative of this group is *Pseudomonas aeruginosa* (*P. aeruginosa*). For simplicity, I refer further to the OTU750018 isolated from *H. oligactis* as *Pseudomonas.* This specific bacterium was isolated in clear culture and confirmed by re-sequencing its 16s rDNA gene fragment for use in further experiments. The spirochaete OTU4017244 amplified from tumor-bearing *H. oligactis* polyps clusters close to the unculturable bacterium CN-20 (source: nitrification and denitrification reactors; KP054233.1) (Fig. 2.9b). Not surprisingly, all efforts to cultivate the spirochaete OTU4017244 from *H. oligactis* failed. Therefore, I further used in my experiments the closest, well characterized and culturable isolate *Turneriella parva* strain DSM21527, further referred to as *T. parva*.

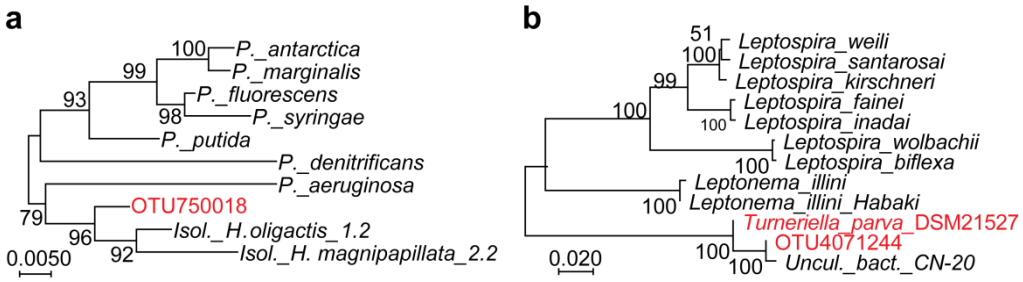

Fig. 2.9: Phylogenetic analysis reveals closely related species of *Pseudomonas* and *Turneriella*. (a) The analysis of *Pseudomonas* species clusters the isolate OTU750018 from healthy *H. oligactis* together with other *Hydra*-associated *Pseudomonas* isolates close to the *P. aeruginosa* species. Neighbour-joining phylogram with numbers at nodes representing bootstrap support values calculated by 1000 iterations. (b) Phylogenetic tree of Leptospiracea family clusters the spirochaetes OTU4017244 amplified from tumor-bearing *H. oligactis* with an unculturable bacterium CN-20 and the reference *T. parva* strain DSM21527. For sequence accession numbers see Suppl. table 1. Neighbour-joining phylogram with numbers at nodes representing bootstrap support values calculated by 1000 iterations.

2.3 Injection of *Turneriella parva* results in tumor formation

To test the causative relation between the presence of spirochaetes, as an alteration in the microbiome, and the tumor formation in *Hydra*, I tried to colonize control polyps with spirochaetes in a so called “common garden” experiment, *i.e*. by co-incubating control and tumor polyps (*n*=50) (Fig. 2.10a). Surprisingly, neither of the control polyps showed a tumorous phenotype after 3 months co-culture. Consistently with that, neither of the control polyps showed a presence of spirochaetes in the mesoglea. This indicates that the commensal microbiota protects itself and its host from colonization with some foreign bacterial, and thus strongly suggests the presence of “colonization-resistance” - a phenomenon long described in mammalian intestine[47,124,125], yet never uncovered in *Hydra* and other invertebrate models.

In order to bypass this resistance, I inoculated the medium with healthy control polyps with a pure culture of *T. parva* DSM21527 and incubated polyps in on container for 72 hours without changing the medium (Fig. 2.10b) (*n*=50). Still, after 40 days post treatment none of the polyps was colonized by *T. parva*, and not surprisingly, none of the polyps developed tumorous phenotype.

In another effort to circumvent the colonization resistance, I introduced *T. parva* directly into healthy *H. oligactis* polyps by injecting a high-density pure inoculate into gastric cavity and the body wall with a fine glass microcapillary. As a negative healthy polyps were injected with pure spirochaete culture medium. Within the following weeks some polyps inoculated with *T. parva* culture gradually developed a tumorous phenotype (Fig. 3.11a), very similar to the naturally occurring tumor-bearing polyps (Fig. 2.10a). Four weeks after the injection over 20% of the injected polyps (22/96) demonstrated a clear tumorous phenotype. In the rest of the cases (74/96) no phenotype changes have been detected within even longer timeframe. Consistently with that, 16S rDNA sequence corresponding to *T. parva* was barely detected in these polyps (Suppl. Fig. 6.1) and no coiled bacteria were revealed in the mesoglea, indicating that the colonization was not successful in these cases.

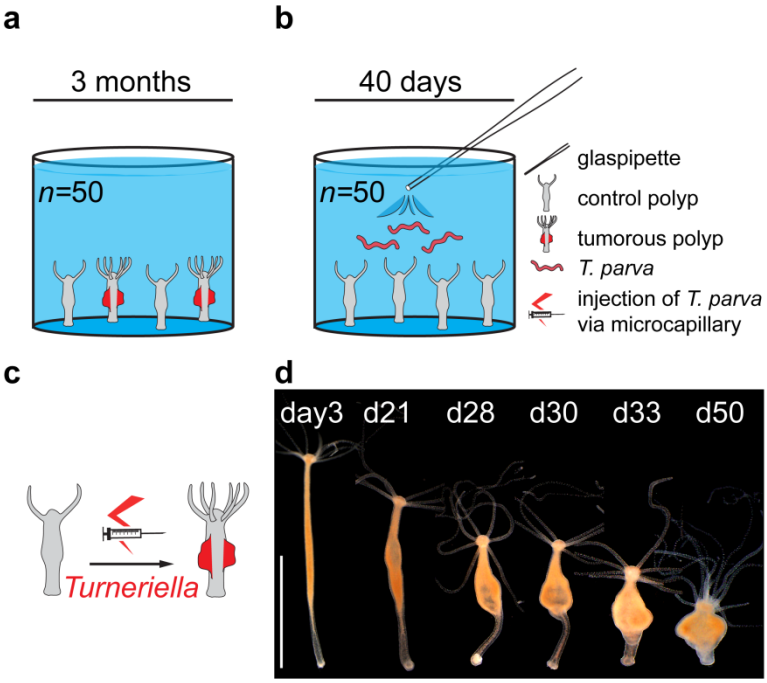

Fig. 2.10: Intact healthy polyps possess a colonization resistance. (a) Experimental setup of co-cultivation of control polyps with tumorous polyps for three months (*n*=50). (b) Experimental setup of control polyps incubated with a pure culture of *T. parva* for 3 days followed by 40 days of observation (*n*=50). Direct injection of *T. parva* leads to successful colonization and tumor development. (c) *T. parva* injection into a healthy control polyp of *H. oligactis*. (d) Series of images taken from the same animal in course of 50 days post *T. parva* injection. After around 30 days the previous characterized tumor phenotype is clearly recognizable (scale bar: 5mm).

In order to verify that the phenotype changes are caused by the colonization of *T. parva*, I conducted confocal microscopy (Fig. 2.11a/b). The analysis clearly indicated that in all polyps that developed a tumorous phenotype the ECM was successfully colonized by the helically coiled *T. parva*. Importantly, rod-shaped *Pseudomonas* cells naturally present in the health recipient polyps were also detected (Fig. 3.12a).

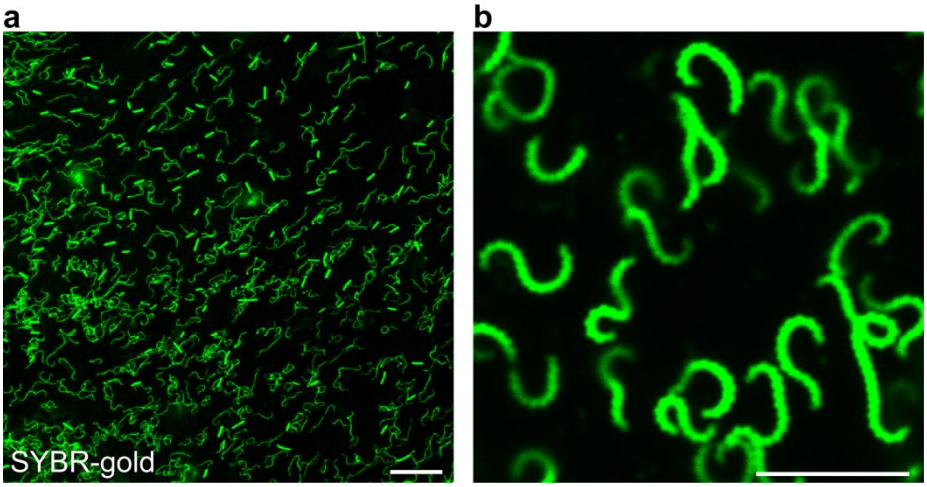

Fig. 2.11: *T. parva* colonizes the extracellular matrix. (a) After injection *T. parva* starts to spread over the entire ECM of injected polyps and is in close proximity to *Pseudomonas* (scale bar: 10µm).

(b) Staining with SYBR gold reveals the typical helical *T. parva* cells in the mesoglea isolated from injected polyps (scale bar: 5µm).

Furthermore, to characterize the microbiota composition in the polyps with introduced *T. parva*, I performed 16s rDNA analysis. As anticipated, *T. parva* was highly abundant in the microbiome of the injected polyps that developed tumors (Fig. 2.12a). Overall, the microbiota composition of polyps injected with *T. parva* resembled that of polyps with naturally-occurring tumors: Spirochetales, Pseudomonadales and Sphingobacteriales were dominating in the microbiome. Only members of Burkholderiales were poorly represented in *T. parva*-inoculated polyps. Notably, the abundance of *Pseudomonas* was greatly reduced in the injected polyps (Fig. 2.12a), suggesting that *T. parva* may displace the commensal *Pseudomonas* from its niche in the mesoglea.

In the *T. parva* injected polyps the microbiota was though slightly different from that of natural tumor polyps (see Fig. 2.5b), the marked domination of spirochaetes appears sufficient to induce tumor formation. Enrichment of spirochaetes and depletion of *Pseudomonas* in the injected polyps was statistically supported by LEfSeq analysis (Fig. 2.12b/c). LEfSeq analysis comparing injected and control polyps highlights the significant enrichment of *T. parva* (OTU4017244) in tumorous polyps. In contrary *Pseudomonas* (OTU750018) is enriched in the healthy control *H. oligactis* (Fig. 2.12b/c).

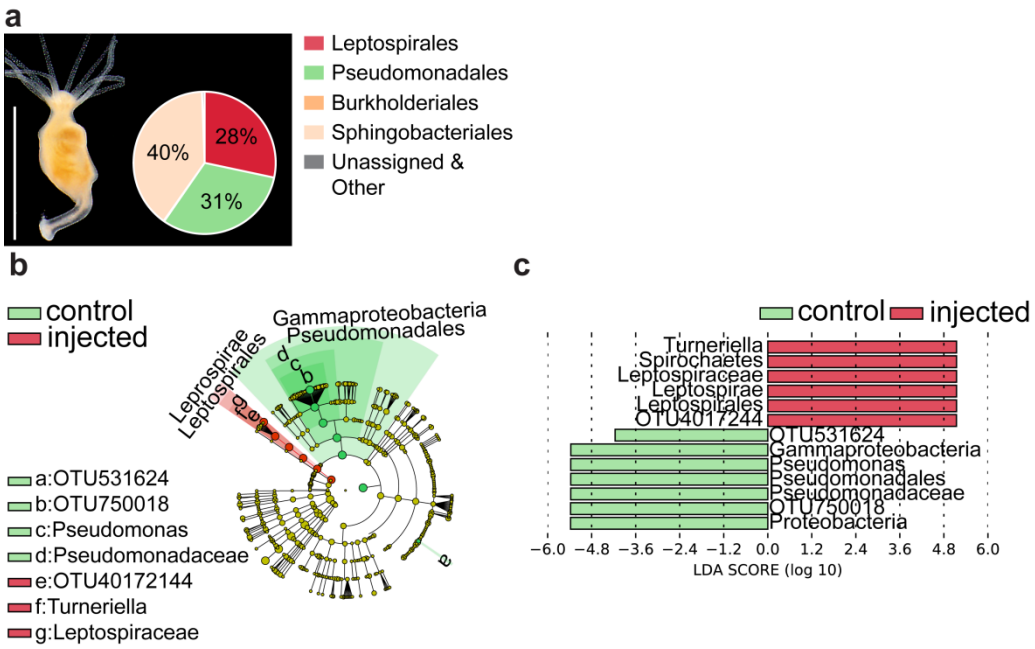

Fig. 2.12: Injected spirochaetes dominate the microbiota of tumorous polyps. (a) Injected healthy polyps colonized by *T. parva,* exhibit a tumorous phenotype and show a microbial composition resembling that of naturally-occurring tumours (scale bar: 5mm). (b) Taxonomic cladogram presenting OTUs differentially represented in the microbiota of control and tumor polyps generated using LEfSe analysis; red - taxa enriched in tumor polyps; green – taxa enriched in healthy polyps. (c) The

enrichment of certain taxa in tumor polyps is statistically supported by high positive LDA score values (red), and the taxa strongly enriched in control polyps are supported by negative score values (green).

In sum, I demonstrate that *T. parva* is capable of colonizing *H. oligactis* and triggering the tumorous phenotype. Importantly, *Turneriella* is normally not found in association with *H. oligactis* species (Fig. 2.4,[80]), and is likely present only in the environment (such as pond water), and in the low quantities. Similarly, *T. parva* strains have been isolated from tap water[126]. These data suggest that spirochaetes are not members of *Hydra* commensal microbiota. Instead, they act as opportunistic bacteria and colonize the host only if its immune barrier and/or normal microbiota are compromised. To test this hypothesis, I challenged control *Hydra* polyps by high temperature (22°C for 3 days, Fig. 2.13a). Surprisingly, a subsequent injection of *T. parva* into these polyps resulted in much higher colonization rates and tumor outcomes (60%, Fig. 2.13a) compared to injection into intact polyps (20%). Bacterial abundances are visualized on the class level on the bar plots (Fig. 2.13b). However, it was not clear why the phenotype first appeared after 40 days post injection. Therefore, I performed a qRT-PCR analysis for the 16s rDNA of *T. parva* to estimate the changes in abundance of this bacterium over time. Results showed that *T. parva* is first detectable after 20 days post injection independent on the stress treatment and still increases until day 40 after injection. These results implicate that *T. parva* has to reach a certain density threshold to affect the host phenotype.

Taken together, my results unequivocally indicate that injection of *T. parva* into the polyps circumvents the natural colonization resistance of the polyps and results in a stable persistence of introduced spirochaetes in the host. The localization of *T. parva* in the mesoglea (Fig. 2.11) perfectly recapitulates the distribution of natural spirochaetes OTU4017244 in *Hydra* (Fig. 2.6). Even more, the injection experiments uncover the same trends as detected in naturally occurring tumors polyps: the presence of spirochaetes in the mesoglea (OTU4017244) reduces the density of *Pseudomonas* (Fig. 2.5, Fig. 2.12 & Fig. 2.13). These observations provide evidence that the two spirochaete strains, *T. parva* DSM21527 and *Turneriella* isolated from *H. oligactis* (both share the same OTU4017244) are not only phylogenetically similar (based on 16s rDNA analysis, see Fig. 2.9b), but demonstrate similar biology as well. This allows addressing further the role of spirochaetes in tumor formation in this artificial model.

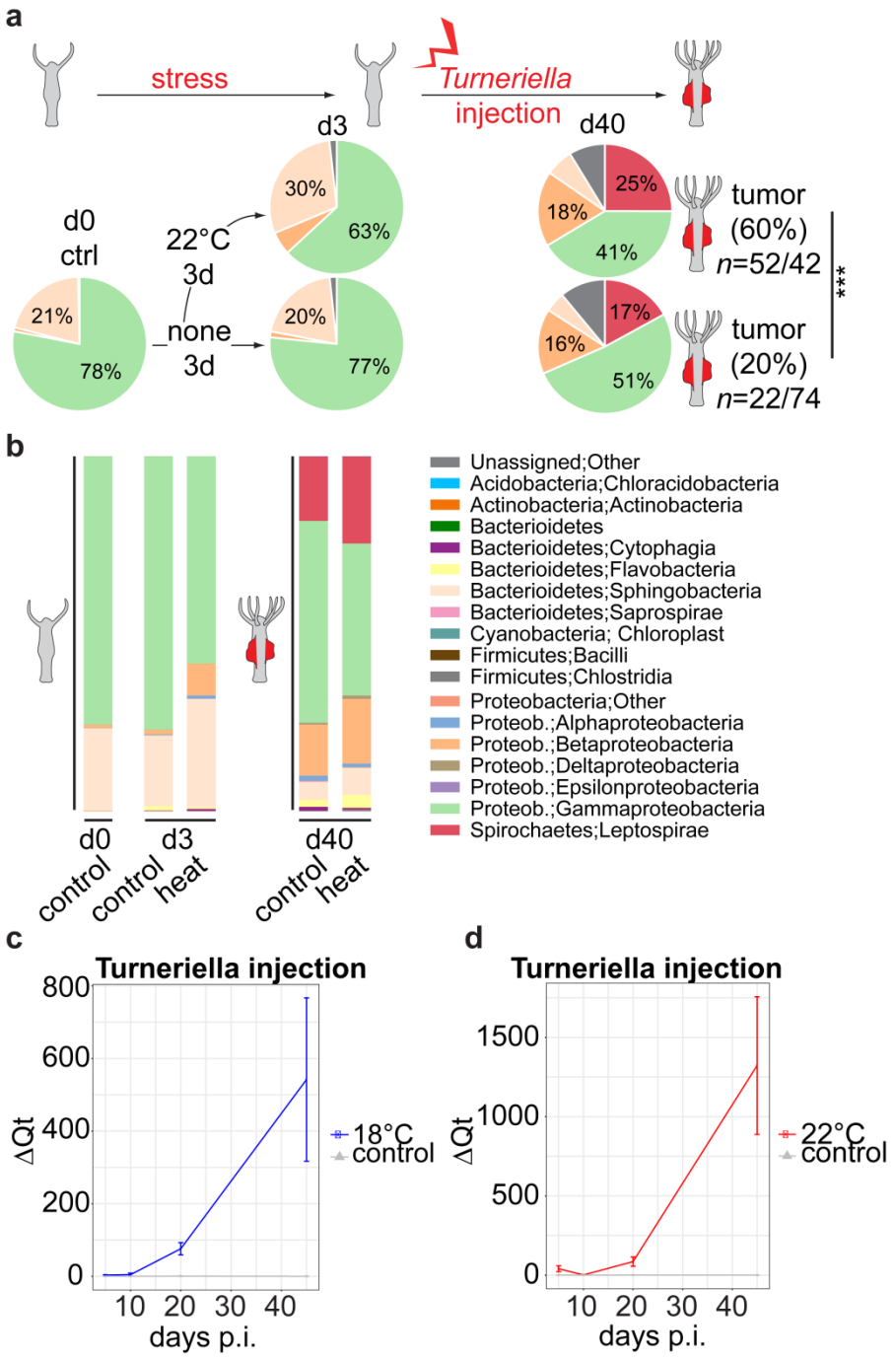

Fig. 2.13: Heat stress increases the efficiency of *Hydra* colonization by *T. parva*. (a) *T. parva* colonizes the ECM of *H. oligactis* more successfully if the host was pre-stressed with high temperatures (22°C; 52 of 94 injected polyps; ~60%) (chi-square statistic: χ^2=20.9; df=2; P<10-5). (b) Abundance plots of the microbial composition of healthy (control), stressed & untreated polyps and stressed & untreated polyps with a successful *T. parva* colonization 40 days post injection on the bacteria class level. (c/d) The qRT-PCR results uncover that *T. parva* needs at least 20 days to reach detectable levels in both (c) untreated (18°C) and (d) prestressed (22°C) polyps (delta Qt: normalized Cq value to the actin housekeeping gene of *Hydra oligactis*).

The successful introduction of *T. parva* into the healthy *H. oligactis* polyps consistently resulted in tumorous transformation of the polyps. This indicates that *T. parva* is capable of triggering the tumor phenotype in the host. These findings highlight the role of the environment, and its both – microbial (*T. parva* in the water) and abiotic (e.g. temperature stress) properties, in tumor initiation.

2.4 Antibiotic treatment eliminates tumor

To test further the role of microbiota in tumor formation, I treated the tumor-bearing *H. oligactis* polyps with an antibiotic cocktail for two weeks. This protocol is known to effectively eliminate bacteria from *Hydra* and thus – to generate germfree animals[127]. Remarkably, already 10 days after beginning of the treatment tumorous polyps showed a recovering from the tumor phenotype (Fig. 2.14a). Tumor bulges disappeared completely within 10-14 days, polyps gained a normal shape (Fig. 2.14b) and were not distinguishable anymore from the healthy control polyps. Importantly, the polyps retained the normal phenotype further, after the antibiotic treatment was over, and did not develop tumors again in the following months.

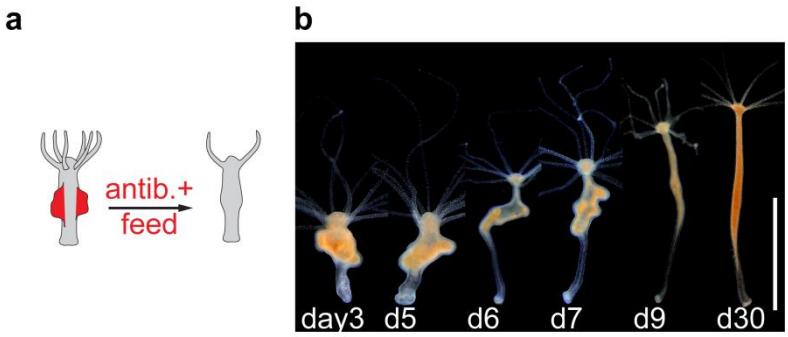

Fig. 2.14: Antibiotic treatment of tumor polyps eliminates the tumor phenotype. (a) Experimental setup of antibiotic treatment of tumorous polyps. (b) Time-series of the same tumor-bearing polyp over 30 days. Antibiotic treatment over two weeks with subsequent feeding eliminates the tumor phenotype after 10 days (scale bar: 0.5 cm). Feeding after 14 days restores a healthy phenotype.

Further 16S rDNA sequence analysis uncovered dramatic changes in the polyp's microbiota (Fig. 2.15a/b). First of all, *T. parva* was absent from antibiotic-treated polyps: no OTUs could be assigned to the Spirochaetes phylum. Second, the relative abundance of *Pseudomonas* decreased substantially. Finally, bacteria of other orders, such as Sphingobacteriales, became highly represented in the microbiome of antibiotic-treated polyps. These bacteria

were introduced, most likely, by feeding normal, not sterile, *Artemia* nauplii to the germ-free polyps. Consistently with the 16S sequencing results, no bacteria could be found in the ECM of antibiotic-treated polyps (Fig. 2.15b). Note, while some antibiotic agents solely were highly effective against spirochaetes on the mesoglea, some of the tested antibiotics failed in vivo completely to eliminate the bacteria from the ECM (Fig. 2.15c/d). While Neomycin in 100 % of the cases eliminates the tumor phenotype of the tumor-bearing polyps, Rifampicin, Doxycyclin, and Vancomycin have no impact on *Turneriella* and thus the tumor bulges *in vivo.* The absence of bacteria was verified by a 30-cycle PCR using the universal 16s bacteria Primer EUB_27F and Eub_1492R[128] (data not shown).

Taken together, our results clearly indicate that elimination of spirochaetes from the tumorous polyps effectively obliterates the tumors. Along with the fact that injection of *T. parva* into healthy control *H. oligactis* induces the tumor formation (Fig. 2.10), our observation strongly suggests spirochaetes as causative agent of tumorigenesis in *Hydra oligactis.*

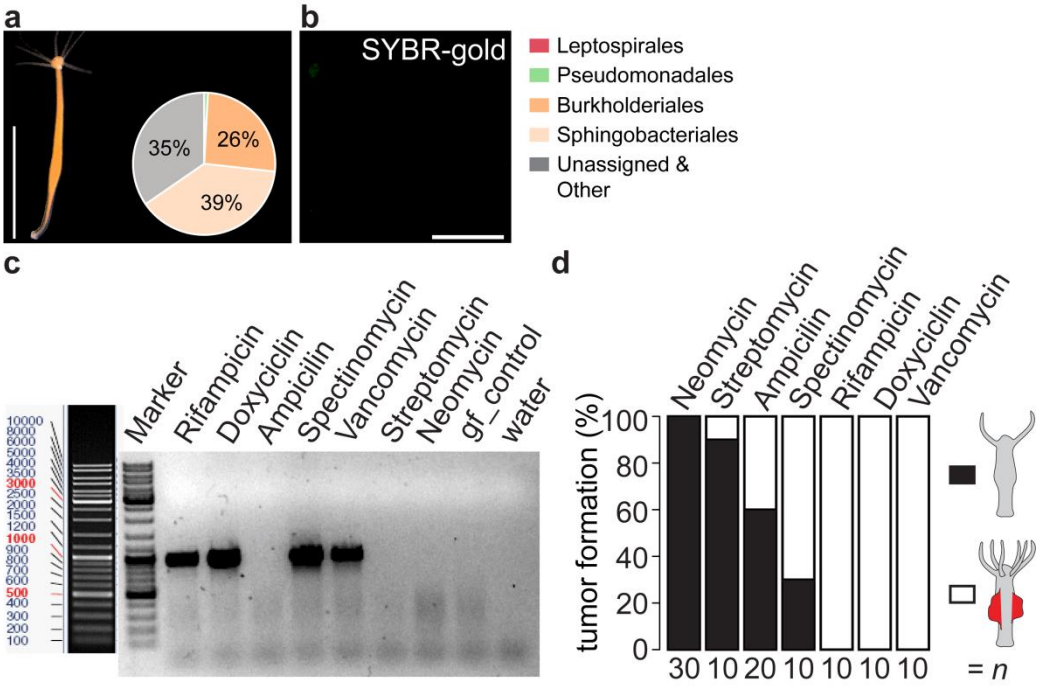

Fig. 2.15: Antibiotic treatment eliminates spirochaetes from mesoglea and obliberates the tumor. (a) Image of an ex-tumor polyp treated with antibiotics The antibiotic treatment and following feeding with non-sterile food restores the healthy phenotype but disturbs the microbiota (scale bar: 0.5 cm). (b) Antibiotic treatment eliminates virtually all bacteria present on the mesoglea including *Turneriella* and *Pseudomonas* (scale bar: 5µm). (c) Only specific antibiotics are sufficient to eliminate spirochaetes from the polyps, visualized here with an agarose-gel and a *T. parva* specific primer (d) Success rate (%) of removing the tumor phenotype with different antibiotics.

2.5 *T. parva* colonization causes morphology alterations and fitness decline

The phenotype of naturally-occurring tumors in *H. oligactis* is not limited to conspicuous tissue budges. In fact, it encompasses multiple changes in the overall morphology of the polyps (Fig. 2.1), growth dynamics (Fig. 2.3), in the architecture of epithelial layers and mesoglea (Fig. 2.2, Fig. 2.3 & Fig. 2.4), and behavior of germ-line interstitial stem cells (Fig. 3.5). In order to prove that the spirochaetes are capable of eliciting the entire complex tumor phenotype, I measured the morphological criteria and fitness parameters of the tumorous polyps generated by injecting the *T. parva*, of the tumor-free polyps obtained by antibiotic treatment of tumorous polyps, and compared them to the both, naturally occurring tumorous strain of *H. oligactis* and healthy control polyps.

While population growth and thus fitness was significantly decreased in the presence of *Turneriella* in natural tumor polyps, population growth was even more decelerated in *T. parva* injected polyps (Fig. 2.16). Remarkably, population growth of tumorous polyps could be restored with antibiotic treatment to the healthy state of control polyps (Fig. 2.16a). One factor which could influence the population growth is the time a bud needs to detach from its mother polyp. Therefore, I computed the detachment time as previous described (2.2). Again, the injection of *T. parva* into healthy polyps recapitulates the natural tumor phenotype, while antibiotic treatment abolishes the delayed detachment phenotype (Fig. 2.16b). Additional to these fitness phenotypes further morphological alterations have been previously described (Fig. 2.1). Tentacle number in healthy animals amounts to 6-8 tentacles but is significantly increased in tumor polyps (Fig. 2.16c). Remarkably, injection of *T. parva* recapitulates the increase of tentacle number comparable to the natural tumor, while antibiotic treatment reduces the number to the level of healthy control animals (Fig. 2.16c). Importantly, the changes described above are gradual, and develop in the timeframe of 2-3 weeks after *T. parva* injection or antibiotic treatment. For instance, the number of tentacles gradually increases in the polyps injected with *T. parva* and reaches the level characteristic for naturally-occurring tumors (~12 per polyp) only 3-4 weeks post injection (Fig. 2.16d). This dynamic can be explained by the previously described (Fig. 2.13c/d) slow increase in the density of *T. parva* in the polyps.

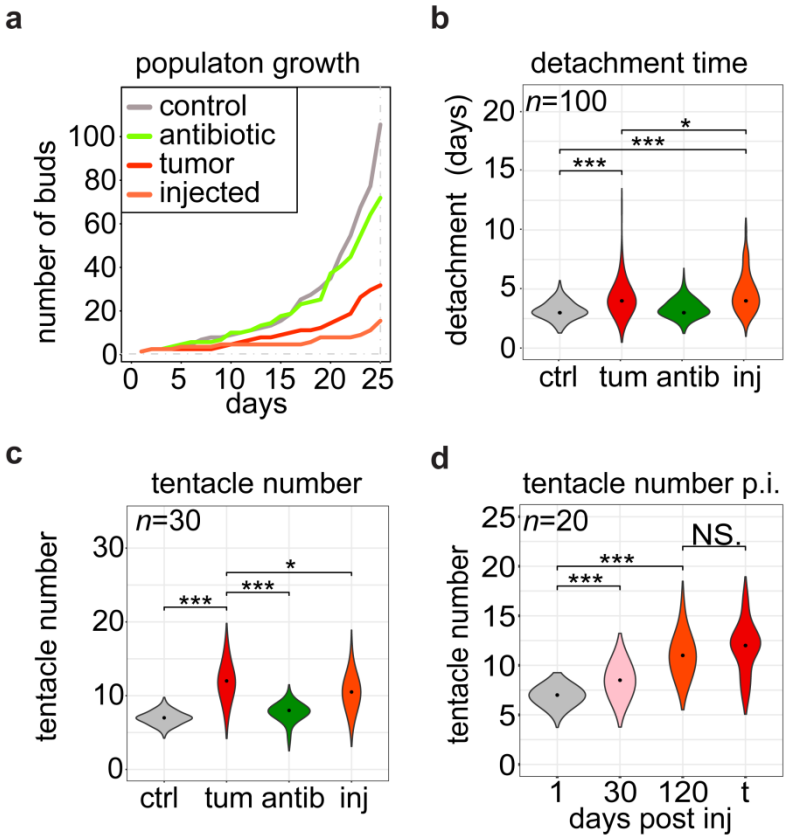

Fig. 2.16: Injection of *T. parva* fully recapitulates the tumor phenotype, while elimination of spirochaetes obliterates the tumors. (a) Population growth of control (ctrl), tumor (tum), injected (inj) and antibiotic (antib) treated animals. The presence of *Turneriella* in the naturally-occurring or injected tumorous polyps results in decrease in asexual reproduction rate, but can be cured by antibiotic treatment. (b) Detachment time of control, tumor, injected and antibiotic treated polyps (*n*=100). Detachment time in tumor and injected tumor polyps is delayed, but can be restored by antibiotic treatment to the level of the control. (c) Tentacle number of control, tumor, injected and antibiotic treated animals (*n*=30). Tumor and injected polyps show an increase in tentacle numbers, but can be normalized to the number of the control by antibiotic treatment. (d) Tentacle number of injected polyps increases after 30 and 120 days post injection (p.i.) and reaches after 120 days a tentacle number comparable to natural tumor animals. ***:$p \leq 0.001$, *:$p \leq 0.05$.

I could already demonstrate that in the naturally-occurring tumor polyps actin cytoskeleton is greatly disorganised, and aberrant germline precursor cells are accumulated (Fig. 1.6 & Fig. 2.4). In order to test the impact of *T. parva* on the actin cytoskeleton and the aberrant germline cells, I performed further immunostainings of injected tumor polyps. The actin cytoskeleton in healthy polyps is parallel structured but disorganized in natural tumor polyps (Fig. 2.4). Very similar cytoskeletal alterations were observed in the polyps injected with *T. parva* three months post inoculation (Fig. 2.17a). Antibiotic treatment of tumor-bearing polyps, conversely, leads to establishing a normal architecture of the actin fiber cytoskeleton could be rescued (Fig. 2.17c). In natural tumor polyps aberrant female precursor cells accumulate and spread over the entire body column[101] (Fig. 2.4). Three Months after

injection with *T. parva,* similar clusters of GCII cells can be detected in the gastric region of injected polyps (Fig. 2.17b/e). Interestingly, antibiotic treatment though decreases the size of the GCII cell clusters (Fig. 3.18d), does not eliminate them entirely. After 15 days post antibiotic treatment I could still detect small clusters of these cells in antibiotic treated polyps (Fig. 2.17d/f).

In sum, the presence of spirochaetes triggers the entire complex tumorous phenotype, which is virtually identical in the polyps infected with the natural *Turneriella* strain or injected *T. parva* strain. Eradication of the spirochaetes fully eliminates tumorous traits. Taken together, my findings provide an unequivocal evidence for spirochaetes as drivers of tumor formation in *Hydra*.

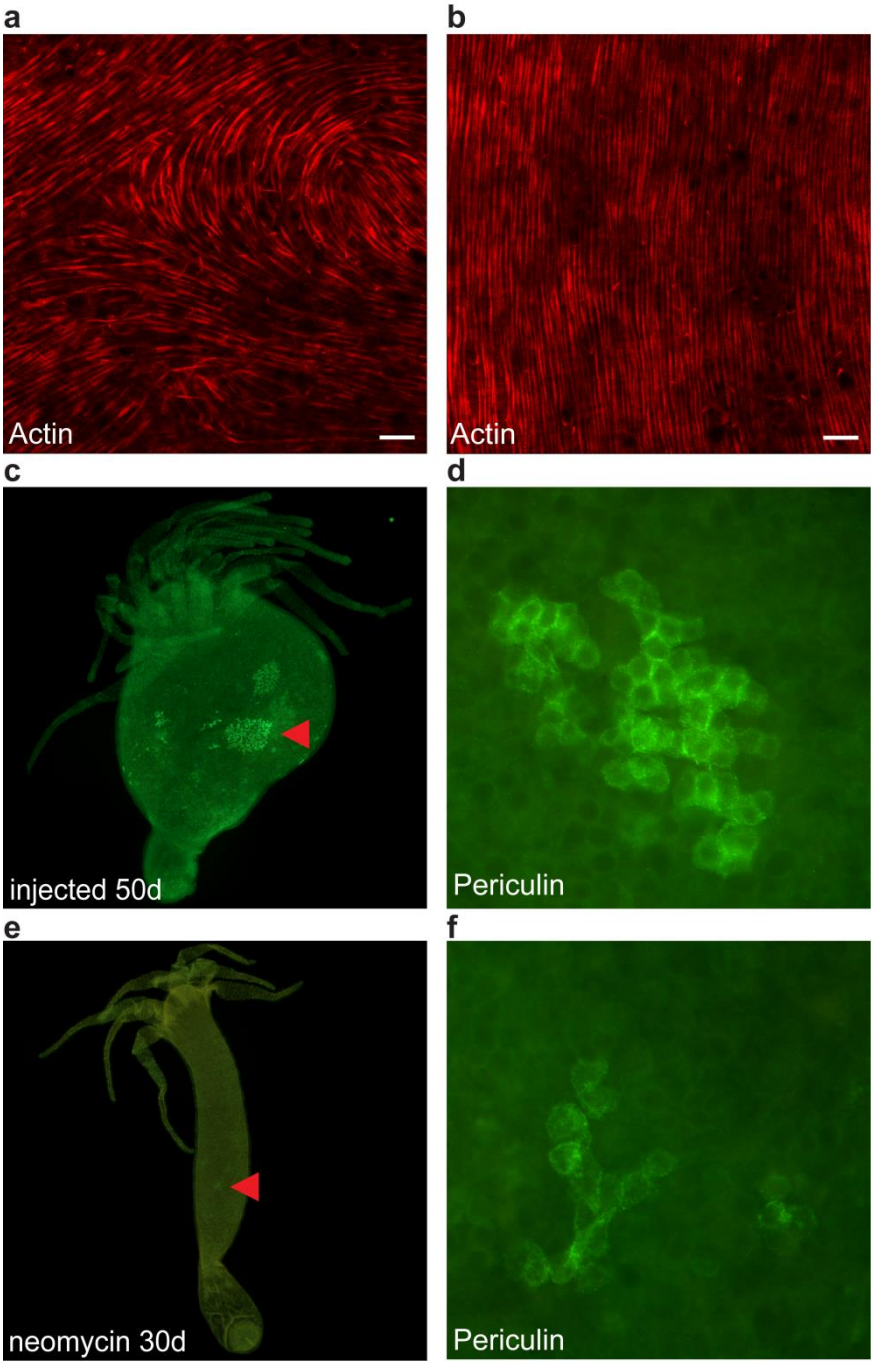

Fig. 2.17: Injection of *T. parva* recapitulates the disturbances of the actin cytoskeleton and the occurrence of aberrant germline cells, and antibiotic treatment reverts to the phenotype. (a) Injection of *T. parva* results in disturbances of the actin fiber patterning (scale bar: 10 µm) and (b/e) accumulation of aberrant female germline precursor cells (red arrow). (c) Antibiotic treatment stabilizes the parallel pattern of the actin fibers in antibiotic-treated tumor polyps (scale bar: 10 µm) and (d/f) drastically reduces the presence of aberrant germline precursor cells on large scale (red arrow).

2.6 Aberrant germline precursor cells are secondary effect of spirochaete colonization

Accumulation of aberrant female germ-line precursor cells (GCII) was considered as a main cause of tumor formation in two *Hydra* species, *H. oligactis* and *P. robusta*[101]. My data suggest that the presence of spirochaetes might be a true prime trigger of tumorigenesis, and the accumulation of female GCII cell clusters appears as secondary effect of the colonization of *Turneriella.*

In order to test this hypothesis, I performed three experiments. First, I eliminated aberrant GCII-cells by Hydroxyurea-treatment (HU) and transplanted this tissue into healthy control polyps. Hydroxyurea is a toxic agent which eliminates all fast replicating cells[129] and therefore eliminates all interstitial and germline cells from the tumor polyps (Fig. 2.18a/b). By this treatment, I generated tumorous polyps without aberrant germline cells. Surprisingly, transplantation of grafts from these tumor-bearing polyps which lack the aberrant GCII-cells into healthy control polyps still resulted in the tumor formation (Fig. 2.18c/d). Immunocytochemical staining of the polyps with an antibody against periculin protein, known to label *Hydra's* female germline precursor cells[93], confirmed that the resulting polyps though had a clear tumor phenotype, lacked GCII cells. Since the HU treatment does not affect the slow-growing *Turneriella*, and this bacterium was transplanted along with the tissue graft, the most plausible scenario is that the presence of *Turneriella* in the tissue of the HU-treated animals was sufficient for formation of tumors in the recipient polyps.

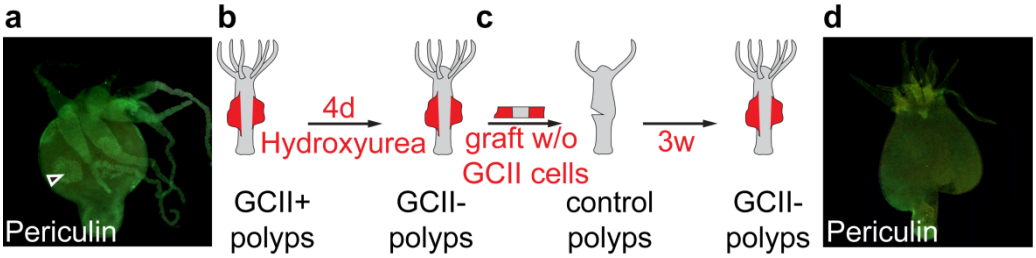

Fig. 2.18: Tissue free of aberrant GCII-cells induces tumorigenesis in *H. oligactis.* (a) Immunocytochemistry of whole mount tumor polyps of *H. oligactis* with an antibody against periculin protein highlights big clusters of aberrant GCII-cells in the gastric region. (b). Hydroxyurea-treatment of tumor polyps over four days (4d) eliminates all stem cells including the aberrant GCII cells. (c) Transplantation of a small fraction of the tumor tissue which lacks now aberrant GCII-cells, but is still colonized by *Turneriella,* into healthy control tissue results in tumor growth (d) which is visible by immunocytochemistry of whole mount tumor polyps.

In the second experiment, I treated tumor polyps with antibiotics to make them germfree and thus eliminate the tumor phenotype (Fig. 2.19a). Antibiotic treatment diminishes the presence of aberrant GCII-cell clusters over time but does not eliminate all cell clusters which could be

visualized by periculin-AB immunocytochemistry. Subsequent transplantation of these spirochaete-free ex-tumorous polyps into healthy polyps never resulted in a tumorous phenotype (Fig. 2.19c/d), in spite of presence of GCII cells.

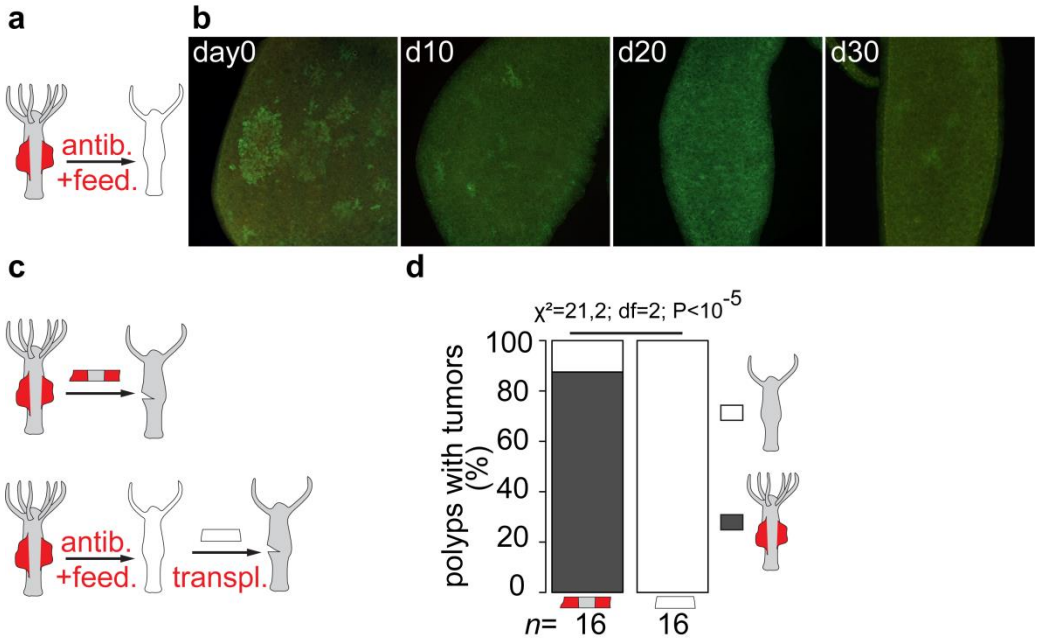

Fig. 2.19: Antibiotic treatment diminishes aberrant GCII-cell clusters. (a) Experimental setup of antibiotic treatment and post feeding of tumor polyps which results in a healthy phenotype. (b) Time line of immunocytochemistry images (periculin-AB) of tumor polyps after 0, 10, 20 and 30 days during and post treatment. Number of aberrant GCII-cells decreases significant over time. (c) Transplantation-scheme of tumor tissue and antibiotic treated tumor tissue into healthy control polyps. (d) Transplants of antibiotic treated polyps never result in tumor formation in the healthy control. In contrary tumor tissue transplants show a high success rate of resulting in tumor formation (chi-square statistic: χ^2=21.2; df=2; P<10^{-5}).

In the third experiment (Fig. 2.20), I used a male *H. oligactis* line that was free of spirochaetes and female germline cells. I injected these polyps with *T. parva* and monitored the phenotypic changes over following two months. Remarkably, the injection of *T. parva* was sufficient to trigger tumor formation in male polyps (Fig. 2.20b). Immunocytochemical staining for the periculin marker confirmed absence of any female germ-line cells in these tumorous polyps (Fig. 2.20b). Finally, gametogenesis was induced in these polyps by lowering the temperature and changing feeding regime[79,106]. All injected polyps demonstrated development of only male gonads (testes, Fig. 2.20c), clearly indicating absence of any female germ-line contribution. Taken together, these three experiments provide clear evidence that spirochaetes are the origin of tumorigenesis in *Hydra* and the accumulation of aberrant germline precursor cells is a secondary effect.

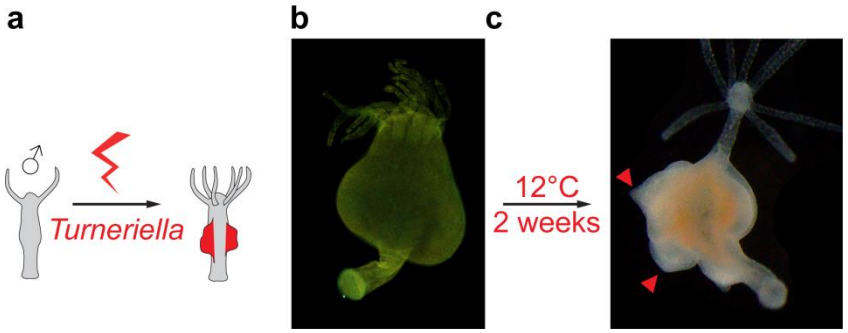

Fig. 2.20: Injected *T. parva* induces tumors in male *H.* oligactis polyps in the absence of aberrant female germline cells. (a) Scheme of the injection of male *H. oligactis* polyps. (b) Immunocytochemistry with the Periculin-AB revealed GCII-cell free male polyps. (c) Tumor bearing polyps were screened for maleness by triggering sexual reproduction with a temperature shift (12°C/ 2 weeks). Male polyps are highlighted by gonads (red arrows).

2.7 Spirochaetes are not sufficient to cause tumorigenesis in *H. oligactis.*

Since my experiments revealed that presence of spirochaetes is necessary for tumor growth (Fig. 2.10), I questioned whether it is sufficient to elicit tumorigenesis. To test this hypothesis, I injected the *T. parva* into germ-free polyps obtained by antibiotic treatment of healthy *Hydras*. Unexpectedly, none of 158 injected polyps developed tumors (Fig. 2.21). Microscopic analysis and 16S rDNA analysis (data not shown) revealed no colonization of the polyps with the spirochaetes, suggesting that presence of other bacteria is necessary for establishing a *T. parva* persistence. Since these manipulated polyps harbored a microbiota composed mainly of Burkholderiales and Sphingobacteriales members, acquired via feeding on *Artemia*, but lacked *Pseudomonas*, I speculated that the presence of particularly this bacterium is necessary for *T. parva* settlement and subsequent tumor development.

Fig. 2.21: Injection of *T. parva* into germ-free *H. oligactis* never results in tumor formation. Presence of some bacteria on *Hydra* is necessary for *T. parva* to colonize the host. *T. parva* injected into antibiotic-treated polyps free of bacteria were not able to settle, and none of injected polyps (0/158) developed the tumorous phenotype.

Additional evidence for the essential role of a second player came from the long-term observation on the culture of tumorous *H. oligactis* strain. Most of the buds produced by tumor-bearing polyps developed tumors, which was consistent with the previous observations[101]. However, very rarely some buds emerged that remained healthy and did not develop tumorous phenotypes for months (Fig. 2.22a). Analysis of microbiota composition of these tumor-free polyps revealed, unexpectedly, that *Turneriella* OTU4017244 became even more dominant compared to the parental culture (Fig. 2.22b), comprising over 65% of the total microbiota. On the contrary, *Pseudomonas* OTU750018 was virtually absent, with an abundance below 0.5% (Fig. 2.22b) suggesting a spontaneous loss of this bacterium by the polyps. The rest of the microbiota composition, including Sphingobacteria and Betaproteobacteria, remained unaffected (Fig. 2.22). These observations clearly indicate that the presence of *Turneriella* alone is not sufficient to elicit tumorigenesis. Instead, a substantial presence of *Pseudomonas* appears needed for tumor formation.

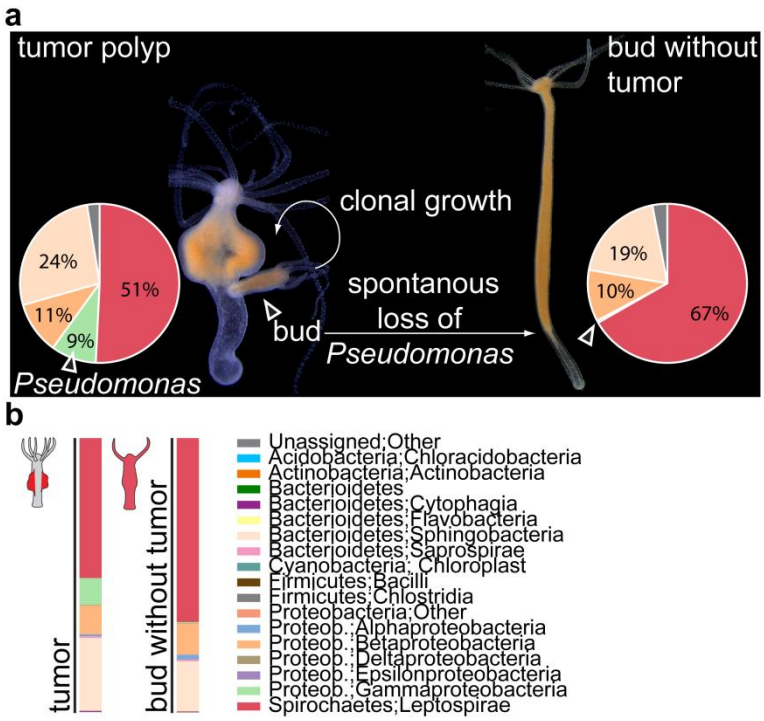

Fig. 2.22: Spirochaetes are not sufficient to cause tumorigenesis in *H. oligactis*. (a) In rare cases, tumor-bearing polyps generate buds that result in healthy tumor-free polyps. These polyps harbor a microbiota dominated by spirochaetes, but devoid of Gammaproteobacteria, indicating a spontaneous loss of *Pseudomonas.* (b) Abundance plots of the microbial composition of parental tumorous polyps (tumor) and spontaneously recovered polyps (bud without tumor) on the bacteria class level.

In order to investigate the need of the presence, and possible interaction of a second player - likely *Pseudomonas,* with *Turneriella* I conducted transplantation experiments (Fig. 2.23a). As donors for grafting, I used first healthy control polyps with high abundance of

Pseudomonas in the mesoglea. Secondly, antibiotic treated and fed polyps with no bacteria in the ECM were used as donors. Finally, tumor buds that lacked *Pseudomonas* but had a dense colonization of *Turneriella* (Fig. 2.22) were used. I tested, whether these three kinds of grafts are capable of eliciting tumor formation being transplanted onto recipients' polyps with a high density of only *Turneriella* on the ECM (tumor buds without tumor, Fig. 2.22). In most of the cases (78.8%, Fig. 2.23b), when I transplanted a piece of a healthy polyp harboring a microbiota dominated by *Pseudomonas* (Fig. 2.23b), tumors were effectively elicited (Fig. 2.23b). On the contrary, transplantation of tissue fragments from the polyps lacking *Pseudomonas*, only rarely resulted in tumor outgrowth. Grafts from polyps with no microbes in the mesoglea, obtained by antibiotic treatment (Fig. 2.14) and grafted onto polyps densely colonized with *Turneriella* (Fig. 2.22) elicited tumorigenesis only in 12.8% cases (Fig. 2.23b). Finally, the autologous transplantation of a *Pseudomonas* depleted tissue onto a tumor-free recipient led to tumorous outcome in only 7.7% cases (Fig. 2.23b). In sum, these observations confirm the crucial role of *Pseudomonas* in tumorigenesis. Only the presence of both bacteria, *Turneriella* and *Pseudomonas*, in the mesoglea elicits tumor growth in *H. oligactis.*

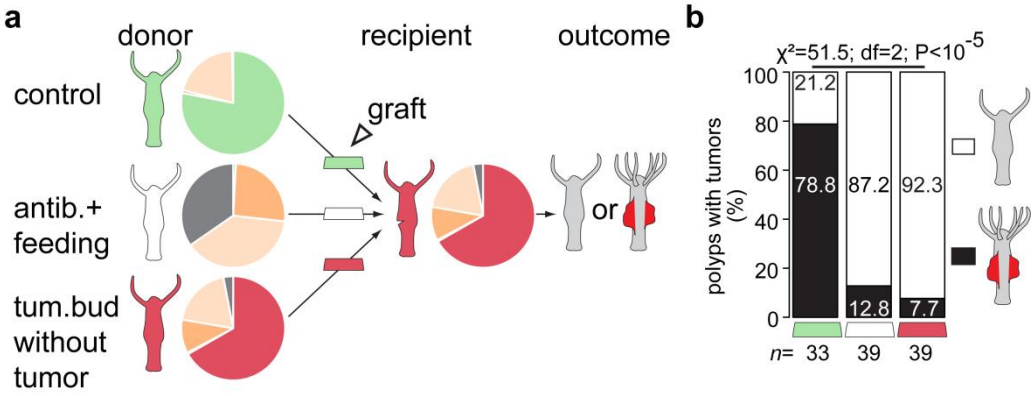

Fig. 2.23: Only the presence of *Pseudomonas* and *T. parva* elicits tumorigenesis in *H. oligactis.* (a) Setup of the transplantation experiment to prove that both bacteria, *Turneriella* and *Pseudomonas*, are necessary and sufficient to elicit tumorous phenotype in *H. oligactis.* A tissue fragment from a healthy donor polyp (control) provides a source of *Pseudomonas*. This graft, or the grafts from an antibiotic-treated polyp devoid of *Pseudomonas* and spirochaetes (antib.+feeding), or a tissue fragment from a spontaneously recovered polyp enriched in spirochaetes, but free from *Pseudomonas,* (tum. bud without tumor) are transplanted onto tumor-free recipients devoid of *Pseudomonas,* but harboring spirochaetes. The tumor formation of the resulting polyps is evaluated. (b) While only a small fraction of the recipients grafted with only *T. parva* (red), or no bacteria (white) on the ECM develop tumors, the recipients with grafts from tissue with *Pseudomonas* (green) have the highest rate of tumor formation.

Therefore, my results uncover that the presence of two bacteria, *Pseudomonas* and a spirochaete (native *Turneriella* or *T. parva*) is essential for tumor growth, and suggest that these two bacteria might interact with each other and the host to elicit the tumorigenesis.

2.8 *Pseudomonas* and *T. parva* possess a variety of virulence factors

My results demonstrate a dual role of the commensal microbe *Pseudomonas* in *H. oligactis.* First, it is required for the colonization of *T. parva* to occur, likely providing a niche for the spirochaetes to settle (Fig. 2.13). Second, the interaction with *Pseudomonas* contributes to the tumorigenesis, once spirochaetes populate the mesoglea. Therefore, I speculate that an interaction between the environmental bacterium *Turneriella* and the commensal *Pseudomonas* in the mesoglea context alters the phenotype of *Pseudomonas* and turns it into a pathobiont (Fig. 2.24). Alternatively, the spirochaetes may unveil their tumorigenic potential only in the presence of *Pseudomonas*.

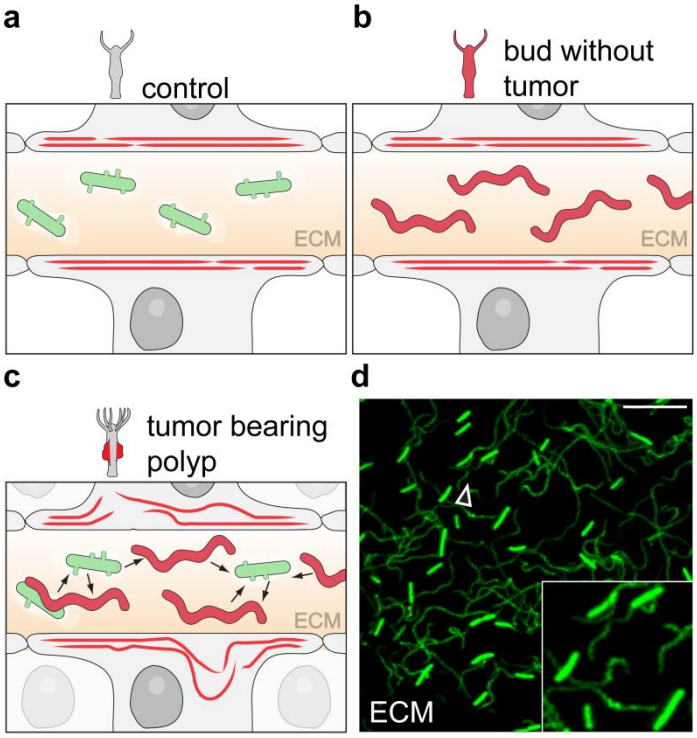

Fig. 2.24: Interplay between the commensal *Pseudomonas* and environmental spirochaetes within *Hydra* mesoglea induces tumor formation. (a) In normal healthy *H. oligactis* polyps the mesoglea (ECM) is colonized only by *Pseudomonas*, the actin cytoskeleton of the epithelial cells (red lines) is well organized, and no developmental abnormalities can be observed. (b) In the polyps that spontaneously lost *Pseudomonas*, the mesoglea is colonized only by *T. parva*, and the phenotype is normal. (c) If the both bacteria, *Pseudomonas* and *Turneriella*, are present in the ECM of a polyp, an interaction between them occurs and likely causes adverse effects onto the host, such as actin fiber disorganization (red curved lines) and tumor outgrowth. (d) In the tumor-bearing polyps, both bacteria – rod-shaped *Pseudomonas* and helically coiled *T. parva,* are found in close proximity in the ECM (revealed by SYBR-gold staining; scale bar: 5 µm), suggesting an immediate interaction.

In order to gain insights into the pathogenic potential of the both bacteria, *Pseudomonas* (from culture isolated OTU750018) and *T. parva*, I sequenced the genome and mined them for the presence of putative virulence factors. These data served to identify putative molecular mechanisms of the bacteria interfering with the tissue homeostasis in *Hydra*. Analysis of the *Pseudomonas* genome revealed an unexpectedly rich repertoire of putative pathogenicity factors. Among others, genes coding for the entire flagellum assembly (Fig. 2.25, Suppl. Fig. 6.2), type II and VI secretion systems, and the Sec-SRP complex (Suppl. Fig. 6.4) were detected along with multiple ABC-transporters (Suppl. Fig. 6.6), bacteriocins, and toxin/antitoxin systems (Suppl. table 3,4&5). Moreover, a complete prophage was found integrated into the *Pseudomonas* genome (Fig. 2.25, Suppl. Fig. 6.8, Suppl. table 6). Finally, multiple genes coding for secreted enzymes, such as collagenases and hydrolases, were detected. These findings are consistent with the observation (Fig. 2.7) that *Pseudomonas* cells are always located in the mesoglea within lacune-like electron-transparent areas free from fibrillary components (Fig. 2.7a/b; red arrows). *Pseudomonas* appears to actively digest the extracellular matrix of *Hydra*. Furthermore, high-resolution electron microscopy analysis allowed detecting conspicuous outer membrane vesicles being released from the surface of *Pseudomonas* within the mesoglea of *Hydra* (Fig. 2.7c-f).

I was not able to isolate a pure culture of *Turneriella* spirochaetes from tumor-bearing *H. oligactis*. Therefore, I analyzed the genome of *T. parva* DSM21527[130] that has been previously sequenced and annotated. Importantly, this strain is phylogenetically very closely related to the native *Turneriella* strain found in *H. oligactis* (Fig. 2.9b) and is equally capable of eliciting tumorigenesis in *Hydra* as the native strain. The phenotype induced by *T. parva* is virtually indistinguishable from that triggered by native spirochaetes. Hence, I speculate, that both strains may contain similar toolkit of pathogenicity factors, and described the repertoire in the *T. parva* DSM21527 genome. In contrast to *Pseudomonas*, *T. parva* turned out to harbor only few pathogenicity factors. Only the genes coding for flagellum assembly machinery (Suppl. Fig. 6.3), few bacteriocin-like proteins (Supp. Table 7,8&9) and several ABC-transporters (Suppl. Fig. 6.7) are present in the *T. parva* genome. The genes coding for the components of the type II secretion system and Sec-SRP complex were only partially represented in this spirochaete (Suppl. Fig. 6.5). Interestingly, putative collagenase and hydrolase enzymes are also encoded in the *T. parva* genome (Suppl. table 2,8), suggesting a possible mechanism for colonizing the mesoglea and thus – for competing with *Pseudomonas* for a niche. Interestingly, although *Turneriella* is characterized by extremely slow growth *in vitro* in a pure culture[130], it effectively outcompetes *Pseudomonas* in the host's mesoglea context and in some cases (Fig. 2.22) even displaces it completely.

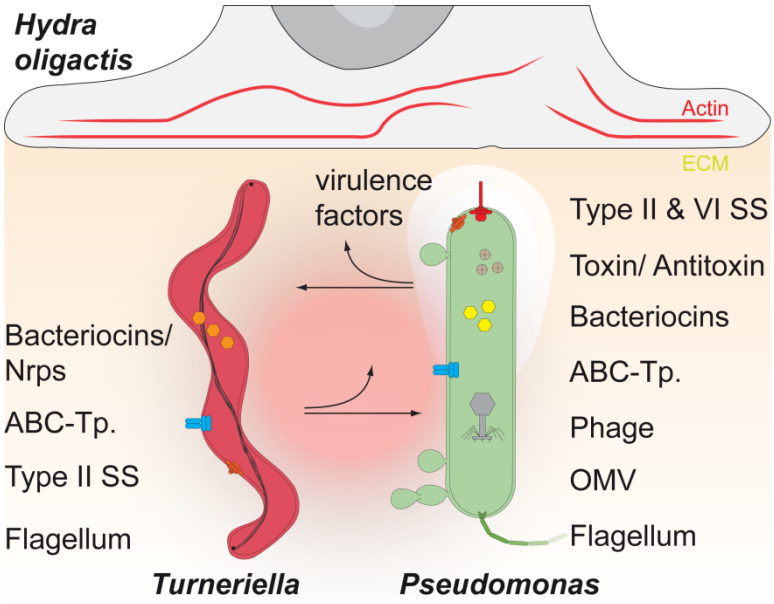

Fig. 2.25: Putative virulence factors uncovered in the genomes of *Pseudomonas* and *T. parva* may mediate their interactions and contribute to tumorigenesis. Analysis of genome sequences from *Pseudomonas* OTU750018 isolated from *H. oligactis* and *T. parva* reference strain DSM21527, capable of inducing tumors in *Hydra*, uncovers their repertoires of pathogenicity factors. In the *Pseudomonas* genome (left), among others, genes coding for the entire flagellum assembly, type II and VI secretion systems (Type II & VI SS) and the Sec-SRP complex are detected along with multiple ABC-transporters (ABC-Tp), bacteriocins, and toxin/antitoxin systems. Additionally, a complete prophage (Phage) is integrated into the *Pseudomonas* genome. The genome of *T. parva* (right) harbors the genes coding for flagellum assembly machinery, few bacteriocin-like proteins and several ABC-transporters (ABC-Tp), few genes coding for components of type II secretion system (Type II SS) and Sec-SRP complex. I speculate that the interplay between two bacteria (arrows) and virulence factors produced by them affect the *H. oligactis* cells, their morphology (including the actin cytoskeleton depicted as red curved lines), disturb the tissue homeostasis and cause tumor formation.

In sum, both bacteria offer a variety of virulence factors which could directly and indirectly interact with the host cell homeostasis. The location of the bacteria in the mesoglea, their putative enzymatic activity degrading the ECM, and close proximity to the actin filament fibers located at the basis of epithelial cells and gravely disturbed in tumors (Fig. 2.4a/b), stimulated me to focus on the interaction of the bacteria with the ECM and the actin cytoskeleton. In order to understand the impact of the bacteria interplay on the *Hydra* host, a metatranscriptomic analysis was performed.

2.9 The actin cytoskeleton as bacterial target

In order to uncover the molecular processes that are responsible for the tumorous phenotype, I sequenced 15 total cDNA libraries to identify differences in gene expression between *H. oligactis* control, female, and tumor animals with five replicates each. The transcriptome of female polyps served to exclude the oogenesis driven changes on the tumorigenesis (similar to the study of Domaszet-Lošo and co-authors[101]). I identified the genes differentially expressed between tumor and control animals to highlight the impact of the bacteria on the tumor formation. Importantly, since the isolated tissue contained the mesoglea and thus – the colonizing *Pseudomonas* and *Turneriella*, and since I isolated a total RNA, the resulting transcriptome can be considered as a metatranscriptome and includes the information of gene expression of the both, *H. oligactis* host and its microbiome. Analysis of the transcriptomic data using principal coordinate analysis (PCoA) showed that the replicates of control, tumor, and female animals cluster closely together (Fig. 2.26). The percent of variation explained by each principal component is indicated on the axes. I removed from each group one outlier. The x-axis separates control and tumor polyps from the female cluster, while the tumor cluster is located in between control and the female cluster. Therefore I can conclude that the first principle component explaining 70,4% of variance among the samples corresponds to oogenesis process, which could be already detected in the microarray data[101]. The second principle component, explaining 13.7% of variance, can be assigned specifically to the tumorigenesis process, since it segregates healthy control and female polyps from tumor polyps (Fig. 2.26a).

I performed differential expression analysis on contigs containing an open reading frame (ORF) of at least 100 amino acids in length and therefore refer to these as genes. In sum I found 760 genes dysregulated in female and tumor polyps compared to control polyps. Of these, 208 genes were only dysregulated in tumor polyps, while 552 were dysregulated by induced oogenesis. Therefore, I focused further on detailed analysis of these 208 genes (Fig. 2.26b; red). In these 208 genes, highly dysregulated in tumor polyps compared to control polyps, 93 were of bacterial origin and 115 mapped to the *Hydra* transcriptome (generated by the study of Domazet-Lošo and co-authors: db454_holi_female_newbler_final). Interestingly the majority of the 93 bacterial genes mapped to the *Pseudomonas* genome (OTU750018) encompassing gene categories belonging to the secretion system or the flagellum and were mainly downregulated in tumor. Almost every gene which mapped to *Pseudomonas* was roughly 2-fold downregulated in tumor polyps compared to control polyps, consistently with the lower abundance of *Pseudomonas* in the tumorous context (Fig. 2.5). These effects of different colonization density compromised further analysis of *Pseudomonas* genes higher

expressed in tumorous polyps. However, I could still find bacterial genes highly upregulated only under tumor conditions which mainly mapped to the genome of *T. parva*. This is again not surprising, because *Turneriella* is not present in control polyps. Among the top differentially genes, several genes were of particular interest. Some genes coding for putative peptidases, proteases, and hydrolases known to effect the actin cytoskeleton and the extracellular matrix (ECM)[131–135], were only upregulated in tumor polyps (Fig. 2.26c; left; cluster9741 & cluster24403). This could explain how the tumorous phenotype occurred. Bacterial peptidases, proteases, and hydrolases affect the normal growth of the actin cytoskeleton and the extracellular matrix in *Hydra* polyps resulting in dysfunction of shape and development in these polyps.

From the host side, a number of genes among the 115 genes significantly dysregulated in tumor polyps encompass interesting categories like antimicrobial peptides (3), energy & metabolism (12), actin cytoskeleton, (41) and tumorigenesis (12) (Fig. 2.26c; right). Interestingly, a high number of genes are dysregulated mapping to the actin cytoskeleton and the ECM. Except three genes, all others are upregulated compared to control polyps. Most of them are important in remodelling and renewing the extracellular matrix, like collagens (cluster3330, cluster1195, cluster23577, cluster107774 and others), thrombospondins (cluster8464 & cluster17492), fibrillins (cluster35379, cluster11907 & cluster10024), and actin linker proteins (cluster10518, cluster30109 & cluster73235). Surprisingly, some of them are specific for the non-canonical planar cell polarity, like laminins[136,137], which regulates the cytoskeleton that is responsible for the shape of the cell[68] and thus – the overall host morphology/anatomy (cluster17885, cluster19305, cluster7998, cluster8657 & cluster24317) (Fig. 2.26c, Suppl. Table 2). However, the most interesting category includes genes which are inhibitors of protease, peptidase, and metallopeptidase activity (cluster26153, cluster25203, cluster12134, cluster12384 & cluster11047). Interestingly, especially the counterparts (proteases & peptidases) were upregulated from the bacterial side.

Taken together, the results of transcriptome analysis strongly supported the microscopic observations on tumorous polyps. First, they provide support for the hypothesis that both bacteria colonizing the ECM of *Hydra. Pseudomonas* and *Turneriella,* produce proteins that are able to interfere and digest the ECM, likely as nutrition source, which I could already show in the electron microscopy images (Fig. 2.7). The direct activity of bacterial proteases, hydrolases, and peptidases, or the ECM disturbance caused by them, disrupt the actin cytoskeleton and thus may interfere with planar cell polarity[138,139] (genes dysregulated in the tumor context: cluster19305, cluster24317, cluster17885, cluster8657, cluster14821 & cluster7998) of the epithelial cells in *Hydra*. How bacterial effectors act on the actin

cytoskeleton was recently reviewed[131,135,140]. The host cell appear to respond to these enzymatic ECM degradation and cytoskeleton modifications by producing inhibitors of peptidases and proteases to countervail the bacterial disturbance[141] (Fig. 2.26d).

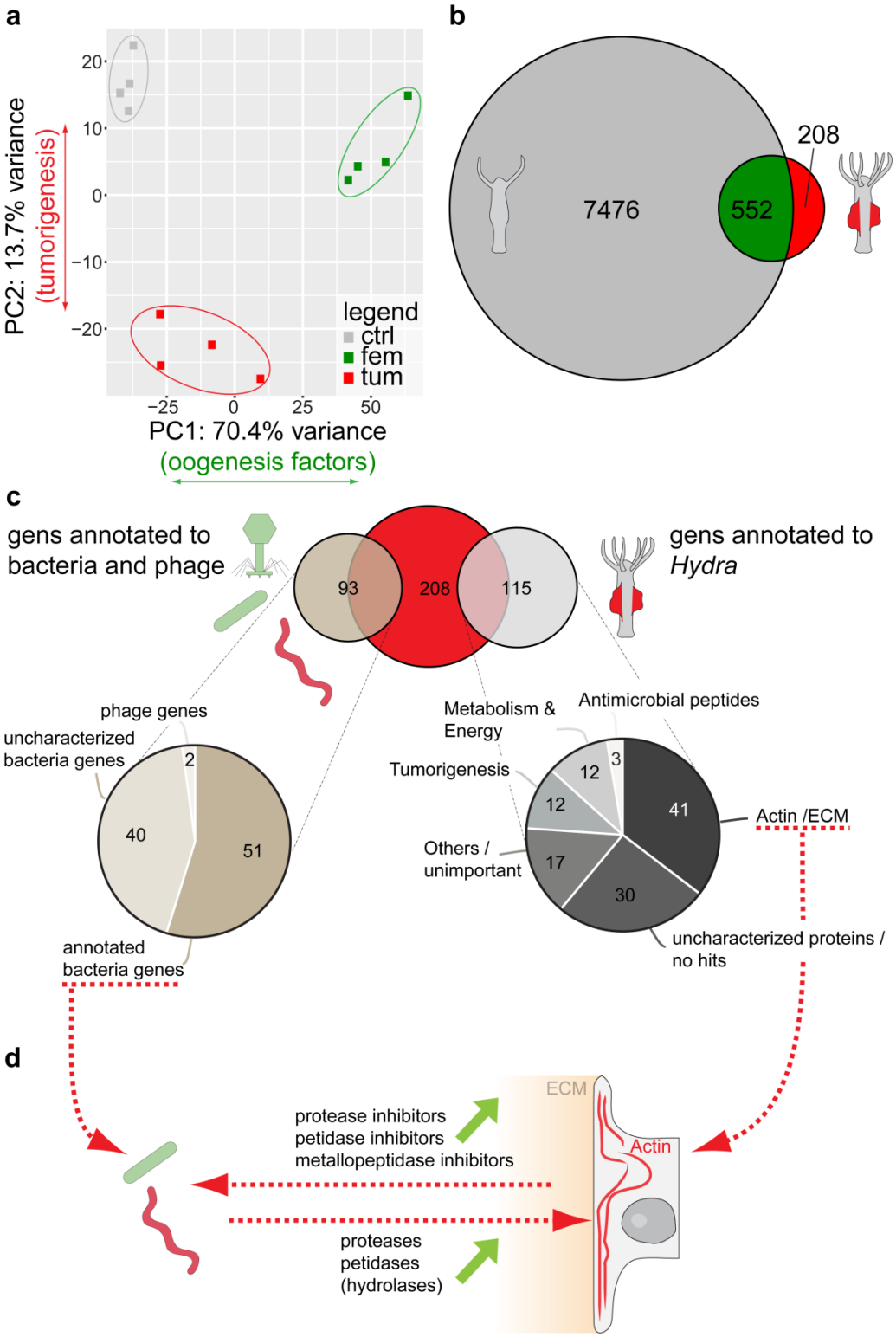

Fig. 2.26: Transcriptomic analysis reveals putative mechanisms of bacterial interactions with the host. (a) Analysis of the transcriptomic data of each individual sample using principal component analysis (PCoA). Note, that control, tumor, and female animals cluster together. Ellipses were added

manually. The percent variation explained by the PCoA is indicated on the axes. One outlier has been removed from each group. (b) Venn diagram showing the overlap of significantly ($p \leq 0.001$) differential expressed genes in control (7476, grey), for tumor and female polyps compared to control (green; 552) and only tumor versus control animals (red; 208). Focus was put on the genes significantly different expressed in tumor polyps compared to control animals (red). (c) Analysis and separation of the specific gene categories differentially expressed in tumor compared to control animals. Of the 208 highly dysregulated genes 93 match to bacterial and virus transcriptomes, while 115 match to the transcriptome of *Hydra.* (d) Model of an interaction between dysregulated bacterial and *Hydra* genes. Note, while from the bacteria side (proteases, peptidases, hydrolases) are upregulated (green arrow), *Hydra*, as counteraction, upregulates inhibitors of these gene products.

In conclusion, the transcriptomic data could reveal a possible initiation of the tumor formation. I propose here, that the disturbance of the ECM and actin cytoskeleton by bacterial proteases and peptidases[132,134,135,142] leads to loss of the actin cytoskeleton integrity and the planar cell polarity and, disrupts the normal tissue homeostasis and morphogenesis in a polyp, and thus initiates tumorigenesis in *Hydra.*

2.10 Tumorigenesis in Pelmatohydra robusta

Originally, the tumor phenotype has been investigated in two different species of *Hydra* - *Hydra oligactis* strain St. Petersburg and *Pelmatohydra robusta* strain L7[101]. In my thesis, I focused predominantly on *H. oligactis* and uncovered the leading role of microbiome in tumorigenesis of this species. In order to test, whether the tumor phenotype of *P. robusta* is also driven by the microbiome alterations, I performed first phenotypic characterizations and microbiome studies of the healthy control and tumorous polyps of *P. robusta.* For the characterizations of the phenotype, I focused on the decisive hallmarks I could already observe in *H. oligactis* comprising shape, presence of tumor bulges, tentacle number, actin cytoskeleton, and presence of aberrant germline precursor cells (Fig. 2.27).

Healthy control animals of *P. robusta* polyps show a tube-like body column and show an average tentacle number of six tentacles per polyp (Fig. 2.27a-c). In contrary, tumorous polyps of *P. robusta* show similar but not as distinct tumor bulges in the gastric region comparable to tumorous polyps of *H. oligactis*. In addition, tumor polyps show an increase in tentacle number up to an average of nine tentacles per polyp (Fig. 2.27c-e). While control polyps have no germline precursor cells (GCII) in the entire body column (Fig. 2.27f), tumor polyps show big clusters especially in the gastric region (Fig. 2.27h). The ectodermal actin fibers in control polyps are aligned in a parallel pattern (Fig. 2.27g). In contrast, tumor polyps show slight changes in the organisation of the actin fibers. In the regions of the tumor bulges minor disorganisation of the actin cytoskeleton could be detected (Fig. 2.27i). Therefore, the

anatomical changes in tumorous *P. robusta* polyps resemble those in tumor-bearing *H. oligactis* strain, though appear less prominent.

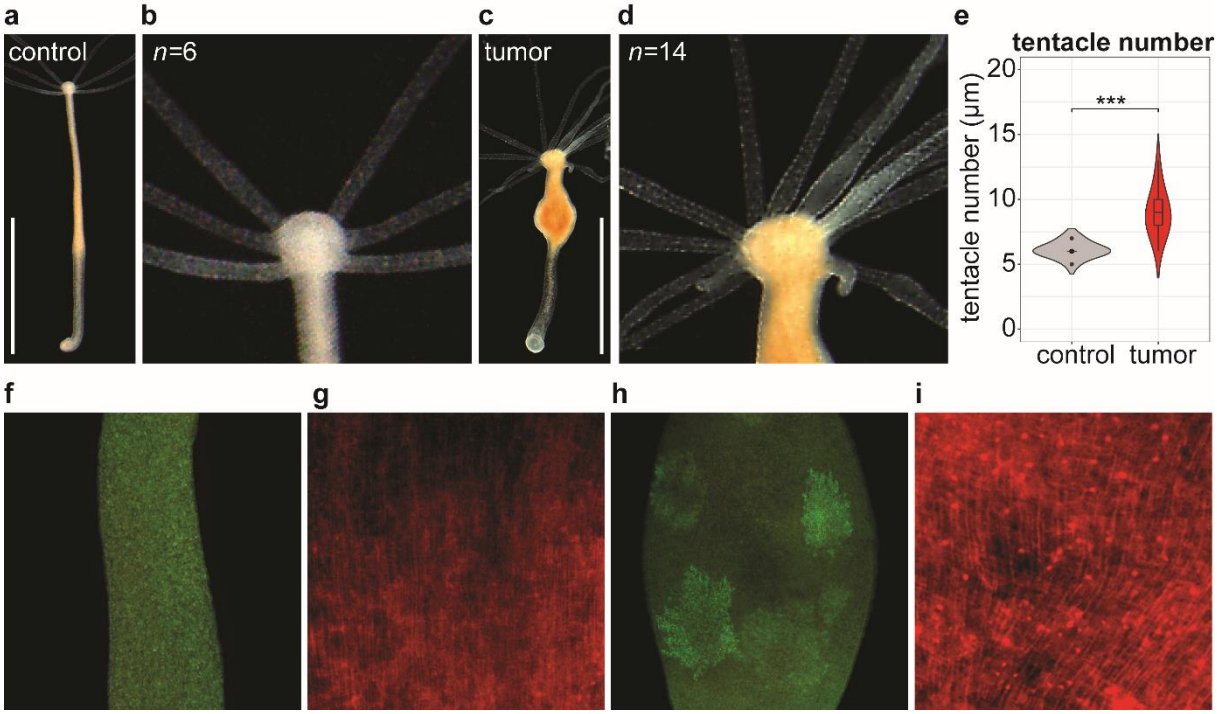

Fig. 2.27: Tumorigenesis phenotype in *P. robusta* shows similarity to *H. oligactis*. (a) Healthy control animals of *P. robusta* polyps show a tube-like body column (scale bar: 0.5 cm). (b/e) the tentacle number is in average 6 tentacles per healthy control polyp. (c) Tumorous polyps of *P. robusta* show similar tumor bulges in the gastric region comparable to tumorous polyps of *H. oligactis* (scale bar: 0.5 cm). (d/e) Tumor polyps in *P. robusta* show an increase in tentacle number up to an average of 9 tentacles per polyps. (f) While control polyps have no germline precursor cells (GCII) in the entire body column, (h) tumor polyps show big clusters especially in the gastric region. (g) The ectodermal actin fibers in control polyps are aligned in a parallel pattern. (i) In contrast tumor polyps show slight changes in the organization of the actin fibers. In the regions of the tumor bulges minor disorganization could be detected. ***:$p \leq 0.001$.

Previous results connected tissue homeostasis and microbiota composition in *Hydra oligactis* and demonstrated a mutual interdependence (Fig. 2.11). Therefore, I hypothesized that the bacterial community in tumor-bearing *P. robusta* in comparison to healthy control animals might be altered. To test this hypothesis, I compared the microbiome of tumorous and healthy polyps by 16S rDNA sequencing. My analysis revealed that the microbiota of healthy polyps, further referred to as control, was dominated by Bacterioidetes and Proteobacteria (Fig. 2.28). Surprisingly, I could not detect any alterations in the microbial community, except a slight and poorly statistically supported increase in the abundance of the Alphaproteobacteria (Fig. 2.28b). Only a small number of OTUs was significantly altered between control and tumorous polyps (Fig. 2.28c/d). Noteworthy, the family of the Cytophagaceae in control polyps increased. Remarkably, only three OTUs (3368, 42267 and

8338) were significantly enriched in tumorous polyps. In sum, only minor changes in the microbiome between control and tumor polyps in *P. robusta* occurred.

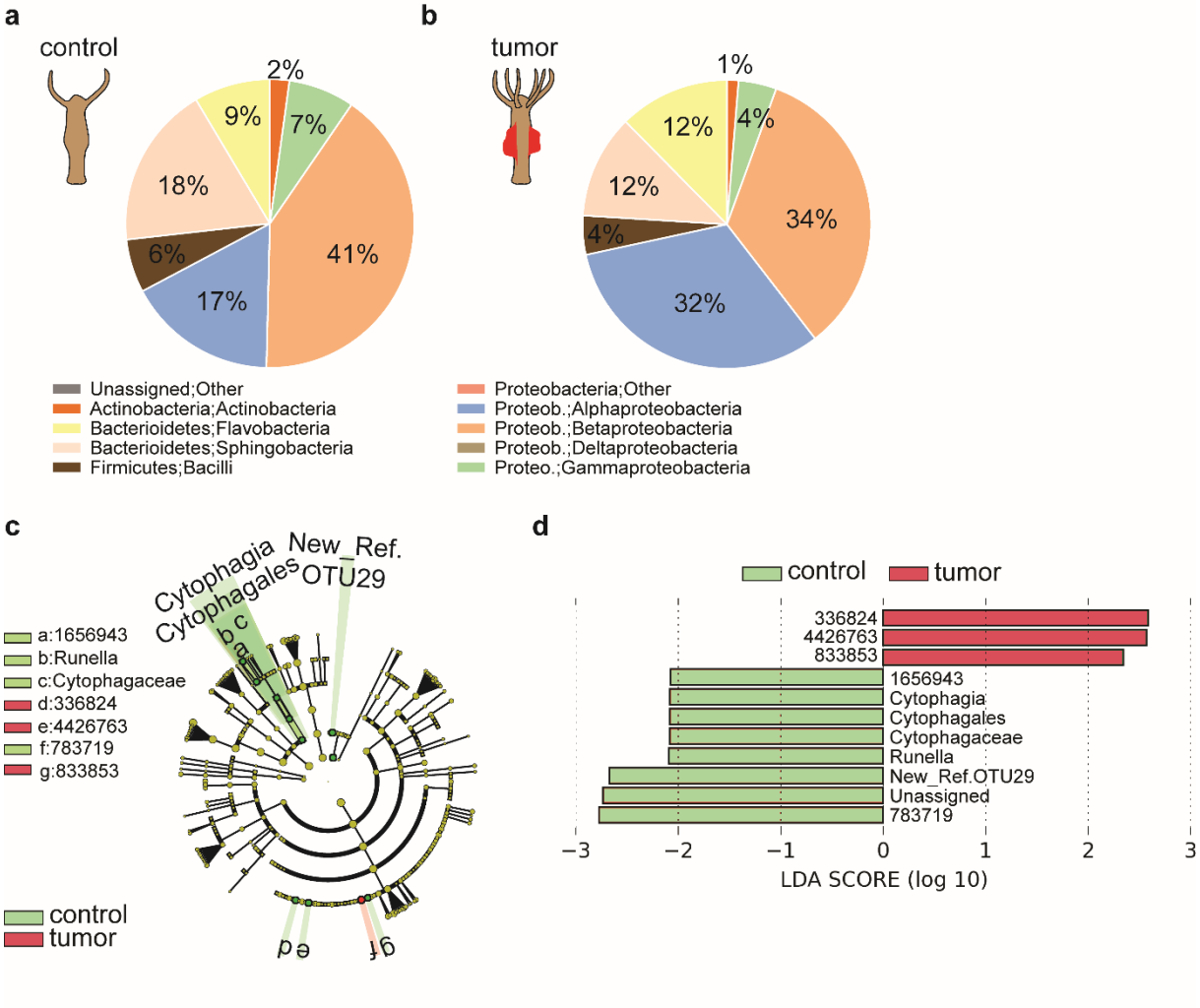

Fig. 2.28: Microbiome of tumor polyps in *P. robusta* is not altered. (a) Control polyps of *P. robusta* are colonized by Proteobacteria and Bacterioidetes. (b) Surprisingly, the microbiome of tumorous polyps showed no major differences to healthy control polyps. (c/d) Taxonomic cladogram presenting OTUs differentially present in the microbiota of control and tumorous polyps of *P. robusta* generated using LEfSe analysis; red - taxa enriched in tumor polyps; green – taxa enriched in intact control polyps. The enrichment of certain taxa in *T. parva*-injected polyps is statistically supported by a positive LDA score values (red), and the taxa strongly enriched in intact control polyps are supported by negative score values (green). In sum, only a few OTUs are significantly altered in control compared to tumor polyps. While no presence of spirochaetes could be detected.

To test further the role of microbiota in tumor formation of *P. robusta*, I treated the tumor-bearing polyps with antibiotics for two weeks (Fig. 2.29). In contrary to the observations on *H. oligactis* (Fig. 2.14), I could not detect any morphological changes in tumor bearing *P. robusta* polyps. After two weeks of antibiotic treatment and post feeding all tumorous polyps (*n*=30/30) still exhibited the tumor bulges and elevated number of tentacles. Collectively, my results indicate that the tumor phenotype in *P. robusta* is independent of the microbiome and likely has a different origin in comparison to *H. oligactis*.

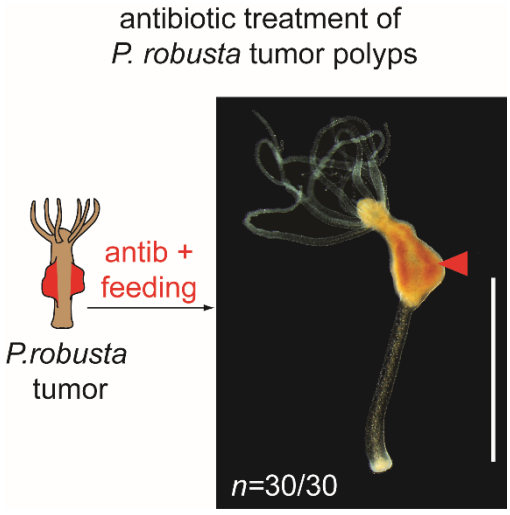

Fig. 2.29: Antibiotic treatment of *P. robusta* tumor polyps hast no effect on polyp's morphology. Germfree-treatment and post feeding of *P. robusta* tumor polyps (*n*=30/30) shows no effect on the tumor phenotype (scale bar: 0.5 cm).

2.11 Spirochaetes presence in other species of *Hydra*

I could demonstrate in previous chapters, that the colonization of *H. oligactis* by *Turneriella* is essential for triggering the complex tumorous phenotype. Noteworthy, *Turneriella*-like spirochaetes are constantly present in some *Hydra* species, such as *H. circumcincta* or *H. carnea*[80]. Even more, there is evidence that the spirochaetes occasionally may colonize the mesoglea in *H. pseudoligactis*[119]. However, no tumors have been described in these species so far. This is consistent with our observation[80] that diverse *Pseudomonas* bacteria, though present in microbiota of these *Hydra* species, do not colonize the ECM. In order to confirm the necessity of *Pseudomonas* (OTU750018) on the ECM to trigger the bacteria interaction and thus tumor formation even in other species than *H. oligactis*, I performed injection experiments with only *T. parva* into two species of *Hydra, Pelmatohydra robusta,* and *Hydra vulgaris* (Fig. 2.30). I hypothesized that the injection of a pure culture of *T. parva* into a host with a bacteria-free mesoglea should have no impact on the phenotype. Remarkably, in all injected animals, *H. vulgaris* AEP (Fig. 2.30a) and *P. robusta T. parva* (Fig. 2.30b) the presence of *T. parva* could be verified by PCR (Fig. 2.30a/b bottom-left corner) indicating a successful colonization. Interestingly, no phenotype changes could be observed in all injected animals. Therefore, consistent with our prediction, *T. parva* is not capable of eliciting tumors without a presence of *Pseudomonas* in the same niche – the mesoglea.

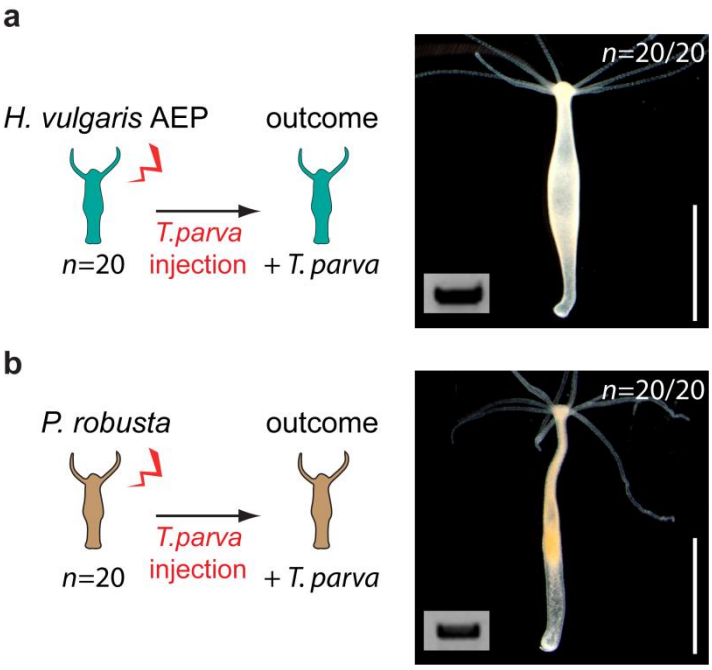

Fig. 2.30: Injection of *T. parva* in different *Hydra* species does not cause tumorigenesis. (a) Injection of a pure culture of *T. parva* in *Hydra vulgaris* AEP (*n*=20). *T. parva* could be detected 30 days post injection via PCR (positive gel band, *T. parva* primer, image bottom left) but polyps lacked the tumor phenotype (scale bar: 0.5 cm). (b) Injection of a pure culture of *T. parva* in *Pelmatohydra robusta* (*n*=20). *T. parva* could be detected 30 days post injection via PCR (positive gel band, *T. parva* primer, image bottom left) but polyps lacked the tumor phenotype (scale bar: 0.5 cm).

As already mentioned, spirochaetes can be constantly present in some *Hydra* species[80]. One outstanding example is *H. circumcincta*. This species shows a microbiome actually dominated by one spirochaete[80]. Since there are no further insights in this spirochaete species, I analysed the previously published data[80] to estimate the relative abundance of spirochaetes in microbiome. Spirochaetes demonstrated indeed a very high relative abundance – over 75%. Further, 16s analysis categorized the dominating spirochaete species as a closely related strain to the spirochaete *Leptospira biflexa serovar* (Fig. 2.9b). Consistently with that, using confocal microscopy I detected spirally-coiled bacteria cells colonizing the mesoglea of *H. circumcincta* with an extremely high density (Fig. 2.31). Noteworthy, the microbiome of *H. circumcincta* also harboured a *Pseudomonas* species. However, its 16s rDNA gene sequence was clearly different from the species colonizing *H. oligactis* mesoglea (Fig. 2.31a). Furthermore, neither rod-shaped cells typical for *Pseudomonas*, nor other bacteria besides the spirochaetes have been detected in the mesoglea of *H. circumcincta*. This is consistent with our model (Fig. 2.24), that spirochaetes are not able to induce tumorigenesis in the absence of *Pseudomonas* colonizing the same niche.

In order to investigate the potential of the spriochaete colonizing the mesoglea of *H. circumcincta* to trigger tumorigenesis, I performed transplantation experiments where the *H. circumcincta* served as a donor of a graft, and healthy *H. oligactis* – as a recipient (Fig. 3.32). One has to take into account, that during interspecies transplantation, the graft, including the epithelial tissue and mesoglea, is connected to the recipient only for a few hours before it is rejected[143]. Still, the time is enough to connect both mesogleas and permit bacteria movement and exchange (Fig. 2.31c). Astonishingly, even by transplanting a different spirochaete species (*Leptospira biflexa* like strain instead of *Turneriella* or *T. parva*) on *H. oligactis*, tumorigenesis was effectively triggered. Similar to the experiments with *Turneriella* injection, development of the tumorous phenotype was gradual and took over three weeks post transplantation (Fig. 2.31c). Further, I was able to amplify the 16s rDNA sequence specific for *Leptospira biflexa* from the resulting tumorous polyps, indicating a successful persistent colonization.

Together, these observations show that any spirochaete species (*T. parva*, *Turneriella*, and spirochaetes from *H. circumcincta)*, presumably every bacterium that can colonize the ECM, is able to trigger tumorigenesis in *Hydra oligactis*. A presence of *Pseudomonas* (OTU750018) in the same niche, the ECM, is a prerequisite for tumor growth to take place.

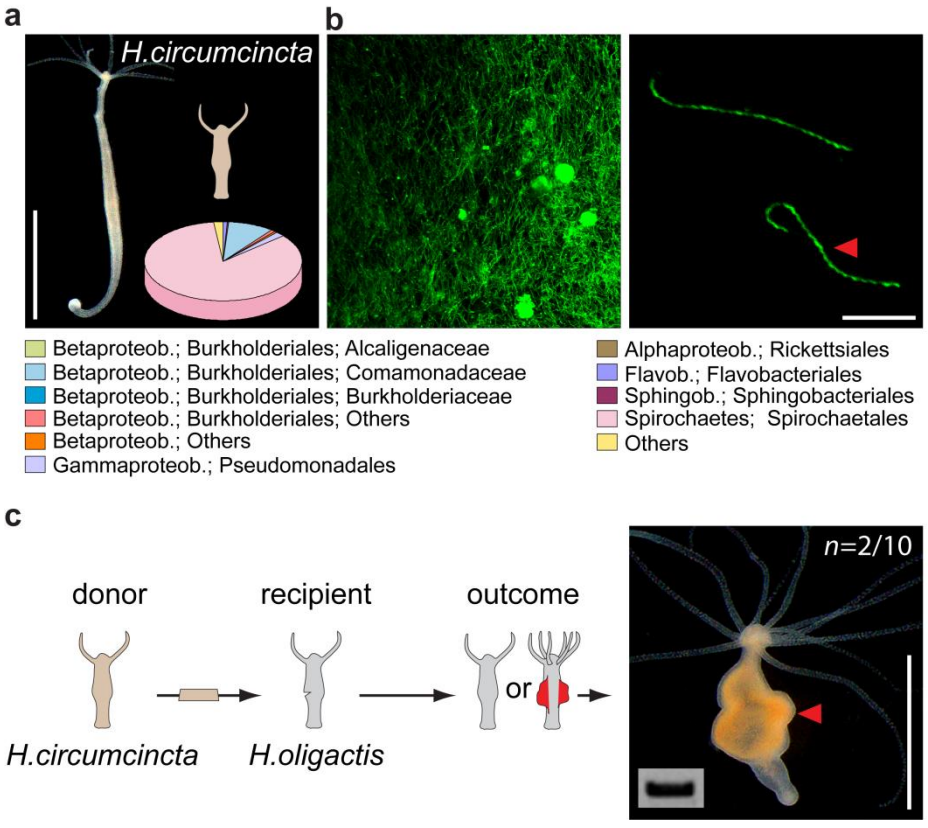

Fig. 2.31: Spriochaetes from *H. circumcincta* can induce tumors in *H. oligactis*. (a) Phenotype of *Hydra circumcincta* polyps is defined by a tube-like body column and a specific microbiome dominated

by spirochaetes (scale bar: 0.5 cm). (b) Helical-coiled spirochaetes colonize the entire *Hydra* ECM visualized on isolated mesoglea with SYBR-gold staining and reach a remarkable body-length (right) (scale bar: 5 µm). (c) In order to proof that this spirochaete is also able to elicit tumorigenesis in *H. oligactis* in the context of *Pseudomonas* (OTU750018), transplantation experiments were performed. Grafts of *H. circumcincta* harboring spirochaetes on the ECM were transplanted on healthy control polyps of *H. oligactis* (*n*=10). 20% of the transplants elicited tumor growth in the recipient. Presence of spirochaetes was screened by PCR (image bottom-left corner) (scale bar: 0.5 cm).

3 Discussion

All animals are prone to tumorigenesis[24,57,112]. All animals species also harbor specific consortia of associated microorganisms – the microbiome[1,5,6,144]. These bacterial communities can affect both, normal physiology and pathological processes, in the host. To what extent and employing what mechanisms does the commensal microbiome contribute to maintaining tissue homeostasis and pathogen defense in its host, remains a fundamental question. Here, using the experimentally traceable model organism, *Hydra,* I uncover the role of the commensal microbiome and environmental bacteria in driving tumorigenesis. My results demonstrate that the interaction of an environmental spirochaete and a commensal pathobiont *Pseudomonas*, both sharing a niche in the extracellular matrix (ECM), elicits tumor formation in *H. oligactis* (Fig. 2.24).

3.1 Environmental spirochaetes drive tumorigenesis in *Hydra*

In a series of experiments (Fig. 2.5-Fig. 2.17), I consistently identified spirochaetes as a causative agent of tumorigenesis. A natural presence of the environmental *Turneriella*-like spirochaete or experimental introduction of *T. parva* or *Leptospira biflexa spec.* effectively elicited tumorigenesis in *H. oligactis*. Remarkably, in all the cases the colonization by spirochaetes caused multiple morphological alterations, developmental changes, and fitness decline in the polyps. Complementary, antibiotic treatment reversed the entire tumor phenotype (Fig. 2.14). All these observations unequivocally point to a high tumorigenic potential of the spirochaetes. On the one hand, since spirochaetes are clearly environmental bacteria typically present in fresh water[145], my observations highlight an essential role of the environment as a source (reservoir) of opportunistic pathogenic microbes that, upon favorable conditions, may colonize a novel habitat - the multicellular host. This role of the environment has to be considered in the context of disease evolution[146,147].

On the other hand, my study uncovered a tumorigenic potential of spirochaetes. Surprisingly, the tumors were elicited by three closely related, yet different spirochaete species. Overall, spirochaetes are known to possess a pathogenic potential and to be implicated in multiple diseases of human and domestic animals. For instance, spirochaetes are chief drivers of pathologies like Syphilis and Lyme disease[148]. However, the spirochaetes have never been reported in association with oncogenic cell transformation.

My results should draw a particular attention to the spirochaetes as widely-spread waterborne infectious agents, capable of inducing tumor formation. Further studies are needed to estimate, whether *Turneriella*-like freshwater spirochaetes can indeed, upon certain circumstances, colonize vertebrate hosts and trigger tumorigenesis in animals and human.

3.2 Bacterial molecules interfere with the tissue homeostasis of *Hydra*

Identification of the virulence of a bacterium is quite intricate. Virulence factor analysis of the genomes from *Pseudomonas* (OTU750018) and *T. parva* (DMSM21527) revealed that both species possess a variety of these virulence factors, which were dysregulated in the transcriptomic data of tumor polyps (Fig. 2.26). Remarkably, the repertoire of pathogenicity factors encoded in the *Pseudomonas* genome is much wider, still it appears to be harmless (benign), when it solely colonizes the mesoglea of *H. oligactis*. Therefore, these factors seem to be only activated or produced, when this bacterium feels threatened or stressed. The variety of virulence factors in *Pseudomonas* can be explained by the close phylogenetic connection to *Pseudomonas aeruginosa* (Fig. 2.9), a well characterized bacterium known for its pathogenic potential[120,140,149]. Moreover, this bacterium is known to be involved in cancer formations[150]. However, the virulence potential of spirochaetes in diseases like Syphilis and lyme disease[148] has been described, but never in cases of tumor formation. Still, there is no pathogenicity effect on mammals known for *Turneriella parva*[151].

Interestingly, the interaction between both bacteria upregulates peptidases and proteases, including collagenases, in the tumor context (Fig. 2.25; Suppl. table 2), which are able to interfere with the ECM (Fig. 2.7) and thus the development of the planar cell polarity[138,139]. This degradation of the ECM and subsequently the actin cytoskeleton disorganization may be the initial damages to *Hydra* (Fig. 2.4 & Fig. 2.7). Factors known to directly manipulate the actin cytoskeleton could be described for a variety of bacteria, including *Pseudomonas*[135,140,152–155] and may explain the tissue disturbance in *H. oligactis*. Notably, the patterning of the actin cytoskeleton determines how and in which direction the tissue growths and subsequently dictates the outgrowth of the bud[156–159]. As a possible defence response *Hydra* produces inhibitors of these peptidases and proteases to countervail the bacterial disturbance[141] as seen in the transcriptomic data (Fig. 2.26d; Suppl. table 2).

In sum, I could identify putative molecular mechanisms of both bacteria, *Pseudomonas* and *Turneriella,* that interfere with the tissue homeostasis of *Hydra*. Above-mentioned bacterial

molecules may disturb the tissue homeostasis and cause alterations in the actin fiber organization (Fig. 2.4), known to be important for cell fate, shape, and development in *Hydra*[68,78] .

3.3 *Pseudomonas* provides colonization resistance

In this study, I could show that the commensal bacterium *Pseudomonas* protects its host *Hydra*, from settlement of the environmental pathogen *Turneriella* (Fig. 2.21). This explains why the "common garden" experiments failed (Fig. 2.10a/b). Only the harsh disturbance by injecting the spirochaetes directly into the mesoglea managed them to settle (Fig. 2.10). Here, the invasion of spirochaetes can be explained due to fluctuations in the abundance of *Pseudomonas* caused by secondary environmental stressors like temperature (Fig. 2.13). Diverse studies have demonstrated a similar principle: the commensal microbiome protects its host from settling of pathogenic bacteria and thus has a beneficial impact on the host's fitness[125,160]. This phenomenon, known as colonization resistance, has been previously described in vertebrate model systems, such as zebra-fish[161] and mouse[162,163], but not in invertebrate taxa. My observations in *Hydra*, an organism phylogenetically distant from the vertebrates, allow considering the colonization resistance in the evolutionary context. In light of my results, colonization resistance provided by the commensal microbiome appears to have deep evolutionary origin and might have emerged equally early as stable associations between microbes and their multicellular hosts - the first metaorganisms.

3.4 *Pseudomonas* contributes to tumorigenesis

Surprisingly, spirochaetes are not sufficient to cause tumorigenesis in *Hydra.* The presence of an environmental stimulus, the spirochaetes, is needed to initiate the interaction of the commensal bacterium *Pseudomonas* and an environmental intruder to form the tumor in *Hydra* (Fig. 2.23). On the one hand, *Pseudomonas* remains a silent commensal bacterium on the mesoglea of healthy *Hydra* polyps. On the other hand, in the presence of the spirochaetes it turns into a pathobiont, whereby it expresses a rich repertoire of pathogenicity factors and likely interferes with the host tissue homeostasis resulting in tumor formation.

Therefore, my study demonstrated that a member of the normal microbiome may become pathogenic and induce tumor formation. Recently an increasing number of studies highlights

that the interaction between commensal bacteria, termed as pathobionts, elicits and/or fuels tumor formation[43,48,164,165]. One study describes the link between early neoplasia of the colon and tumorigenic bacteria. Interestingly, both bacteria are naturally appearing in humans but only by changing the niche in its host and cooperation they become pathogenic[48]. The fact that the presence of a single pathogen or the ongoing interaction between a pathobiont and a pathogen elicits tumor formation has been reported[25,48]. Taken together, these findings provide a new perspective onto the normal commensal microbiome as a source of putative tumorigenic microbes.

My results also uncovered the conditions that trigger *Pseudomonas* to unveil its pathogenic potential, namely – the infestation with spirochaetes. Indeed, *Pseudomonas* acts cooperatively with spirochaetes in triggering the tumorigenesis. Similar synergistic interactions, between bacteria that manipulate tissue homeostasis in the host, were previously described in other systems[44,48,164]. Taken together, these observations highlight the role of interactions within complex microbial communities in disease aetiology, and urge to move away from the simplistic paradigm “one microbe – one disease”[166].

Experiments like the spontaneous loss of *Pseudomonas* (Fig. 2.22) and the bacteria transplantation experiments (Fig. 2.23) onto the tumor phenotype demonstrate the importance of *Pseudomonas* in tumor formation. The spontaneous loss of *Pseudomonas* can hereby be explained by the spatial occurrence of *Pseudomonas* in tumorous polyps (Fig. 3.1) like it was observed in several experiments (Fig. 2.6 & Fig. 2.8).

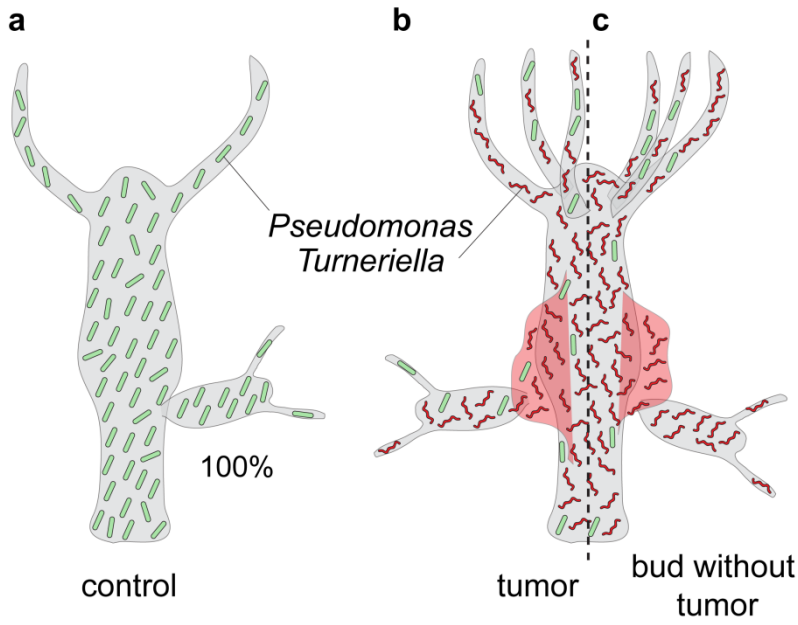

Fig. 3.1: Spontaneous loss of *Pseudomonas* during budding caused by bacterial spatial distribution. (a) In control polyps *Pseudomonas* solely colonized the mesoglea and is transferred to the offspring (bud) in 100 % of the cases. (b) In tumorous polpys *Turneriella* mainly colonizes the mesoglea especially the gastric region. *Pseudomonas* is present but displaced in the hypostome, tentacles or the peduncle. Still, it manages to be transferred, next to *Turneriella*, into the next generation by asexual budding. (c) If the bud of a tumor polyp generates in an area with no presence of *Pseudomonas* and high density of *Turneriella* it results in a non-tumorous polyp with a mesoglea densely colonized by *Turneriella*.

Pseudomonas (OTU750018) has never been observed in other species of *Hydra.* This could imply that the *Pseudomonas* species itself is an invader which is only able to colonize the mesoglea of *H. oligactis* St. Petersburg. A higher fragility of tissue homeostasis or a different ECM nutrient composition in *H.* oligactis[69,119,167] could be explanations for the colonization of *Pseudomonas*. Thus, tumor formation only occurs in *H. oligactis* St. Petersburg and not in other species which are colonized by spirochaetes.

The tumorous polyps show morphology alterations, fitness problems (Fig. 2.2, Fig. 2.3 & Fig. 2.4) and further characteristics which have been partially prior to this thesis, described[101]. Unlike at that time findings can be interpreted differently. For example, the transplantation experiments which resulted in tumorous growth in the recipient, at that time only explained by the migration of germline precursor cells, is now clearly driven by the pathobiont-pathogen interaction on the mesoglea into the healthy host.

Taken together, my findings clearly indicate that antagonistic interactions between two microbiota members, *Pseudomonas* and *Turneriella*, have profound effects onto their host tissue homeostasis and fitness.

3.5 Continuous presence of both bacteria is necessary to sustain tumorigenesis

The effect of single microbes which can drive cancer has been repeatedly reported[29,168]. In some patients the infection by *Helicobacter pylori* can cause long-lasting inflammation in the stomach and stomach ulcers that elevate the risk of gastric cancer development[28]. Once bacteria triggered the inflammation of the host tissue the tumor growth is not reversible.

For most cases, where bacteria are described in association with tumors, an initial infection is sufficient to trigger the oncogenic transformation[34,169]. Further tumor growth and development is independent of the presence of the initial trigger. Surprisingly, in my study, I uncovered the opposite: a continuous interaction of both bacteria, *Pseudomonas* and spriochaetes, is necessary to sustain the tumor formation. In fact, it is possible to ameliorate some cancer types by antibiotic treatment[170]. However, the clearance of the entire tumor phenotype by a single antibiotic treatment, like it has performed in this study (Fig. 2.14), has never been described before. In all, this finding brings new perspectives in medical therapy.

3.6 Plausible scenario of tumor development in *Hydra*

Previously, the naturally occurring tumors in *H. oligactis* have been described[101]. However, two aspects remained unclear. First, what was the initial trigger that caused appearance of the first tumor in the founder polyp? Second, the molecular events underlying the tumor growth remained exclusive. My work provided insights into the both questions.

Turneriella is evidently constantly present in the environment, yet is not able to colonize the host unless its colonization resistance, partially provided by the commensal microbiome, is breached by stress. It is likely, that the initial founder polyp in the mass *H. oligactis* culture has experienced some kind of stress, likely – short water temperature increased. This allowed the spirochaetes to colonize the polyp. Overall, all my experiments indicate that the colonization of *Hydra* by spirochaetes is a low efficiency process. Therefore, it is not surprising, that just a single polyp among hundreds got infected.

Further, *Turneriella* colonized the mesoglea of the polyp – the niche already occupied by *Pseudomonas*. There, in the ECM, both bacteria interact and produce multiple factors which are primarily active to defend from other bacteria and further digest the ECM, but secondarily affecting the host. These virulence factors disturb the organization of the actin fibers and dissolve the ECM. Epithelial and aberrant germline precursor cells accumulate, tentacle

number increases, and fitness problems occur which in the end complete the given tumorous phenotype. Further, upon budding, both bacteria are typically transferred into the bud, leading thus to a clonal propagation of tumorous polyps. This process lasts already over 10 years, since the first discovery and isolation of the tumorous founder polyp[101].

Since the initial colonization requires a co-occurrence of multiple factors (presence of spirochaetes in the medium in sufficiently high concentration, stress-induced weakening of the polyps resistance, and presence of a specific *Pseudomonas* strain in the host mesoglea), it is not surprising that spontaneous occurrence of tumors have not been repeatedly observed. Tumors in *Hydra* induced by environmental spirochaetes remain a serendipity, yet uncovers fundamental principles of host-microbiome interactions.

This work shows the dual role of a commensal pathobiont interacting with an environmental intruder, which acts as a stimulus, to elicit autonomously tumor formation in *Hydra*. This could be further underpinned by the transcriptomic- and genomic analyses (Fig. 2.26). Here, I try to sum up the results which describe the etiology of the tumor phenotype in *H. oligactis.*

In brief, during a stressed period of *Hydra* infection, augmentation of *Turneriella* takes place. *Turneriella* replaces *Pseudomonas* on the ECM on large scale and the interaction of both bacteria produces a potential effector which reaches a causal potential to the host. In the following way, I tried to visualize (Fig. 3.2) the occurrence of all events in the following hierarchy.

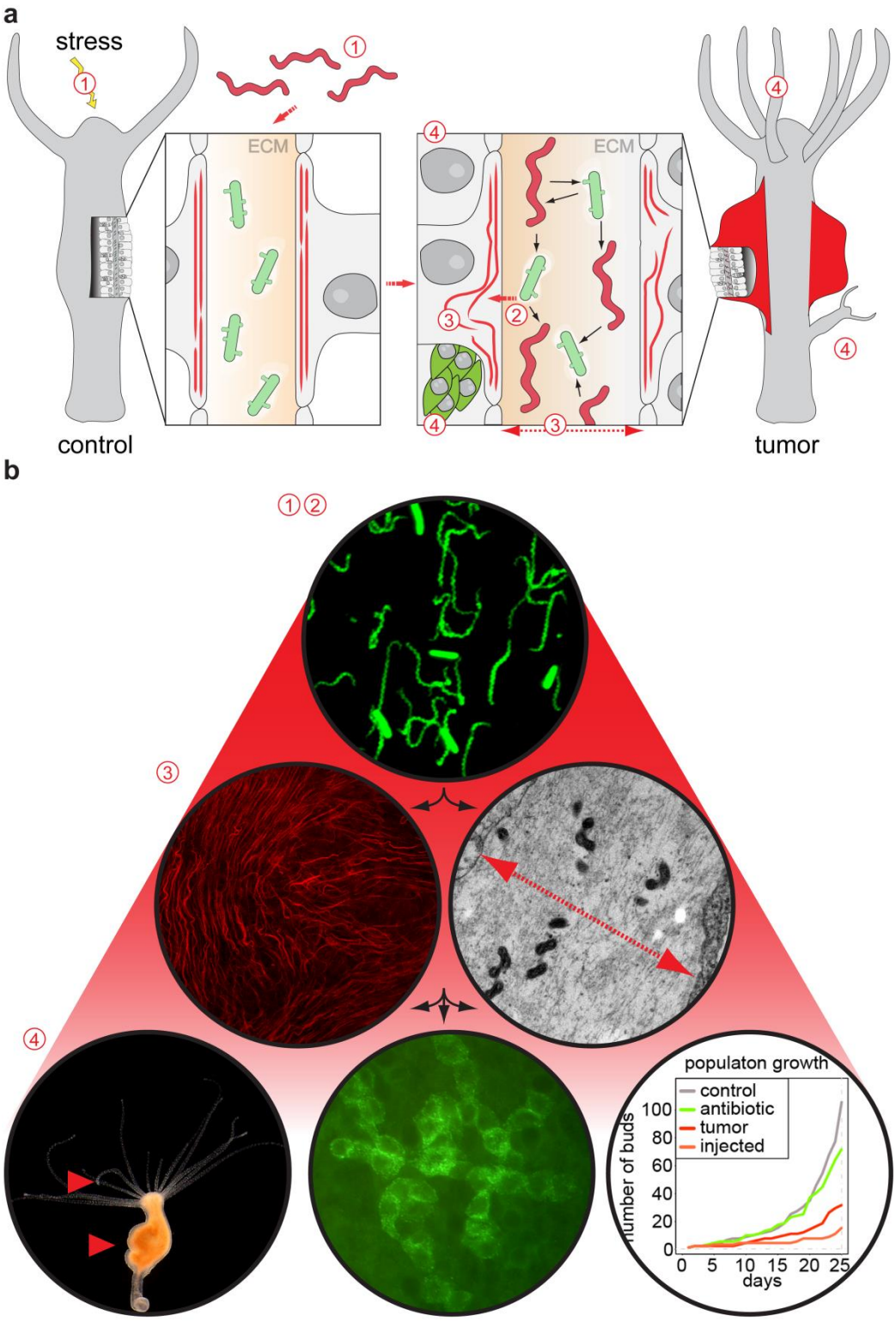

Fig. 3.2: Hierarchy of events happening during tumorigenesis in *Hydra*. (a) (1) Environmental stress to the host and mesoglea degrading *Pseudomonas* opens the niche for spirochaetes to settle. (2) Interaction between *Turneriella* and *Pseudomonas* replaces *Pseudomonas* and produces virulence factors which induce tumorigenesis. (3) First host responses are disturbances of the actin fiber cytoskeleton and thickening of the mesoglea. (4) Disturbances of these factors results in the last wave of events including increase of epithelial cell number and occurrence of aberrant germline precursor cells resulting in the gastric region (red arrow; bottom). Further tentacle number increases (red arrow; top) and fitness loss - decelerated asexual reproduction is caused by reduced detachment time. (b) Visualization of the different, hierarchical ordered subitems 1-4.

4 Conclusion and outlook

In this study, I aimed to identify the origin of tumorigenesis in *Hydra.* I demonstrated that the tumor growth in *H. oligactis* affects the development, morphology, and fitness of these polyps. I could show that the microbiome in tumorous polyps is changed in comparison to healthy control polyps. Here, tumor polyps are invaded by an environmental spriochaete. Further experiments showed that the disruption of the microbiome is sufficient to elicit tumorigenesis in *H.* oligactis. The interaction between the environmental pathogen *Turneriella* and the commensal *Pseudomonas* was able to induce tumor formation in *Hydra.* Genomic and transcriptomic studies of the host and the both bacteria indicate putative genes (virulence factors) which are able to interfere with the tissue homeostasis in *Hydra*. This data suggests that the commensal bacterium *Pseudomonas* has a dual role as a pathobiont. Solely, on the mesoglea, it protects from pathogens by colonization resistance. If an intruder, like *Turneriella*, enters its field it promotes tumorigenesis by niche competition.

Future perspectives in this project will focus on the identification of these virulence factors. This analysis could include tracing of potential molecules secreted by both bacteria in the tumor context by proteomics (Fig. 4.1).

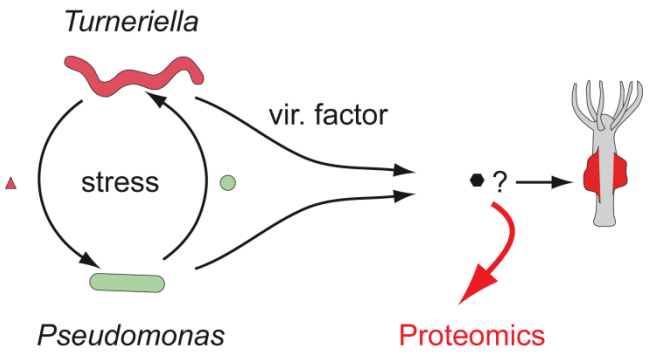

Fig. 4.1: Bacterial interaction uncouples pathogenicity. Model how the interaction between the both bacteria, *Pseudomonas* and *Turneriella,* produce one or multiple unknown virulence factors which in the end elicit tumor growth in *Hydra.*

Finding answers to this remaining question will expand our understanding of bacterial driven tumorigenesis and especially how commensal bacteria interact with environmental pathogens and thus become pathogenic themself. The research of bacteria driven tumorigenesis is only in the beginning. Investigations, in a phylogenetically basal organism like *Hydra* are instrumental in uncovering the fundamental mechanisms of tumorigenesis and interactions within a metaorganism.

Altogether, these findings point to the evolutionary conserved defying role of the commensal bacteria in maintaining the host tissue homeostasis. Finally, I demonstrated that phylogenetically basal organisms, like *Hydra,* are instrumental in uncovering the fundamental mechanisms of tumorigenesis and interactions within a metaorganism.

5 Methods

5.1 Animals and culture conditions

Experiments were carried out using *Hydra oligactis* strain St. Petersburg, *Pelmatohydra robusta* (strain L7), *Hydra vulgaris* strain AEP and *Hydra circumcincta*. Animals were maintained under constant environmental conditions, including *Hydra* medium (HM: 0.28 mM $CaCl_2$, 0.33 mM $MgSO_4$, 0.5 mM $NaHCO_3$ and 0.08 mM KCO_3), temperature (18°C) and feeding regime (twice a week) according to standard procedures[171]. Natural occurrence of tumor polyps has been already described[101]. Tumor buds have been separated from the original cultures and been kept in pure tumor cultures. The majority of the buds attain the tumor phenotype after around 4 weeks. In rare cases buds do not exhibit the tumor phenotype and remain healthy. These specific buds were separated and kept in culture. In this study experiments were primarily performed with the *H. oligactis* St. Petersburg species (2.1-2.11). All animals which were used in the experiments were clones from the same culture.

5.2 Fitness measurement

Success of asexual reproduction by budding defines fitness in *Hydra* and is measured by its population growth rate. For this a single polyp for each treatment served as founder for a clonal population. Progeny of this polyp and all other following offspring's were set individually in single 12-well plate cavities until at least 100 polyps were generated by feeding five times a week. Developmental stages and detachment rate of all polyps were assessed every 24 h. For population growth rate calculation the experiment was split in sub-experiments at the second generation. Since *Hydra* grows clonally and the genotype is the same for one line, the resulting sub-experiments were treated as independent replicates. For growth rate calculation a regression of the $\log^2$-transformed polyp number per time unit was performed and the slope of the curve as descriptor for growth rate was used. For data analysis a MySQL-database as well as custom written python and R functions have been developed.

Bud detachment time is the time a bud needs from the first visible protrusion to full detachment from the mother-polyp. This time points were taken out of the population growth

data (*n*=100 for each treatment). The number of tentacles was counted on randomly picked polyps of each condition under the microscope.

5.3 Isolation of the mesoglea

Isolation of the *Hydra* mesoglea was performed as previously described[167]. Adapted from the protocol IGEPAL ® CA-630 was used (1:1000 in ddH_2O, Sigma-Aldrich, Germany) to separate the mesoglea from the *Hydra* cells. The isolated mesoglea was used for the Isolation of *Pseudomonas* (OTU750018) in a pure culture and additional SYBR-gold immunostainings.

5.4 Transplantation experiments

Transplantation of interspecies grafts were performed as described[172,173]. If otherwise not mentioned the method of axial transplantation was performed using a fishing line (35mm) to line up the graft and the recipient and rubber stoppers to keep the animals together for 2 h to let the tissues attach. After 2 h the fishing line and stoppers were removed and animals were kept in separate dishes with fresh HM. Overlaying grafts were cut off after 24 h. Phenotypes could be observed and evaluated after 4 weeks post transplantation.

5.5 Elimination of interstitial cells

Hydroxyurea treatment was performed to evaluate the importance and influence of aberrant female germline precursor cells (GCII cells) during tumor formation. *Hydra* were treated with 0,01M hydroxyurea (HU) as described[174]. This treatment consisted of 4 cycles of 24 h each in HU separated by 30 min in HM. Treated animals were subsequently cultured comparable to normal cultures. After 4 cycles of treatment animals were washed several times in sterile filtered HM and kept in sterile filtered HM for 7 days until evaluation.

5.6 Immunohistochemistry

Immunohistochemical detection of periculin protein in whole mount *Hydra* preparations was performed as earlier decribed[93] using polyclonal mouse antisera against periculin 1a protein (1:500 diluted, produced by the Bosch lab) and Alexa conjugated donkey anti mouse secondary antibodies (2 µg ml^{-1}; Invitrogen, USA). Phalloidin stainings were conducted as described previously[175]. Microscopy images were performed using the TCS SP1 laser-scanning confocal microscope (Leica, Germany). SYBR-gold staining of *Pseudomonas* (OTU750018), *Turneriella* (OTU4017244), and *Turneriella* on the mesoglea was performed after the isolation of the mesoglea. After three times of washing in sterile ddH_2O the mesoglea was stained with SYBR-gold (1:20,000 in ddH_2O; Thermo Fisher Scientific, USA) for 3 min in the dark at room temperature. After staining the mesoglea was washed three times for 5 min. in ddH_2O, placed on object slide and embedded in Moviol-Dabco[176].

5.7 Transmission electron microscopy

For images of the cross sections of control and tumor animals including the present bacteria on the mesoglea polyps were not fed for three days. Protocol for the TEM was performed like previously described[177]. TEM pictures were taken using the Tecnai™ G^2 Spirit/BioTWIN (FEI Company™, Thermo Fisher Scientific, USA).

5.8 Measuring mesoglea thickness

To measure the thickness of the individual mesoglea cross sections (60 nm) through the polyp's body column were taken. For each conditions (control and tumor) the average thickness of each mesoglea was measured and calculated (n=12). The average mesoglea thickness of each cross section was calculated from 10 measuring locations in the same distribution (clockwise).

5.9 Tissue digestion and cell number measurement using flow cytometry

To compare the number of cells between control and tumor polyps, single polyps were digested and subsequent cell number was measured by flow cytometry[114]. Only animals of the early budding stage were selected from each culture. Individual polyps were digested in 100 µl of 50 U/ml Pronase E (Serva, USA) in an isotonic culture medium[178] and inverted continuously after 10 minutes for 4 hours at 18 °C. The living cells were measured using the BD FACSCalibur with CellQuestPro v5.2 (Becton-Dickinson, USA) using forward and side scatter with a blue 488 nm laser to gate the epithelial cells. Localization of epithelial cells was previously determined by measuring transgenic GFP expressing epithelial *H. vulgaris* (AEP) lines[179] using the FL-1 filter (530/30 nm). Further analyses including gating were performed with FCSalyzer 0.9.13 alpha (https://sourceforge.net/projects/fcsalyzer/).

5.10 RNA-Seq analyses

For metatranscriptome sequencing 5 replicates of control, female, and tumor polyps of both species (*H. oligactis* & *P. robusta*) were taken. The results for *P. robusta* are not shown in this work. Each replicate contained a pool of 15 to 20 animals. After sampling, animals were frozen in TRIzol (Thermo Fisher Scientific, USA) at -20 °C until RNA extraction with the PureLink RNA Mini Kit (Ambion, Germany) according to the manufacter's protocol. The optional on-column rDNA-digestion was additionally performed. The RNA was eluted in 30 µl of elution buffer and tested for sufficient quality and quantity and frozen at -80°C until further use. Total RNA sequencing was performed for 30 libraries on the Illumina HiSeq2500 v4 platform, with 125 bp paired-end sequencing of 12 libraries per lane. This resulted in 30 million reads per sample after quality control. Adapter and quality were trimmed using PRINSEQ-lite 0.20.4[15] and Cutadapt 1.13[180]. Mapping against the transcriptome[181] of db454_holi_female_newbler_final, *Turneriella parva* DSM21517 and *Pseudomonas* (OTU750018) pas performed using Bowtie2 2.2.9[182] All downstream analyses were conducted in "R"[183]. Differentially expressed contigs were identified with the package DESeq2 1.16.1[184] after batch correction with SVA[185].

5.11 Bacteria culture conditions and generation of germfree *Hydra*

To obtain germfree (GF) *H. oligactis* polyps were kept for 2 weeks in an antibiotic solution containing 50 µg/ml each of ampicillin, rifampicin, streptomycin, spectinomycin, and neomycin with exchange of the solution every second day. After the treatment, the polyps were transferred into sterile-filtered and autoclaved HM for one week again changed every second day. The absence of bacteria was verified by a 30-cycle PCR using the universal 16s bacteria Primer EUB_27F and Eub_1492R[128], whereas the positive control of none-treated (DMSO) polyps showed a positive signal. *Turneriella* from *H. oligactis* was not cultivable, therefore the closest relative *Turneriella parva*[151] DSM 21527 was ordered and kept in Leptospira semisolid medium which was produced and handled based on the manufactures protocol (Difco™ Leptospira Medium Base EMJH & Difco™ Leptospira Enrichment EMJH; Thermo Fisher Scientific,USA). *Turneriella* was inoculated twice a week to new bacterium media (2 µl) to keep the culture alive because glycerol stocks and other storing methods failed. To test specific for the presence of *Turneriella* (OTU4017244) following primers have been used: For: GAGGAACACGTAGGAATCTACC; Rev: AACCCAACATCTCACAACACGAG & qRT For: TACAGAGGGACGCAATGCC; qRT Rev: GTTGGCACCAGCCTCTTCG). To test specific for the presence of *Pseudomonas* (OTU750018) following primers have been used: For: CCGTTGGGAGTCTTGAGCTC; Rev: CGTGGTAACCGTCCTCCCTA & qRT For: CCTAGTGGTGGGGGATAACG; qRT Rev: GGTGGAGCCATTACCTCACC (Suppl. Table 10).

5.12 Isolation of Pseudomonas

Hydra oligactis Pseudomonas (OTU750018) was isolated from the ECM of *Hydra oligactis* control polyps. The ECM was isolated as described before to get rid of all bacteria present on the glycocalyx to simplify the isolation. *Pseudomonas* was singularized from a bacterial mixture on R2A-AGAR (Carl Roth, Germany) plates and identified by 16s Sanger sequencing (IKMB, Kiel).

5.13 Quantification of Bacterial 16S Genes by qRT-PCR

Total bacterial quantification was performed with the original DNAs used for 16S rDNA high troughput-sequencing. Template amounts were equilibrated for the *Hydra* actin gene

(hy_actinF 5´-TTCACGTTCAGCAGTAGTAGT-3´ and hy_actinR 5´AAGGATATGCTCTTCCCCATG-3´). Bacterial DNA was quantified with the universal primers Eub341_F and Eub534_R[186]. For *Turneriella* (OTU4017244) the primers under 5.11 have been used.

Fold-change was calculated using the formula fold-change = $2^{-\Delta\Delta Ct}$ with Ct being the PCR threshold cycle. Fold-changes were normalized to the given control polyps.

5.14 Common garden & injection of *Turneriella parva* DSM21527 in *Hydra oligactis*

Common garden experiments, to colonize control polyps with spirochaetes, were performed in specific coincubation chambers. These separated control and tumor polyps (*n*=50) by a thin net but allowed the exchange of media and thus bacteria. Polyps were treated equally under normal culture conditions (5.1). The experiment was stopped after three months. Inoculation of 50 control polyps with a pure culture of *T. parva* ($20*10^6$ bacteria per 50 ml tube) was performed for three days. Polyps were evaluated 40 days post treatment for the presence of *T. parva* and the tumor phenotype.

Polyps of *Hydra oligactis* were injected with a pure culture of *Turneriella parva* DSM21527 (*T. parva*). The injection solution (grown culture & sterile ddH_2O) was adjusted to 20,000 bacteria per 1 µl by counting the bacteria with a C-Chip Disposable Hemocytometer DHC-N01 (NanoEnTek, USA). For visualization under the counting chamber bacteria were stained with methylene blue. *T. parva* was injected directly in the tissue by carefully mouth-blowing the bacterial mixture with an self-made aperture (self-pulled glass-needles connected to a rubber tube and a sterile 0,2 µm filter (Filtropur, Sarstedt, Germany)) to not harm *Hydra* by the air pressure. Polyps were kept in the bacterial media for 24 h and subsequent moved into new dishes with fresh HM. Phenotypes were observed after 40 days post injection (positive) if not the injection for these polyps was counted as negative.

5.15 DNA Extraction and Sequencing of bacterial 16S rRNA and genomes

For total DNA extraction, single polyps (six replicates for each treatment) were washed three times in sterile HM and subjected to the DNeasy Blood & Tissue Kit (Qiagen, Germany). Extraction was performed following the manufacturer's protocol, except that DNA was eluted

in 30 µl and kept at -20°C until sequencing. Before sequencing, the variable regions 1 and 2 (V1V2) of the bacterial 16S rRNA genes were amplified using the primers 27F and 338R[187]. Bacterial 16S rRNA profiling was performed in the Illumina MiSeq platform with paired-end sequencing of 2x 300bp. Sequence analysis was executed by using QIIME 1.9.0 package (RRID:SCR_008249)[188]. SeqPrep was used to assemble Paired-end reads (RRID:SCR_013004), chimeric sequences were screened with ChimeraSlayer (RRID:SCR_013283)[189] and manually checked prior to the removal from the data set. Sequences were kept in the analysis if they have been present at least in two independent samples. For the genome sequencing of the *Pseudomonas* (OTU750018) a pure culture was grown over night in R2A media, purified by several washing steps in sterile PBS and then subjected to the DNeasy Blood & Tissue Kit (Qiagen, Germany). To get the genome of *Turneriella* (OTU4017244) the mesoglea was isolated from tumor-bearing animals, purified by several washing steps in sterile PBS, and subjected to the DNeasy Blood & Tissue Kit (Qiagen, Germany). Nextera XT kit (Illumina, USA) was used for library preparation and paired-end sequencing was conducted on a MiSeq platform (Illumina, USA) at Centre for molecular biology in Kiel. Genomes and metagenomes were assembled with spades 3.12 (standard settings). Several complementary approaches were used to annotate the assembled sequences. First annotation was performed with Dfast_core (v.1.0.8). The genes were annotated by aligning the sequence with sequences previously deposited in diverse protein databases including the National Center for Biotechnology Information (NCBI; https://www.ncbi.nlm.nih.gov/) non-redundant protein (Nr) database, UniProt/Swiss-Prot (https://www.uniprot.org/[190]) and Kyoto Encyclopedia of Genes and Genomes (KEGG; https://www.kegg.jp/[191]). Additional annotation was carried out using the following databases: Virulence Factors of Pathogenic Bacteria (VFDB; http://www.mgc.ac.cn/VFs/main.htm[192]) and antibiotics & Secondary Metabolite Analysis Shell (anti-smash; https://antismash.secondarymetabolites.org/#!/start[193]). Prophages were identified using the PHAge Search Tool (http://phast.wishartlab.com[194]). Nr and GO annotation was carried out using Blast2GO. An E-value of $1e^{-5}$ was used as the cut-off for all basic local alignment search tool. The quality of the metagenome of *Turneriella* from *H. oligactis* was too low that further work and results based on the *T. parva* DSM 21527 species.

5.16 Bacterial community analysis

Picking Operational Taxonomic Units (OTUs) was performed using the pick_open_reference_otus.py script with at least 97% identity per OTU and the UCLUST

algorithm (RRID:SCR_011921) was used to operate the annotation[195] against the GreenGenes database v13.8 (RRID:SCR_002830)[196] implemented in QIIME. To avoid false positive OTUs originated from sequencing errors OTUs with <50 reads were removed from the data set[197]. Read number was normalized to the lowest number of reads in the dataset (8,000). Bacterial groups of control versus tumor and control versus injected were identified by LEfSe (RRID:SCR_014609)[198]. To obtain statistical significance LEfSe couples robust tests (Kruskal–Wallis test) with quantitative tests for biological consistency (Wilcoxon signed-rank sum test). Effect size ranks the differentially abundant and biologically relevant bacterial groups after proceeding linear discriminant analyses. P-values were rectified for multiple hypotheses testing by Benjamini and Hochberg's false-discovery rate correction (q-value). A q-value of 0.001 and an effect size threshold of 4.0 (on a $\log_{10}$-scale) were used for all comparisons discussed in this study.

5.17 Phylogenetic analysis.

For the calculation of the bacteria trees for *Pseudomonas* and *Turneriella*, a nucleotide alignment of the 16s sequence of each bacteria was used (Suppl. table 1). Trees were simplified and adapted from[199] and from[200]. Sequence alignment for the 16s was generated using Clustal_x[201] and subsequently imported into MEGA 5 sequence analysis software package. A model-test was used to estimate the best fit substitution models for phylogenetic analyses. For the maximum-likelihood analyses, genes were tested using the General Time Reversible (GTR + I) model. A bootstrap test with 1000 replicated for maximum likelihood and random seed was conducted[202–205].

5.18 Statistics

Statistical analyses for the 16s rDNA data were performed using two tailed Student's t-test or Mann-Whitney U-test if applicable. If multiple testing was performed, p-values were adjusted using the Benjamini-Hochberg correction[206]. Statistics for the fitness measurements were performed using One-Way-ANOVA (Kruskal-Wallis test) and an additional Dunnett's multiple comparison post-test comparing all values to the control. To test the statistical significance of the variance between different samples the levene-test was performed. All other differences were tested using Wilcoxon rank sum test or ANOVA[183].

6 Supplementary figures

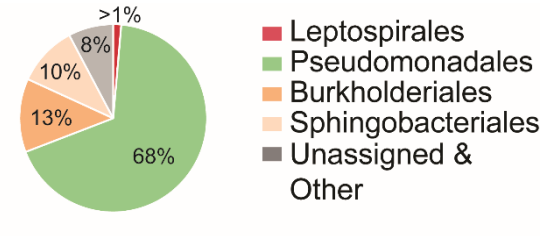

Suppl. Fig. 6.1: Bacterial OTU abundance pi of injected control polyps without the tumor phenotype. Abundance of *T. parva* in injected polyps without a phenotype is below 1%.

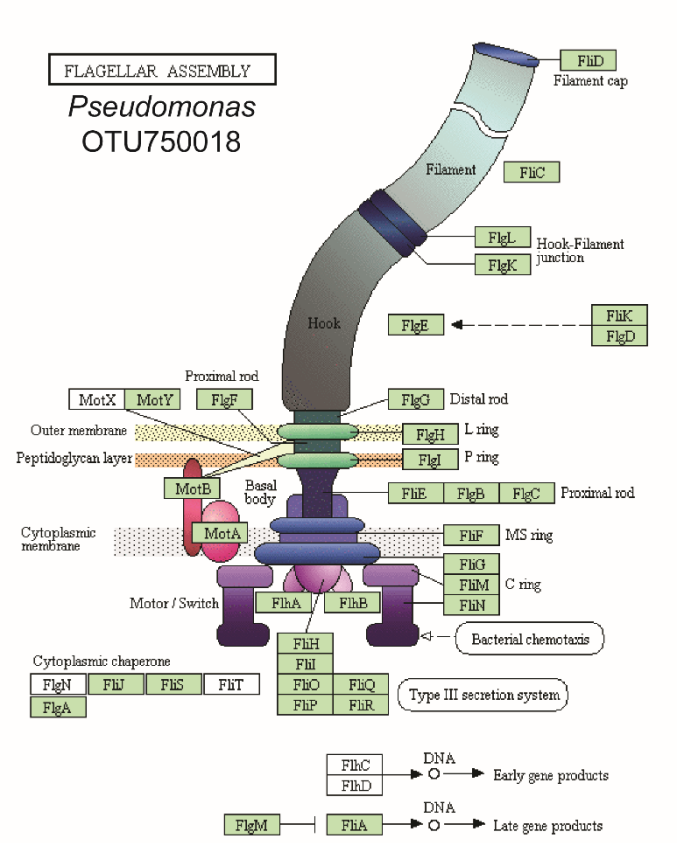

Suppl. Fig. 6.2: The flagellar assembly. Genes linked to the bacterial flagellum and present in the *Pseudomonas* genome are shaded in green other remain white. *Pseudomonas* seems to have an intact flagellum[191].

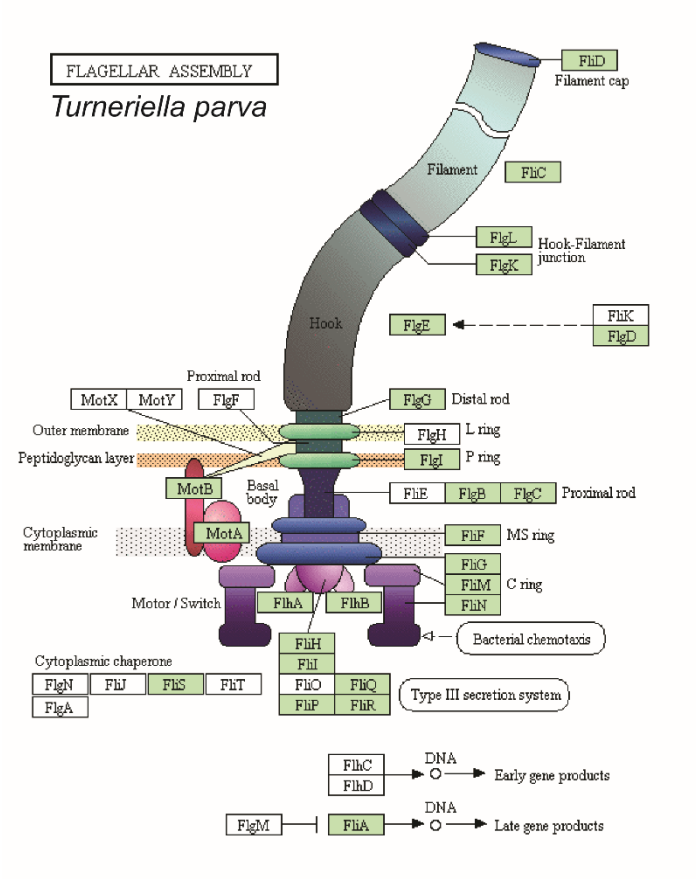

Suppl. Fig. 6.3: The flagellar assembly. Genes linked to the bacterial flagellum and present in the *T. parva* genome are shaded in green other remain white. *T. parva* seems to have an intact flagellum[191]. The endoflagella of the most spirochaete species is located in the periplasm between the inner cytoplasmic membrane and the outer membrane and permits fast motility.

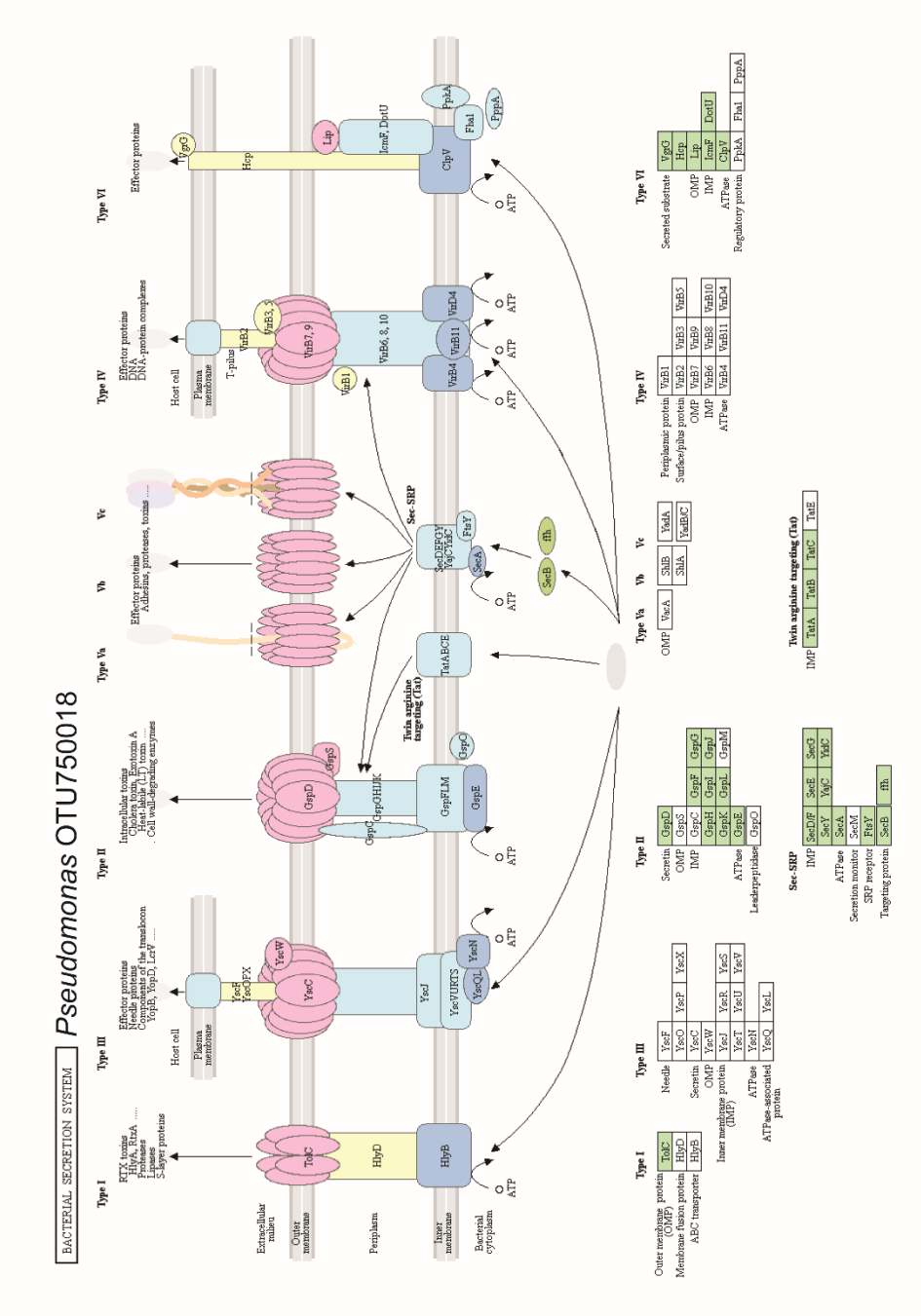

Suppl. Fig. 6.4: The Bacterial secretion systems. Genes linked to the bacterial secretion systems II & VI are present in the *Pseudomonas* genome and shaded in green[191]. Only a few genes are missing in the annotation of KEGG. The secretion system II is a protein secretion machinery found in various of Gram-negative bacteria. It enables the transport of cytoplasmic proteins across the lipid bilayers. The type VI secretion system is also used by a wide range of Gram-negative bacteria species to transport proteins from the cytoplasm of a bacteria cell in the cellular envelope of the adjacent eukaryotic or prokaryotic target cell. The availability of these secretion systems increases the possibility of a pathogenic bacterium.

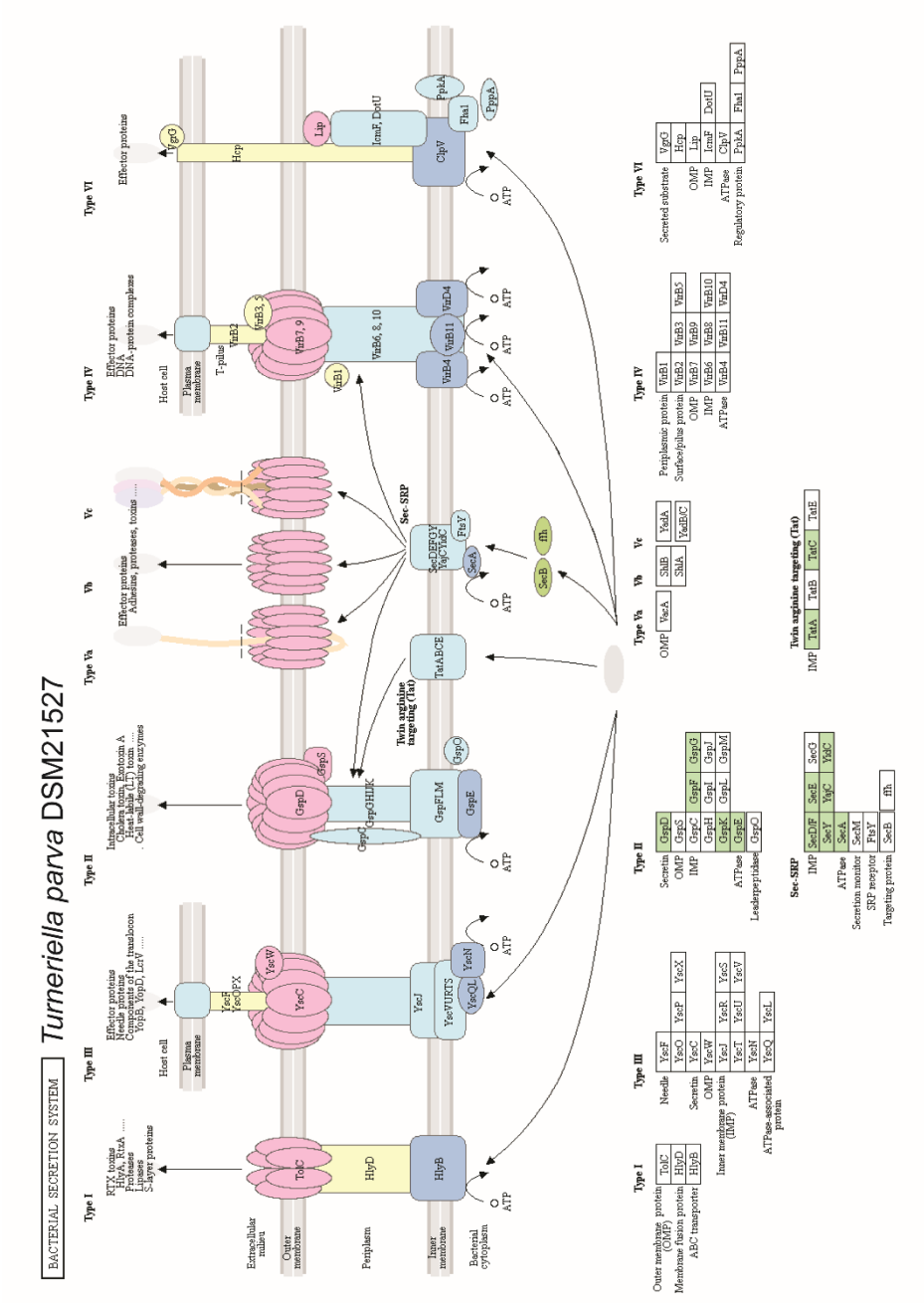

Suppl. Fig. 6.5: The Bacterial secretion systems. Genes linked to the bacterial secretion systems II are partial present in the *T. parva* genome and shaded in green. If the secretions system in *T. parva* is present remains unclear because many genes which are important for the secretion machinery are not present[191].

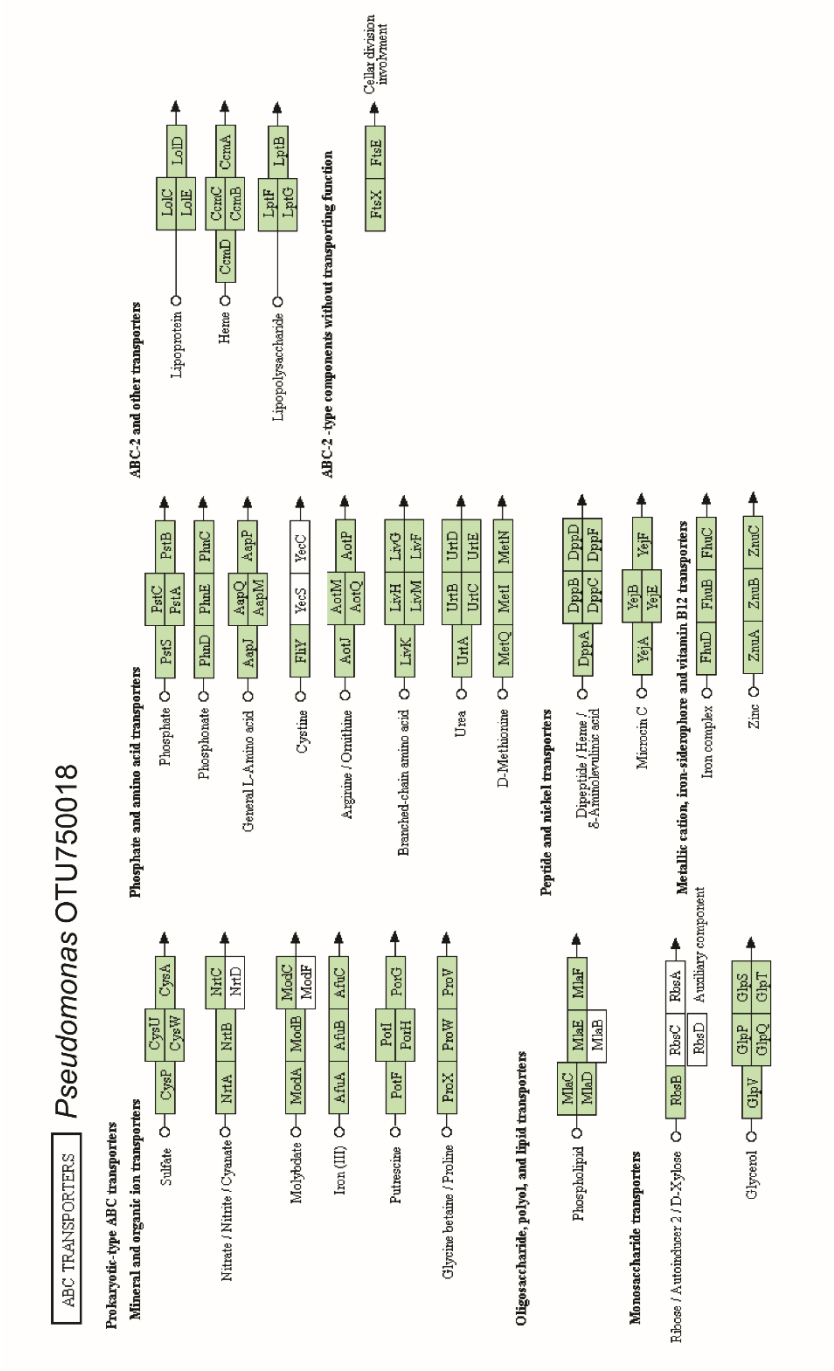

Suppl. Fig. 6.6: The ABC transporters. Genes linked to different ABC transporters and present in the *Pseudomonas* genome are shaded in green[191]. Listed are only ABC-transporters which are present in the *Pseudomonas* (OTU750018) genome. ABC-transporters are important bacterial peptide transporters which serve the bacterium from nutrition to a wide variety of virulence factors.

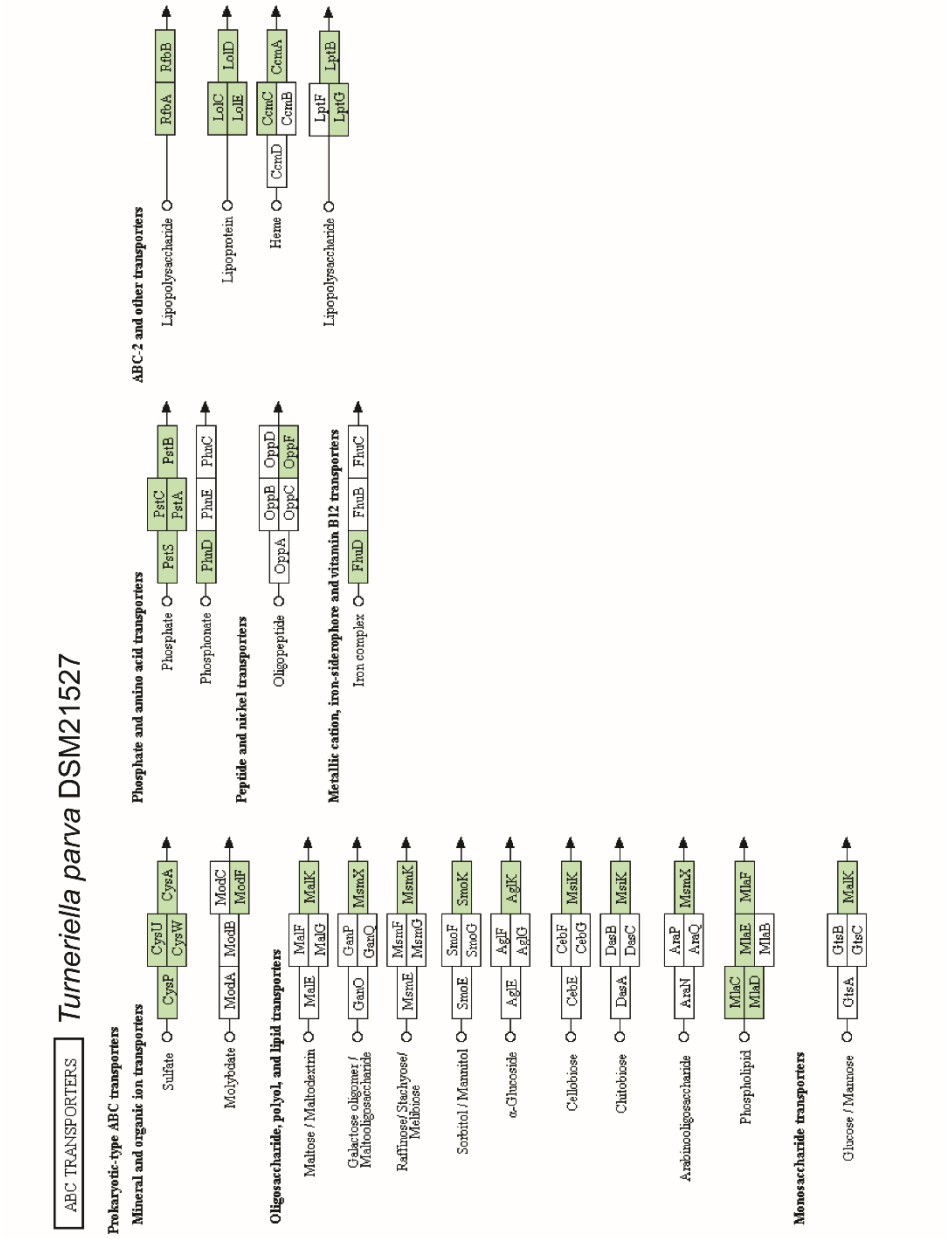

Suppl. Fig. 6.7: The ABC transporters. Genes linked to different ABC transporters and present in the *T. parva* genome are shaded in green[191]. Listed are only ABC-transporters which are present in the *T. parva* (OTU4017244) genome. Most of these ABC transporters are partially complete and thus unlikely active in *T. parva*.

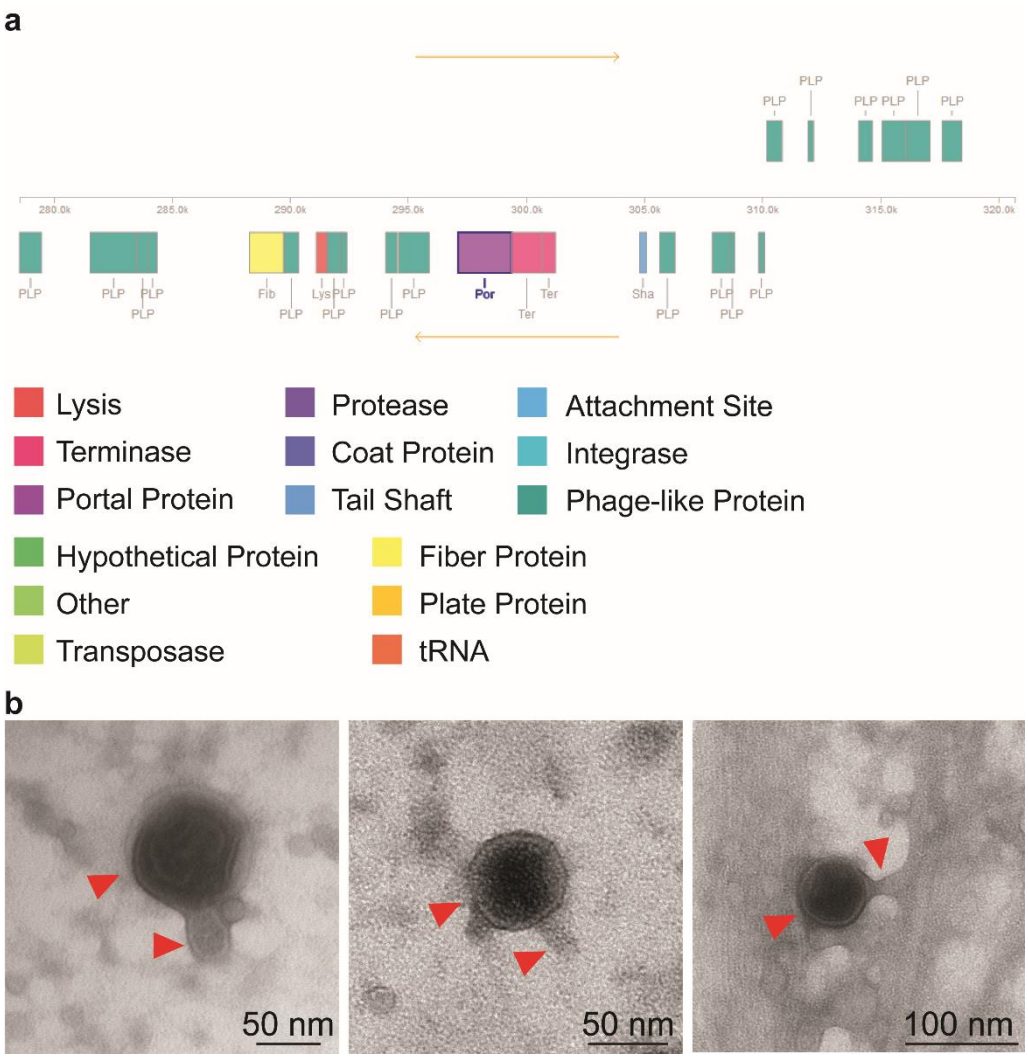

Suppl. Fig. 6.8: Entire phage annotated gene overview of the integrated prophage in *Pseudomonas.* (a) Analysis of the phage genome with phaster[194] highlights the completeness of the prophage. (b) Transmission electron microscopy images of the purified phage from *H. oligactis*. Capsid (dark circle) and tail (attached longitudinal structure) are highlighted by read arrows (scale bar from left to right: 50 nm, 50 nm and 100 nm). From the length of the tail one can conclude that the phage belongs to the phage family of the Podoviridae. It is not to exclude that possible virulence factors are carried out on the prophage, which is triggered by the contact with *T. parva*.

7 Supplementary tables

Supplementary tables and data are present on a compact disc (CD) which is attached to the thesis.

- Suppl. table 1 – tree sequences
- Suppl. table 2 – RNA-Seq
- Suppl. table 3 – antismash *Pseudomonas*
- Suppl. table 4 – Results *Pseudomonas*
- Suppl. table 5 – *Pseudomonas* (OTU750018)
- Suppl. table 6 – *Pseudomonas* Prophage
- Suppl. table 7 – Results T.parva_DSM21527
- Suppl. table 8 – Turneriella parva genome
- Suppl. table 9 – antismash *T. parva* DSM21527
- Suppl. table 10 – primerlist

Additionally, raw data of the RNA-Seq-analysis are attached.

8 Abbreviations

°C	Degree(s) Celsius
Act	Actin
AMP	Antimicrobial peptide
antib	antibitocs/antibiotic
EBFT	Enterotoxogenic *Bacteroides fragilis* toxin
BLAST	Basic Local Alignment Search Tool
bp	Base pairs
BSA	Bovine Serum Albumin
CagA	cytotoxin-associated gene A
CDT	Clostridium-difficile-Toxin
CLSM	Confocal Lase Scanning Microscopy
ctrl	control
DMSO	Dimethyl sulfoxide
DNA	Deoxyribonucleic acid
dNTP	Deoxynucleotide triphosphate
ECM	extracellular matrix
e.g.	Lat.:*exempli gratia*, engl.: for example
et al.	Lat.: *et alii*, engl.: and others
GCII	germline precursor cells stage II
gDNA	Genomic DNA
IACR	International Association of Cancer Registries
Mb	Megabase
mg	Milligram
min.	Minute(s)

ml	Milliliter
mM	Millimolar
mRNA	Messenger-RNA
mya	million years
µg	Microgram
µl	Microliter
n	Number of replicates
NCBI	National Center for Biotechnology Information
PBS	Phosphate buffered saline
PBT	Phosphate buffered saline with Tween-20
PCR	Polymerase chain reaction
pks	Polyketide synthase
qRT	Quantitative real-time
rRNA	Ribosomal Ribonucleic acid
RT	Room temperature
SDS	Sodium dodecyl sulfate
SMART	Simple modular architecture research tool
ssp.	subspecies
Taq	*Thermophilus aquaticus*
T_m	Melting temperature
TEM	Transmission electron microscopy
TLR	toll-like receptor
Tris	Tris-(Hydroxymethyl)-Aminomethane
tum	Tumor
U	Units

9 References

1. Rosenberg, E. & Zilber-Rosenberg, I. Microbes drive evolution of animals and plants: The hologenome concept. *mBio* (2016). doi:10.1128/mBio.01395-15

2. Horiike, T., Hamada, K., Miyata, D. & Shinozawa, T. The origin of eukaryotes is suggested as the symbiosis of pyrococcus into γ-proteobacteria by phylogenetic tree based on gene content. *J. Mol. Evol.* (2004). doi:10.1007/s00239-004-2652-5

3. Dyall, S. D., Brown, M. T. & Johnson, P. J. Ancient Invasions: From Endosymbionts to Organelles. *Science* (2004). doi:10.1126/science.1094884

4. McFadden, G. I. & Van Dooren, G. G. Evolution: Red algal genome affirms a common origin of all plastids. *Current Biology* (2004). doi:10.1016/j.cub.2004.06.041

5. Bosch, T. C. G. & McFall-Ngai, M. J. Metaorganisms as the new frontier. *Zoology* (2011). doi:10.1016/j.zool.2011.04.001

6. McFall-Ngai, M. *et al.* Animals in a bacterial world, a new imperative for the life sciences. *Proc. Natl. Acad. Sci.* (2013). doi:10.1073/pnas.1218525110

7. Esser, D. *et al.* Functions of the Microbiota for the Physiology of Animal Metaorganisms. 393–404 (2019). doi:10.1159/000495115

8. Gilbert, S. F., Sapp, J. & Tauber, A. I. A Symbiotic View of Life: We Have Never Been Individuals. *Q. Rev. Biol.* (2012). doi:10.1086/668166

9. Oldroyd, G. E. D., Murray, J. D., Poole, P. S. & Downie, J. A. The Rules of Engagement in the Legume-Rhizobial Symbiosis. *Annu. Rev. Genet.* (2011). doi:10.1146/annurev-genet-110410-132549

10. Rumpho, M. E., Pelletreau, K. N., Moustafa, A. & Bhattacharya, D. The making of a photosynthetic animal. *J. Exp. Biol.* (2011). doi:10.1242/jeb.046540

11. Dubilier, N., Bergin, C. & Lott, C. Symbiotic diversity in marine animals: The art of harnessing chemosynthesis. *Nature Reviews Microbiology* (2008). doi:10.1038/nrmicro1992

12. Archambaud, C. *et al.* The intestinal microbiota interferes with the microrna response upon oral listeria infection. *MBio* (2013). doi:10.1128/mBio.00707-13

13. Mazmanian, S. K., Round, J. L. & Kasper, D. L. A microbial symbiosis factor prevents intestinal inflammatory disease. *Nature* (2008). doi:10.1038/nature07008

14. Yamashiro, Y. Gut Microbiota in Health and Disease. *Annals of Nutrition and Metabolism* (2018). doi:10.1159/000481627

15. Schmieder, R. & Edwards, R. Quality control and preprocessing of metagenomic datasets. *Bioinformatics* (2011). doi:10.1093/bioinformatics/btr026

16. McFall-Ngai, M., Heath-Heckman, E. A. C., Gillette, A. A., Peyer, S. M. & Harvie, E. A. The secret languages of coevolved symbioses: Insights from the Euprymna scolopes-Vibrio fischeri symbiosis. *Seminars in Immunology* (2012). doi:10.1016/j.smim.2011.11.006

17. Bates, J. M. *et al.* Distinct signals from the microbiota promote different aspects of zebrafish gut differentiation. *Dev. Biol.* (2006). doi:10.1016/j.ydbio.2006.05.006

18. Landmann, F., Foster, J. M., Michalski, M. L., Slatko, B. E. & Sullivan, W. Co-evolution between an Endosymbiont and Its Nematode Host: Wolbachia Asymmetric Posterior Localization and AP Polarity Establishment. *PLoS Negl. Trop. Dis.* (2014). doi:10.1371/journal.pntd.0003096

19. Heijtz, R. D. *et al.* Normal gut microbiota modulates brain development and behavior. *Proc. Natl. Acad. Sci.* (2011). doi:10.1073/pnas.1010529108

20. Lee, Y. K. & Mazmanian, S. K. Has the microbiota played a critical role in the evolution of the adaptive immune system? *Science* (2010). doi:10.1126/science.1195568

21. Garrett, W. S. Cancer and the microbiota. *Science* **348**, 80–86 (2015).

22. Nigro, G. & Sansonetti, P. J. Microbiota and Gut Stem Cells Cross-Talks: A New View of Epithelial Homeostasis. *Current Stem Cell Reports* (2015). doi:10.1007/s40778-014-0005-x

23. Rea, D. *et al.* Microbiota effects on cancer: from risks to therapies. *Oncotarget* (2018). doi:10.18632/oncotarget.24681

24. Athena Aktipis, C. *et al.* Cancer across the tree of life: Cooperation and cheating in multicellularity. *Philos. Trans. R. Soc. B Biol. Sci.* (2015). doi:10.1098/rstb.2014.0219

25. De Martel, C. *et al.* Global burden of cancers attributable to infections in 2008: A review and synthetic analysis. *Lancet Oncol.* (2012). doi:10.1016/S1470-2045(12)70137-7

26. Pisani, P., Parkin, D. M., Muñoz, N. & Ferlay, J. Cancer and infection: Estimates of the attributable fraction in 1990. *Cancer Epidemiology Biomarkers and Prevention* (1997).

27. Plummer, M. *et al.* Global burden of cancers attributable to infections in 2012: a synthetic analysis. *Lancet Glob. Heal.* (2016). doi:10.1016/S2214-109X(16)30143-7

28. Blaser, M. J. & Atherton, J. C. Helicobacter pylori persistence: biology and disease. *J. Clin. Invest.* **113**, 321–333 (2004).

29. Cho, I. & Blaser, M. J. The human microbiome: At the interface of health and disease. *Nature Reviews Genetics* (2012). doi:10.1038/nrg3182

30. Peter, S. & Beglinger, C. Helicobacter pylori and gastric cancer: The causal relationship. *Digestion* (2007). doi:10.1159/000101564

31. Scanu, T. *et al.* Salmonella Manipulation of Host Signaling Pathways Provokes Cellular Transformation Associated with Gallbladder Carcinoma. *Cell Host Microbe* (2015). doi:10.1016/j.chom.2015.05.002

32. Boccellato, F. & Meyer, T. F. Bacteria Moving into Focus of Human Cancer. *Cell Host and Microbe* (2015). doi:10.1016/j.chom.2015.05.016

33. Abdulamir, A. S., Hafidh, R. R. & Bakar, F. A. The association of Streptococcus bovis/gallolyticus with colorectal tumors: The nature and the underlying mechanisms of its etiological role. *Journal of Experimental and Clinical Cancer Research* (2011). doi:10.1186/1756-9966-30-11

34. Mager, D. L. Bacteria and cancer: Cause, coincidence or cure? A review. *Journal of Translational Medicine* (2006). doi:10.1186/1479-5876-4-14

35. Kocazeybek, B. Chronic Chlamydophila pneumoniae infection in lung cancer, a risk factor: A case-control study. *J. Med. Microbiol.* (2003). doi:10.1099/jmm.0.04845-0

36. Louis, P., Hold, G. L. & Flint, H. J. The gut microbiota, bacterial metabolites and colorectal cancer. *Nature Reviews Microbiology* (2014). doi:10.1038/nrmicro3344

37. Elinav, E. *et al.* Inflammation-induced cancer: Crosstalk between tumours, immune cells and microorganisms. *Nature Reviews Cancer* (2013). doi:10.1038/nrc3611

38. Irrazábal, T., Belcheva, A., Girardin, S. E., Martin, A. & Philpott, D. J. The multifaceted role of the intestinal microbiota in colon cancer. *Molecular Cell* (2014). doi:10.1016/j.molcel.2014.03.039

39. Goodman, B. & Gardner, H. The microbiome and cancer. *J. Pathol.* **244**, 667–676 (2018).

40. Abreu, M. T. & Peek, R. M. Gastrointestinal malignancy and the microbiome. *Gastroenterology* (2014). doi:10.1053/j.gastro.2014.01.001

41. Fulbright, L. E., Ellermann, M. & Arthur, J. C. The microbiome and the hallmarks of cancer. *PLoS Pathog.* **13**, 1–6 (2017).

42. Rajagopala, S. V. *et al.* The human microbiome and cancer. *Cancer Prevention Research* (2017). doi:10.1158/1940-6207.CAPR-16-0249

43. Zechner, E. L. Inflammatory disease caused by intestinal pathobionts. *Curr. Opin. Microbiol.* **35**, 64–69 (2017).

44. Manfredo Vieira, S. *et al.* Translocation of a gut pathobiont drives autoimmunity in mice and humans. *Science (80-.).* (2018). doi:10.1126/science.aar7201

45. Hornef, M. Pathogens, commensal symbionts, and pathobionts: Discovery and functional effects on the host. *ILAR J.* **56**, 159–162 (2015).

46. Butler, S. & O'Dwyer, J. P. Stability criteria for complex microbial communities. *Nat. Commun.* (2018). doi:10.1038/s41467-018-05308-z

47. Abt, M. C. & Pamer, E. G. Commensal bacteria mediated defenses against pathogens. *Curr. Opin. Immunol.* **29**, 16–22 (2014).

48. Dejea, C. M. *et al.* Patients with familial adenomatous polyposis harbor colonic biofilms containing tumorigenic bacteria. *Science (80-.).* **359**, 592–597 (2018).

49. Hutter, C. M. *et al.* Gene-environment interactions in cancer epidemiology: A national cancer institute think tank report. *Genet. Epidemiol.* (2013). doi:10.1002/gepi.21756

50. Schwabe, R. & Jobin, C. The microbiome and cancer. *Nat Rev Cancer* **13**, 800–812 (2013).

51. Nishida, A. H. & Ochman, H. Rates of gut microbiome divergence in mammals. *Mol. Ecol.* (2018). doi:10.1111/mec.14473

52. Okabe, S. *et al.* A Great Leap forward in Microbial Ecology. *Microbes Environ.* (2010). doi:10.1264/jsme2.me10178

53. Dewi Puspita, I., Kamagata, Y., Tanaka, M., Asano, K. & Nakatsu, C. H. Are Uncultivated Bacteria Really Uncultivable? *Microbes Environ.* (2012). doi:10.1264/jsme2.me12092

54. Turnbaugh, P. J. *et al.* The Human Microbiome Project. *Nature* (2007). doi:10.1109/SAINT.2010.93

55. Dos Reis, M. *et al.* Uncertainty in the Timing of Origin of Animals and the Limits of Precision in Molecular Timescales. *Curr. Biol.* (2015). doi:10.1016/j.cub.2015.09.066

56. Bosch, T. C. G. *et al.* Back to the Basics: Cnidarians Start to Fire. *Trends in Neurosciences* (2017). doi:10.1016/j.tins.2016.11.005

57. Domazet-Lošo, T. & Tautz, D. Phylostratigraphic tracking of cancer genes suggests a link to the emergence of multicellularity in metazoa. *BMC Biol.* **8**, 1–10 (2010).

58. Jägersten, G. ̈On the early phylogeny of the Metazoa. *Zool. Bidr. Uppsala* 321–354 (1955).

59. Faurot, L. *Etudes sur l'anatomie, l'histologie et le développement des Actinies ...* (typ. A. Hennuyer, 1893).

60. Faurot L. Développement du pharynx des couples et des paires de cloisons chez les Hexactinies. *Arch. Zool. Exp.* **Gén. Sér.**, 359–399 (1903).

61. Bode, H. R. Axial patterning in hydra. *Cold Spring Harbor perspectives in biology* (2009). doi:10.1101/cshperspect.a000463

62. LIU, T. T. & CHANG, J. T. Number of Tentacles in Hydra vulgaris as a Genetic Character. *Nature* **157**, 728 (1946).

63. Bode, H. *et al.* Quantitative analysis of cell types during growth and morphogenesis in Hydra. *Wilhelm Roux Arch. für Entwicklungsmechanik der Org.* (1973). doi:10.1007/BF00577725

64. Galliot, B. Regeneration in Hydra. *Encycl. Life Sci.* (2013). doi:10.1002/9780470015902.a0001096

65. Hemmrich, G. *et al.* Molecular signatures of the three stem cell lineages in hydra and the emergence of stem cell function at the base of multicellularity. *Mol. Biol. Evol.* (2012). doi:10.1093/molbev/mss134

66. Bosch, T. C. G. Hydra and the evolution of stem cells. *BioEssays* (2009). doi:10.1002/bies.200800183

67. Takano, J. Genetic analysis of developmental mechanisms in hydra. IX. Effect of food on development of a slow-budding strain (L4). *Dev. Biol.* **103**, 96–108 (1984).

68. Livshits, A., Shani-Zerbib, L., Maroudas-Sacks, Y., Braun, E. & Keren, K. Structural Inheritance of the Actin Cytoskeletal Organization Determines the Body Axis in Regenerating Hydra. *Cell Rep.* **18**, 1410–1421 (2017).

69. Sarras, M. P. Components, structure, biogenesis and function of the Hydra extracellular matrix in regeneration, pattern formation and cell differentiation. *International Journal of Developmental Biology* (2012). doi:10.1387/ijdb.113445ms

70. Pouille, P. A., Ahmadi, P., Brunet, A. C. & Farge, E. Mechanical signals trigger myosin II redistribution and mesoderm invagination in drosophila embryos. *Sci. Signal.* (2009). doi:10.1126/scisignal.2000098

71. Desprat, N., Supatto, W., Pouille, P. A., Beaurepaire, E. & Farge, E. Tissue Deformation Modulates Twist Expression to Determine Anterior Midgut Differentiation in Drosophila Embryos. *Dev. Cell* (2008). doi:10.1016/j.devcel.2008.07.009

72. Miller, C. J. & Davidson, L. A. The interplay between cell signalling and mechanics in developmental processes. *Nature Reviews Genetics* (2013). doi:10.1038/nrg3513

73. Holz, O. *et al.* Bud detachment in hydra requires activation of fibroblast growth factor receptor and a Rho–ROCK–myosin II signaling pathway to ensure formation of a basal constriction. *Dev. Dyn.* (2017). doi:10.1002/dvdy.24508

74. Sarras, M. P. *et al.* Extracellular matrix (mesoglea) of Hydra vulgaris. I. Isolation and characterization. *Dev. Biol.* (1991). doi:10.1016/0012-1606(91)90266-6

75. Shimizu, H. *et al.* The extracellular matrix of hydra is a porous sheet and contains type IV collagen. *Zoology* (2008). doi:10.1016/j.zool.2007.11.004

76. Savagner, P. *Rise and Fall of Epithelial Phenotype*. *Rise and Fall of Epithelial Phenotype* (2005). doi:10.1007/0-387-28671-3

77. Bosch, T. C. G. & David, C. N. Male and Female Stem Cells and Sex Reversal in Hydra Polyps Male and female stem cells and sex reversal in Hydra polyps (sex switch/female repression/model for sex determination). *Cell Biol.* (1986). doi:10.1073/pnas.83.24.9478

78. Aufschnaiter, R., Wedlich-Söldner, R., Zhang, X. & Hobmayer, B. Apical and basal epitheliomuscular F-actin dynamics during *Hydra* bud evagination. *Biol. Open* (2017). doi:10.1242/bio.022723

79. Littlefield, C. L., Finkemeier, C. & Bode, H. R. Spermatogenesis in Hydra oligactis. II. How temperature controls the reciprocity of sexual and asexual reproduction. *Dev. Biol.* (1991). doi:10.1016/0012-1606(91)90231-Q

80. Franzenburg, S. *et al.* Distinct antimicrobial peptide expression determines host species-speci fi c bacterial associations. *Proc. Natl. Acad. Sci. U. S. A.* **110**, E3730–E3738 (2013).

81. Ericsson, A. C. & Franklin, C. L. Manipulating the gut microbiota: Methods and challenges. *ILAR J.* (2015). doi:10.1093/ilar/ilv021

82. Janda, J. M. & Abbott, S. L. 16S rRNA gene sequencing for bacterial identification in the diagnostic laboratory: Pluses, perils, and pitfalls. *Journal of Clinical Microbiology* (2007). doi:10.1128/JCM.01228-07

83. Fraune, S. *et al.* Bacteria-bacteria interactions within the microbiota of the ancestral metazoan Hydra contribute to fungal resistance. *ISME J.* **9**, 1543–1556 (2015).

84. Schröder, K. & Bosch, T. C. G. The origin of mucosal immunity: Lessons from the holobiont Hydra. *MBio* **7**, 1–9 (2016).

85. Ouwerkerk, J. P., De Vos, W. M. & Belzer, C. Glycobiome: Bacteria and mucus at the epithelial interface. *Best Practice and Research: Clinical Gastroenterology* (2013). doi:10.1016/j.bpg.2013.03.001

86. Moran, A. P., Gupta, A. & Joshi, L. Sweet-talk: Role of host glycosylation in bacterial pathogenesis of the gastrointestinal tract. *Gut* (2011). doi:10.1136/gut.2010.212704

87. Hufnagel, L. A. & Myhal, M. L. Observations on a Spirochaete Symbiotic in Hydra. *Trans. Am. Microsc. Soc.* (1977). doi:10.2307/3225874

88. Margulis, L., Thorington, G., Berger, B. & Stolz, J. Endosymbiotic bacteria associated with the intracellular green algae of Hydra viridis. *Curr. Microbiol. An Int. J.* (1978). doi:10.1007/BF02602848

89. Brucker, R. M. & Bordenstein, S. R. The Hologenomic Basis of Speciation : *Science (80-.).* (2013). doi:10.1126/science.1240659

90. Tlaskalová-Hogenová, H. *et al.* The role of gut microbiota (commensal bacteria) and the mucosal barrier in the pathogenesis of inflammatory and autoimmune diseases and cancer: Contribution of germ-free and gnotobiotic animal models of human diseases. *Cellular and Molecular Immunology* (2011). doi:10.1038/cmi.2010.67

91. Littman, D. R. & Pamer, E. G. Role of the commensal microbiota in normal and pathogenic host immune responses. *Cell Host and Microbe* (2011). doi:10.1016/j.chom.2011.10.004

92. Fraune, S. & Bosch, T. C. G. Long-term maintenance of species-specific bacterial microbiota in the basal metazoan Hydra. *Proc. Natl. Acad. Sci.* (2007). doi:10.1073/pnas.0703375104

93. Fraune, S. *et al.* In an early branching metazoan, bacterial colonization of the embryo is controlled by maternal antimicrobial peptides. *Proc. Natl. Acad. Sci.* **107**, 18067–18072 (2010).

94. Augustin, R. *et al.* A secreted antibacterial neuropeptide shapes the microbiome of Hydra. *Nat. Commun.* **8**, 1–8 (2017).

95. Pietschke, C. *et al.* Host modification of a bacterial quorum-sensing signal induces a phenotypic switch in bacterial symbionts. *Proc. Natl. Acad. Sci.* (2017). doi:10.1073/pnas.1706879114

96. Mortzfeld, B. M., Taubenheim, J., Fraune, S., Klimovich, A. V. & Bosch, T. C. G. Stem cell transcription factor FoxO controls microbiome resilience in hydra. *Front. Microbiol.* **9**, 1–10 (2018).

97. Murillo-Rincon, A. P. *et al.* Spontaneous body contractions are modulated by the microbiome of Hydra. *Sci. Rep.* **7**, 1–9 (2017).

98. Fraune, S., Abe, Y. & Bosch, T. C. G. Disturbing epithelial homeostasis in the metazoan Hydra leads to drastic changes in associated microbiota. *Environ. Microbiol.* (2009). doi:10.1111/j.1462-2920.2009.01963.x

99. Bosch, T. C. G., Miller, D. J., Bosch, T. C. G. & Miller, D. J. The Hydra Holobiont: A Tale of Several Symbiotic Lineages. in *The Holobiont Imperative* (2016). doi:10.1007/978-3-7091-1896-2_7

100. Bosch, T. C. G. & Miller, D. J. *The Holobiont Imperative*. *The Holobiont Imperative* (2016). doi:10.1007/978-3-7091-1896-2

101. Domazet-Lošo, T. *et al.* Naturally occurring tumours in the basal metazoan Hydra. *Nat. Commun.* **5**, 1–8 (2014).

102. Ujvari, B., Roche, B. & Thomas, F. *Ecology and Evolution of Cancer*. *Ecology and Evolution of Cancer* (2017).

103. Scharrer, B. & Lochhead, M. S. Tumors in the Invertebrates: A Review. *Cancer Res.* **10**, (1950).

104. Squires, D. F. Neoplasia in a coral? *Science (80-.).* **148**, 503–505 (1965).

105. Robert, J. Comparative study of tumorogenesis and tumor immunity in invertebrates and nonmammalian vertebrates. *Dev. Comp. Immunol.* **34**, 915–925 (2010).

106. Tardent, P. Gametogenesis in the genus hydra. *Integr. Comp. Biol.* (1974). doi:10.1093/icb/14.2.447

107. Gopalakrishnan, V., Helmink, B. A., Spencer, C. N., Reuben, A. & Wargo, J. A. The Influence of the Gut Microbiome on Cancer, Immunity, and Cancer Immunotherapy. *Cancer Cell* **33**, 570–580 (2018).

108. Goodman, B. & Gardner, H. The microbiome and cancer. *J. Pathol.* **244**, 667–676 (2018).

109. Sears, C. L. & Garrett, W. S. Microbes, microbiota, and colon cancer. *Cell Host and Microbe* (2014). doi:10.1016/j.chom.2014.02.007

110. Hanahan, D. & Weinberg, R. A. Hallmarks of cancer: The next generation. *Cell* (2011). doi:10.1016/j.cell.2011.02.013

111. Hanahan, D. & Weinberg, R. A. The hallmarks of cancer. *Cell* (2000). doi:10.1007/s00262-010-0968-0

112. Albuquerque, T. A. F., Drummond do Val, L., Doherty, A. & de Magalhães, J. P. From humans to hydra: patterns of cancer across the tree of life. *Biol. Rev.* (2018). doi:10.1111/brv.12415

113. Takahashi, T. Hym-301, a novel peptide, regulates the number of tentacles formed in hydra. *Development* (2005). doi:10.1242/dev.01792

114. Mortzfeld, B. M. *et al.* Temperature and insulin signaling regulate body size in Hydra by the Wnt and TGF-beta pathways. *Nat. Commun.* **10**, 3257 (2019).

115. David, C. N. A quantitative method for maceration of hydra tissue. *Wilhelm Roux Arch. für Entwicklungsmechanik der Org.* (1973). doi:10.1007/BF00577724

116. Watanabe, H. *et al.* Nodal signalling determines biradial asymmetry in Hydra. *Nature* (2014). doi:10.1038/nature13666

117. Graf, L. & Gierer, A. Size, shape and orientation of cells in budding hydra and regulation of regeneration in cell aggregates. *Wilhelm Roux's Arch. Dev. Biol.* (1980). doi:10.1007/BF00848806

118. Hausman, R. E. & Burnett, A. L. The mesoglea of hydra. I. Physical and histochemical properties. *J. Exp. Zool.* (1969). doi:10.1002/jez.1401710103

119. Davis, L. E. & Haynes, J. F. An ultrastructural examination of the mesoglea of Hydra. *Zeitschrift für Zellforsch. und Mikroskopische Anat.* **92**, 149–158 (1968).

120. Ellis, T. N., Leiman, S. A. & Kuehn, M. J. Naturally produced outer membrane vesicles from Pseudomonas aeruginosa elicit a potent innate immune response via combined sensing of both lipopolysaccharide and protein components. *Infect. Immun.* (2010). doi:10.1128/IAI.00433-10

121. Guerrero-Mandujano, A., Hernández-Cortez, C., Ibarra, J. A. & Castro-Escarpulli, G. The outer membrane vesicles: Secretion system type zero. *Traffic* (2017). doi:10.1111/tra.12488

122. MacDonald, I. A. & Kuehna, M. J. Stress-induced outer membrane vesicle production by Pseudomonas aeruginosa. *J. Bacteriol.* (2013). doi:10.1128/JB.02267-12

123. Schwechheimer, C. & Kuehn, M. J. Outer-membrane vesicles from Gram-negative bacteria: Biogenesis and functions. *Nature Reviews Microbiology* (2015). doi:10.1038/nrmicro3525

124. Lawley, T. D. & Walker, A. W. Intestinal colonization resistance. *Immunology* **138**, 1–11 (2013).

125. Buffie, C. G. & Pamer, E. G. Microbiota-mediated colonization resistance against intestinal pathogens. *Nature Reviews Immunology* (2013). doi:10.1038/nri3535

126. Wynwood, S. J. *et al.* Leptospirosis from water sources. *Pathog. Glob. Health* (2014). doi:10.1179/2047773214Y.0000000156

127. Franzenburg, S. *et al.* MyD88-deficient Hydra reveal an ancient function of TLR signaling in sensing bacterial colonizers. *Proc. Natl. Acad. Sci.* (2012). doi:10.1073/pnas.1213110109

128. Weisburg, W. G., Barns, S. M., Pelletier, D. A. & Lane, D. J. 16S Ribosomal DNA Amplification for Phylogenetic Study. *J. Bacteriol.* **173**, 697–703 (1991).

129. Sacks, P. G. & Davis, L. E. Production of nerveless Hydra attenuata by hydroxyurea treatments. *J Cell Sci* (1979).

130. Stackebrandt, E. *et al.* Genome sequence of the free-living aerobic spirochete Turneriella parva type strain (HT), and emendation of the species Turneriella parva. *Stand. Genomic Sci.* (2013). doi:10.4056/sigs.3617113

131. Duarte, A. S., Correia, A. & Esteves, A. C. Bacterial collagenases - A review. *Crit. Rev. Microbiol.* **42**, 106–126 (2016).

132. Ribet, D. & Cossart, P. How bacterial pathogens colonize their hosts and invade deeper tissues. *Microbes Infect.* **17**, 173–183 (2015).

133. Singh, B., Fleury, C., Jalalvand, F. & Riesbeck, K. Human pathogens utilize host extracellular matrix proteins laminin and collagen for adhesion and invasion of the host. *FEMS Microbiology Reviews* (2012). doi:10.1111/j.1574-6976.2012.00340.x

134. Alfano, M. *et al.* The interplay of extracellular matrix and microbiome in urothelial bladder cancer. *Nature Reviews Urology* (2016). doi:10.1038/nrurol.2015.292

135. Bugalhão, J. N., Mota, L. J. & Franco, I. S. Bacterial nucleators: actin' on actin. *Pathog. Dis.* **73**, ftv078 (2015).

136. Díaz de la Loza, M. C. *et al.* Laminin Levels Regulate Tissue Migration and Anterior-Posterior Polarity during Egg Morphogenesis in Drosophila. *Cell Rep.* (2017). doi:10.1016/j.celrep.2017.06.031

137. Matlin, K. S., Myllymäki, S. M. & Manninen, A. Laminins in epithelial cell polarization: Old questions in search of new answers. *Cold Spring Harb. Perspect. Biol.* (2017). doi:10.1101/cshperspect.a027920

138. Fuertes-Alvarez, S. *et al.* p73 regulates ependymal planar cell polarity by modulating actin and microtubule cytoskeleton. *Cell Death Dis.* (2018). doi:10.1038/s41419-018-1205-6

139. Yi, K. & Li, R. Actin cytoskeleton in cell polarity and asymmetric division during mouse oocyte maturation. *Cytoskeleton* (2012). doi:10.1002/cm.21048

140. Cowell, B. A., Evans, D. J. & Fleiszig, S. M. J. Actin cytoskeleton disruption by ExoY and its effects on Pseudomonas aeruginosa invasion. *FEMS Microbiol. Lett.* **250**, 71–76 (2005).

141. Marshall, N. C., Finlay, B. B. & Overall, C. M. Sharpening Host Defenses during Infection: Proteases Cut to the Chase. *Mol. Cell. Proteomics* (2017). doi:10.1074/mcp.O116.066456

142. Richard, J. F. Bacterial toxins modifying the actin cytoskeleton. *Int. Microbiol.* **2**, 185–194 (1999).

143. Bosch, T. C. G. & David, C. N. Immunocompetence in Hydra: Epithelial cells recognize self-nonself and react against it. *J. Exp. Zool.* (1986). doi:10.1002/jez.1402380212

144. Sharon, G. *et al.* Commensal bacteria play a role in mating preference of Drosophila melanogaster. *Proc. Natl. Acad. Sci.* (2010). doi:10.1073/pnas.1009906107

145. Canale-Parola, E. Physiology and evolution of spirochetes. *Bacteriol. Rev.* (1977). doi:10.1126/science.203.4375.44

146. Julian, T. R. Environmental transmission of diarrheal pathogens in low and middle income countries. *Environmental Science: Processes and Impacts* (2016). doi:10.1039/c6em00222f

147. Cholera: Environmental Reservoirs and Impact on Disease Transmission. in *One Health* (2014). doi:10.1128/microbiolspec.oh-0003-2012

148. Halperin, J. J. A Tale of Two Spirochetes: Lyme Disease and Syphilis. *Neurologic Clinics* (2010). doi:10.1016/j.ncl.2009.09.009

149. Pollack, M. The virulence of Pseudomonas aeruginosa. *Rev. Infect. Dis.* **6 Suppl 3**, S617–S626 (1984).

150. Markou, P. & Apidianakis, Y. Pathogenesis of intestinal Pseudomonas aeruginosa infection in patients with cancer. *Front. Cell. Infect. Microbiol.* (2014). doi:10.3389/fcimb.2013.00115

151. Levett, P. N., Morey, R. E., Galloway, R., Steigerwalt, A. G. & Ellis, W. A. Reclassification of Leptospira parva Hovind-Hougen et al. 1982 as Turneriella parva gen. nov., comb. nov. *Int. J. Syst. Evol. Microbiol.* (2005). doi:10.1099/ijs.0.63088-0

152. Aktories, K., Lang, A. E., Schwan, C. & Mannherz, H. G. Actin as target for modification by bacterial protein toxins. *FEBS J.* **278**, 4526–4543 (2011).

153. Wessler, S., Gimona, M. & Rieder, G. Regulation of the actin cytoskeleton in Helicobacter pylori-induced migration and invasive growth of gastric epithelial cells. *Cell Commun. Signal.* **9**, 27 (2011).

154. Baldassarre, M. *et al.* Actin dynamics at sites of extracellular matrix degradation. *Eur. J. Cell Biol.* (2006). doi:10.1016/j.ejcb.2006.08.003

155. Alfano, M. *et al.* The interplay of extracellular matrix and microbiome in urothelial bladder cancer. *Nat. Rev. Urol.* **13**, 77–90 (2016).

156. Smethurst, D. G. J., Dawes, I. W. & Gourlay, C. W. Actin - a biosensor that determines cell fate in yeasts. *FEMS Yeast Res.* (2014). doi:10.1111/1567-1364.12119

157. Pocaterra, A. *et al.* F-actin dynamics regulates mammalian organ growth and cell fate maintenance. *J. Hepatol.* (2019). doi:10.1016/j.jhep.2019.02.022

158. Starke, J., Wehrle-Haller, B. & Friedl, P. Plasticity of the actin cytoskeleton in response to extracellular matrix nanostructure and dimensionality. *Biochem. Soc. Trans.* (2014). doi:10.1042/BST20140139

159. Théry, M. *et al.* The extracellular matrix guides the orientation of the cell division axis. *Nat. Cell Biol.* (2005). doi:10.1038/ncb1307

160. Sorbara, M. T. & Pamer, E. G. Interbacterial mechanisms of colonization resistance and the strategies pathogens use to overcome them. *Mucosal Immunology* (2019). doi:10.1038/s41385-018-0053-0

161. Murdoch, C. C. & Rawls, J. F. Commensal Microbiota Regulate Vertebrate Innate Immunity-Insights From the Zebrafish. *Front. Immunol.* (2019). doi:10.3389/fimmu.2019.02100

162. Van Der Waaij, D., Berghuis-de Vries, J. M. & Lekkerkerk-Van Der Wees, J. E. C. Colonization resistance of the digestive tract in conventional and antibiotic-treated mice. *J. Hyg. (Lond).* (1971). doi:10.1017/S0022172400021653

163. Van Der Waaij, D., Berghuis, J. M. & Lekkerkerk, J. E. C. Colonization resistance of the digestive tract of mice during systemic antibiotic treatment. *J. Hyg. (Lond).* (1972). doi:10.1017/S0022172400022464

164. Guerrini, M. M., Vogelzang, A. & Fagarasan, S. A Hen in the Wolf Den: A Pathobiont Tale. *Immunity* **48**, 628–631 (2018).

165. Dingemanse, C. *et al.* Akkermansia muciniphila and Helicobacter typhlonius modulate intestinal tumor development in mice. *Carcinogenesis* **36**, 1388–1396 (2015).

166. Vayssier-Taussat, M. *et al.* Shifting the paradigm from pathogens to pathobiome new concepts in the light of meta-omics. *Frontiers in Cellular and Infection Microbiology* (2014). doi:10.3389/fcimb.2014.00029

167. Sarras, M. P. *et al.* Extracellular matrix (mesoglea) of Hydra vulgaris. I. Isolation and characterization. *Dev. Biol.* **148**, 481–494 (1991).

168. Backert, S. & Blaser, M. J. The role of CagA in the gastric biology of helicobacter pylori. *Cancer Res.* **76**, 4028–4031 (2016).

169. Cover, T. L. & Blaser, M. J. Helicobacter pylori in Health and Disease. *Gastroenterology* (2009). doi:10.1053/j.gastro.2009.01.073

170. Bošković, B. Antibiotics that target mitochondria effectively eradicate cancer stem cells, across multiple tumor types: Treating cancer like an infectious disease. *Acta Med. Acad.* (2015). doi:10.5644/ama2006-124.134

171. Lenhoff, H. M. & Brown, R. D. Mass culture of hydra: an improved method and its application to other aquatic invertebrates. *Lab. Anim.* **4**, 139–154 (1970).

172. Browne, E. N. The production of new hydranths in Hydra by the insertion of small grafts. *J. Exp. Zool.* (1909). doi:10.1002/jez.1400070102

173. Fujisawa, T. Role of interstitial cell migration in generating position-dependent patterns of nerve cell differentiation in Hydra. *Dev. Biol.* (1989). doi:10.1016/0012-1606(89)90298-4

174. Bode, H. R., Flick, K. M. & Smith, G. S. Regulation of interstitial cell differentiation in Hydra attenuata. I. Homeostatic control of interstitial cell population size. *J. Cell Sci.* (1976).

175. Anton-Erxleben, F., Thomas, A., Wittlieb, J., Fraune, S. & Bosch, T. C. G. Plasticity of epithelial cell shape in response to upstream signals: A whole-organism study using transgenic Hydra. *Zoology* **112**, 185–194 (2009).

176. Siebert, S., Anton-Erxleben, F. & Bosch, T. C. G. Cell type complexity in the basal metazoan Hydra is maintained by both stem cell based mechanisms and transdifferentiation. *Dev. Biol.* (2008). doi:10.1016/j.ydbio.2007.09.007

177. Holstein, T. W., Hess, M. W. & Salvenmoser, W. *Preparation techniques for transmission electron microscopy of hydra*. *Methods in Cell Biology* **96**, (Elsevier Inc., 2010).

178. Greber, M. J., David, C. N. & Holstein, T. W. A quantitative method for separation of living Hydra cells. *Roux's Arch. Dev. Biol.* (1992). doi:10.1007/BF00592110

179. Wittlieb, J., Khalturin, K., Lohmann, J. U., Anton-Erxleben, F. & Bosch, T. C. G. Transgenic Hydra allow in vivo tracking of individual stem cells during morphogenesis. *Proc. Natl. Acad. Sci.* (2006). doi:10.1073/pnas.0510163103

180. Martin, M. Cutadapt removes adapter sequences from high-throughput sequencing reads. *EMBnet.journal* (2011). doi:10.14806/ej.17.1.200

181. Taubenheim, J. Growth dynamics and size determination in Hydra. (2018).

182. Langmead, B. & Salzberg, S. L. Fast gapped-read alignment with Bowtie 2. *Nat. Methods* (2012). doi:10.1038/nmeth.1923

183. R Development Core Team, R. *R: A Language and Environment for Statistical Computing*. *R Foundation for Statistical Computing* (2011). doi:10.1007/978-3-540-74686-7

184. Love, M. I., Anders, S. & Huber, W. *Differential analysis of count data - the DESeq2 package*. *Genome Biology* (2014). doi:110.1186/s13059-014-0550-8

185. Leek, J. T., Johnson, W. E., Parker, H. S., Jaffe, A. E. & Storey, J. D. The SVA package for removing batch effects and other unwanted variation in high-throughput experiments. *Bioinformatics* (2012). doi:10.1093/bioinformatics/bts034

186. Muyzer, G., De Waal, E. C. & Uitterlinden, A. G. Profiling of complex microbial populations by denaturing gradient gel electrophoresis analysis of polymerase chain reaction-amplified genes coding for 16S rRNA. *Appl. Environ. Microbiol.* (1993). doi:0099-2240/93/030695-06$02.00/0

187. Rausch, P. *et al.* Analysis of factors contributing to variation in the C57BL/6J fecal microbiota across German animal facilities. *Int. J. Med. Microbiol.* **306**, 343–355 (2016).

188. Bhute, S. S. *et al.* Molecular analysis of gut microbiota in obesity among Indian individuals. *Nature* **9**, 1–15 (2011).

189. Haas, B. J. *et al.* Chimeric 16{S} r{RNA} Sequence Formation and Detection in {S}anger and 454-Pyrosequenced {PCR} Amplicons. *Genome Res.* **21**, 494–504 (2011).

190. Bateman, A. *et al.* UniProt: The universal protein knowledgebase. *Nucleic Acids Res.* (2017). doi:10.1093/nar/gkw1099

191. Kanehisa, M., Furumichi, M., Tanabe, M., Sato, Y. & Morishima, K. KEGG: New perspectives on genomes, pathways, diseases and drugs. *Nucleic Acids Res.* (2017). doi:10.1093/nar/gkw1092

192. Chen, L., Zheng, D., Liu, B., Yang, J. & Jin, Q. VFDB 2016: Hierarchical and refined dataset for big data analysis - 10 years on. *Nucleic Acids Res.* (2016). doi:10.1093/nar/gkv1239

193. Medema, M. H. *et al.* AntiSMASH: Rapid identification, annotation and analysis of secondary metabolite biosynthesis gene clusters in bacterial and fungal genome sequences. *Nucleic Acids Res.* (2011). doi:10.1093/nar/gkr466

194. Zhou, Y., Liang, Y., Lynch, K. H., Dennis, J. J. & Wishart, D. S. PHAST: A Fast Phage Search Tool. *Nucleic Acids Res.* (2011). doi:10.1093/nar/gkr485

195. Edgar, R. C. Search and clustering orders of magnitude faster than BLAST. *Bioinformatics* **26**, 2460–2461 (2010).

196. DeSantis, T. Z. *et al.* Greengenes, a chimera-checked 16S rRNA gene database and workbench compatible with ARB. *Appl. Environ. Microbiol.* **72**, 5069–5072 (2006).

197. Faith, J. J. *et al.* The long-term stability of the human gut microbiota. *Science (80-.).* **341**, (2013).

198. Segata, N. *et al.* Metagenomic biomarker discovery and explanation. *Genome Biol.* **12**, R60 (2011).

199. Anzai, Y. *et al.* Phylogenetic affiliation of the pseudomonads based on 16S rRNA sequence become a dumping ground for incompletely characterized polarly flagellated , of 128 valid and invalid Pseudomonas species , which included almost valid species of the genus Pseudomona. *Int. J. Syst. Evol. Microbiol.* **50**, 1563–1589 (2000).

200. Stackebrandt, E. *et al.* Genome sequence of the free-living aerobic spirochete Turneriella parva type strain (HT), and emendation of the species Turneriella parva. *Stand. Genomic Sci.* **8**, 228–238 (2013).

201. Thompson, J. D., Gibson, T. J., Plewniak, F., Jeanmougin, F. & Higgins, D. G. The CLUSTAL X windows interface: Flexible strategies for multiple sequence alignment aided by quality analysis tools. *Nucleic Acids Res.* **25**, 4876–4882 (1997).

202. Kumar, S., Stecher, G. & Tamura, K. MEGA7: Molecular Evolutionary Genetics Analysis Version 7.0 for Bigger Datasets. *Mol. Biol. Evol.* (2016). doi:10.1093/molbev/msw054

203. Felsenstein, J. Confidence limits on phylogenies: an approach using the bootstrap. *Evolution (N. Y).* (1985). doi:10.2307/2408678

204. Saitou, N. & Nei, M. The neighbor-joining method: a new method for reconstructing phylogenetic trees. *Mol. Biol. Evol.* (1987). doi:citeulike-article-id:93683

205. Tamura, K., Nei, M. & Kumar, S. Prospects for inferring very large phylogenies by using the neighbor-joining method. *Proc. Natl. Acad. Sci.* (2004). doi:10.1073/pnas.0404206101

206. Benjamini, Y. & Hochberg, Y. Controlling the False Discovery Rate : A Practical and Powerful Approach to Multiple Testing Author (s): Yoav Benjamini and Yosef Hochberg Source : Journal of the Royal Statistical Society . Series B (Methodological), Vol . 57 , No . 1 Published by : *J. R. Stat. Soc.* **57**, 289–300 (1995).

10 List of publications

Rathje, K., Mortzefeld, B., Höppner, M, Bosch, T. Klimovich, A. Dynamic interactions within the host-associated microbiota cause tumor formation in the basal metazoan *Hydra*. *PLoS Pathog*. (2019). doi: (in review)

11 Acknowledgements

I always enjoyed working in the group of Thomas Bosch. The working atmosphere and the affectionate people simplified every day. It was not an easy way but I liked to go it. The technical and scientific support was fantastic. Especially, I want to thank some people who supported me during this work.

I would like to thank Prof. Dr. Thomas Bosch for giving me the opportunity to write my thesis in his lab. I was pleasured that he offered me this topic which immediately caught my interest. I appreciate his thoughts and advices on my thesis. I felt honoured when he resigned me the job as a postdoctoral student and his assisting words during my illness. His expectant function as supervisor urged me in my work.

I was really glad to call Dr. Alexander Klimovich my supervisor. I have never met someone with such a broad spectrum of knowledge. His interest to learn more and more was inspiring. His perfectionism was motivating still sometimes arduous. I am really thankful for all his advices on my experiments and thesis. He will make a great group leader.

I thank the members of the thesis committee, Prof. Dr. Thomas Roeder, Prof. Dr. Unterweger and Prof. Dr. Gorb for the time they dedicated for the evaluation of this work.

I thank Martin Blazer and Sladjana Prisic for comments on my manuscript. I am grateful to Antje Thomas, Julia-Vanessa Böge and Daniela Prasse for technical assistance with my manuscript. I thank Marc Höppner and Daniela Esser for putting work in the genomic and RNA-Seq Data. I thank the Institute of Clinical Molecular Biology in Kiel for providing Sanger sequencing service. The manuscript was supported by the Deutsche Forschungsgemeinschaft (DFG) - CRC1182 “Origin and Function of Metaorganisms”.

I thank Dr. Benedikt Mortzfeld and Dr. Jan Taubenheim for being not only lab mates but close friends. Both helped with fruitful discussion and strengthened the predication of this work. I was always pleasured to spend time next to this work with you and hope we will always stay in contact. A friend in need is a friend indeed. 0.5$.

I would never miss the mornings and lunches with Jörg Wittlieb. Even when there was no envy left for this work the time and discussion of all problems the world has to offer have been amazing. I could write so many things about our conversations… but I better not. Thank you!

I thank Tim Lachnit for help with my work. He contributed to the outcome of the TEM images and accounted for statistical support. The stories of his life will always be unreached. He always was one level above us.

I was glad to call Janina Lange and Jay Bathia my colleagues and friends who supported my work and always had time for sweeping discussions.

I want to thank Sebastian Fraune. He liked to discuss the newest results with me and always had a good hint especially if cake was present.

I am grateful for the support of Anika Hintz and Cleo Pietschke. They did not only ordered my life as a graduate student but also have grown as my friends. Very rarely they discussed with me the newest occasions which distracted me from my work. I really appreciate the last point.

Even if they not contributed directly to this work the help of Doris Willoweit-Ohl, Eva Herbst and Maria Franck always supported me with knowledge about protocols, cultures and general lab stuff.

Thanks to all my friends and my girlfriend who discussed with me my work and stand my anger if I have had a rough day. It is always important to have a shoulder to lean on and friends you trust in.

Finally, I want to thank my family for all the support. Even if they do not understand until the end what I was doing they would always lend an ear. Without them I would literally not be here.

12 Erklärung

Hiermit erkläre ich, dass ich die vorliegende Dissertation nach Regeln guter wissenschaftlicher Praxis eigenständig verfasst und keine anderen als die angegebenen Hilfsmittel und Quellen benutzt habe. Dabei habe ich keine Hilfe, außer der wissenschaftlichen Beratung durch meinen Doktorvater Prof. Dr. Dr. h.c. Thomas C. G. Bosch in Anspruch genommen. Des Weiteren erkläre ich, dass ich noch keinen Promotionsversuch unternommen habe.

Teile dieser Arbeit wurden bereits zur Publikation eingereicht.

Kiel, den

_____

Kai Rathje